UNIVERSITY OF COPENHAGEN
FACULTY OF SCIENCE

Master Thesis on

General Relativistic Test Particle Scattering

Jitze Hoogeveen

Supervised by: Poul Henrik Damgaard & Andrés Luna Godoy

Submitted: August 15, 2022

Scattering trajectories are of great importance in general relativistic gravitational studies. The 2016 observation of gravitational waves from binary black holes has increased interest in dynamics of massive systems. Specifically, full two body dynamics are obtainable from an effective framework which considers test particles. Such a theory has been established for non-spinning binary objects. The work on spin is still ongoing.
This thesis presents a novel way of calculating test particle scattering angles of General Relativity. It does so in a weak field expansion in Newtons constant G. The work directly generalizes the previous result [1]. It does so by considering a wider class of integrals. Arbitrary planar test particle scattering can be handled, both with spinning and non-spinning particles. The resulting angle is provided as an expansion in G. It requires introducing special *normal* coordinates applicable to any metric, and a nicely-behaved function $h(r)$ in terms of which the angle can be expressed. The formalism is tested explicitly up to second order in test particle spin. Specific calculations are provided for Kerr (up to $\mathcal{O}(G^6)$) and Schwarzschild metrics (up to $\mathcal{O}(G^{10})$). These cutoffs are arbitrary and higher orders can readily be calculated.
General features are discussed, both of the derivation and the obtained results. Because of its mathematical nature, the formalism presented may have uses beyond test particle scattering. It already naturally reproduces the general mass non-spinning binary result of [1]. Discussed further is an EOB framework based on scattering angles and the possibility of an all-PM order angle in a single expression.

In collaboration with Poul Henrik Damgaard, Andrés Luna Godoy and Justin Vines, an article is in preparation with the findings described in this thesis. [2]

Contents

1 Introduction

Humans have watched the heavens for thousands of years. Ever since the Assyro-Babylonians in present day Iraq, people have meticulously observed the light from the heavens [4]. Their still-existent clay tablets record the beginnings of the earliest natural science, astronomy.

Since these ancient times, light has been the only direct conduit for this research. The ancients relied on their eyes, Newton had telescopes, and present day astronomy is both ground and space-based.

In the beginning of the 20'th century, Einstein revolutionized this viewpoint. He discovered General Relativity, a new theory of gravity. Binary systems, such as a planet orbiting a star, or two black holes orbiting each other, were predicted to emit *gravitational waves*. First observed by LIGO in 2016 [5], gravitational waves are completely different from light. They open the shutters of a completely new window to the Universe.

The search with General Relativity to describe these waves has been intense. It relies heavily on knowing the laws governing binary motion. This thesis is concentrated on a small part of this field - we look specifically at scattering of small particles around a bigger central object. This is called the test particle limit of a full binary problem. We consider scattering trajectories that stay in a single plane. The derivation generalizes an amplitudes results of [1], presented in 3.2. It does so by considering a wider class of integrations.

Before going into depth with this, we will present a general review of both the history and current state of art in gravitational theory. Newtons theory of gravitation will be described, followed by Einsteins general theory of relativity. We will discuss how binary dynamics in such a theory might be found, before turning to gravitational waves. Last, we will describe a different way of obtaining binary dynamics, called the Post Minkowskian expansion. We will work with this method throughout the thesis.

All specific mathematics necessary for our work will be described in later chapters.

1.1 Newtonian theory of motion and gravity

Although the paths of celestial objects could be recorded meticulously by the ancients, predictions as to their future development was largely fuelled by superstition. A proper theory behind the dynamics was lacking. As observational techniques improved, specifically by the advent of the telescope in 1608, so did the understanding of celestial dynamics. In 1609 Johannes Kepler proposed the first mathematical description of the orbits of planets around the Sun. It introduced mathematical methods to astronomy and was the simplest theory in agreement with observations.

The first actual physical principles governing this motion were introduced by Isaac Newton in 1687. The famous work *Philosophiae Naturalis Principia Mathematica* included the first actual law of gravity. The attractive force F between objects of (gravitational) masses m and M separated by distance r was predicted to be

$$F = \frac{GmM}{r^2} \tag{1}$$

Bodies attracted by such a force, will orbit in a common plane. Such orbits include not only bound, Keplerian trajectories, but eq. (1) allows for hyperbolic ones too. this is called a scattering trajectory.

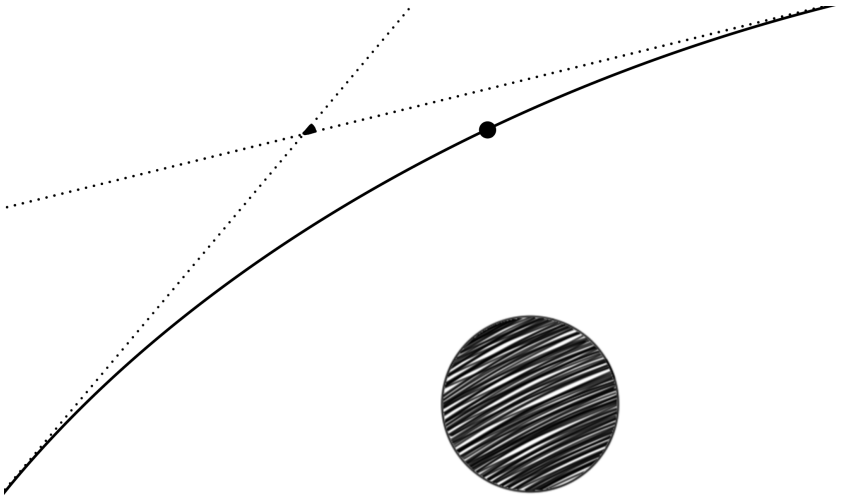

Figure 1: Scattering path of a small object (solid black sphere) orbiting a larger object (striped black sphere). The scattering angle χ between asymptotical incoming and outgoing flight directions (dotted lines) is indicated with a dark triangle. All motion happens in the plane of the paper

Imagine a large mass (perhaps a star) and a much smaller mass (perhaps a planet). The planet flies with great velocity towards the star. If the velocity is large enough, the gravitational pull of the star is not sufficient to capture the planet in a bound orbit. Instead, the planet will just whisk past the star in a slightly bent orbit. The situation is depicted in figure 1. This is known as gravitational scattering. The scattering will be in a single plane, called the *scattering plane.* [1]. The bending angle between incident and outgoing planet trajectories is known as the scattering angle, χ.

Some effects however, were not explainable by Newtons theory. The orbit of mercury provided a great puzzle. Its precession, caused by tidal interactions with the Sun and gravitational forces of other planets, as calculated by Newtons theory deviated about 7% from the observed quantity. The solution revolutionized physics as a whole.

1.2 General theory of relativity

During one of the most remarkable periods of modern physics, Albert Einstein proposed the Special and General Theory of Relativity. Developed in the period 1905 to 1916 [6, 7, 8, 9], Einstein revolutionized physics as a whole. Special Relativity concerns motion without gravity. It topples Newtons idea of absolute time - the experience of time differs with relative velocities. For a review, see appendix A. General relativity (GR) introduces gravity. Gravitational effects are interpreted in a radial new way; gravity can be considered, not a force, but the bending of space and time by matter such that straight lines be bent into orbits. Newtons 3 laws [2], underlying

[1] Situations where scattering is not in a plane are described in section 1.2.7

[2]

the Newtonian theory of gravity, were completely revised. General relativity reduces only to Newtonian gravity when velocities are small and gravity is weak.

General relativity has been very thoroughly tested. Early tests included the correction of the precession of Mercury (to be discussed later), bending of light around massive objects and last the gravitational Doppler effect. [4] [10, 11, 7] All were confirmed with unprecedented accuracy.

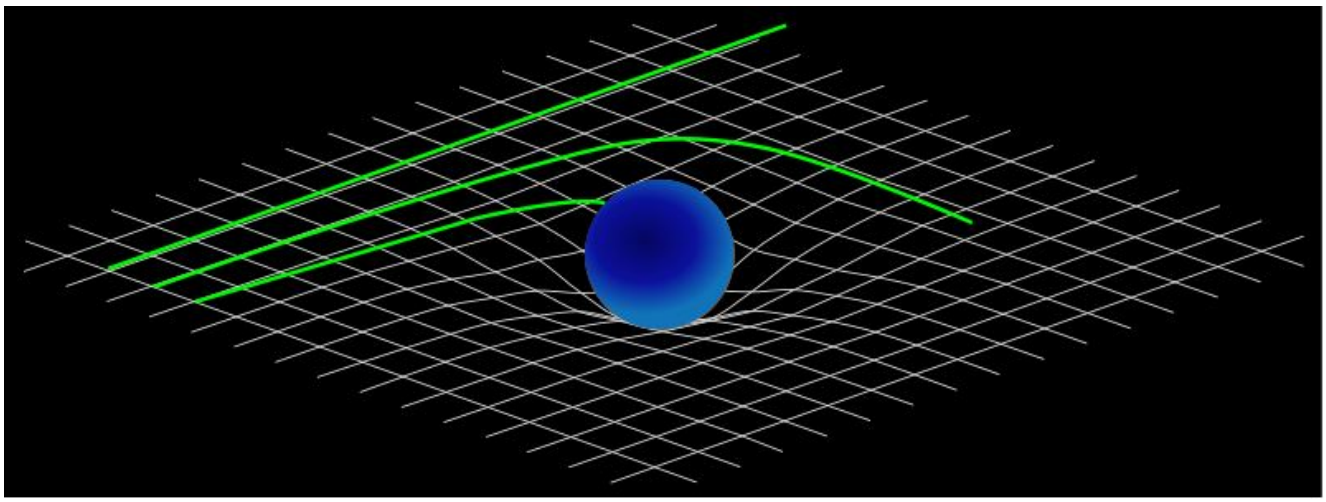

Figure 2: Spacetime being warped by matter. Different test particle trajectories are heading into the paper, marked in green. A large object (blue sphere) warps spacetime (black-white grid), such that the straight line paths followed by particles are bent into curved ones. This is the effect of gravity. The leftmost path travels entirely through flat space. The middle, closer to the mass is bent considerably more. The right trajectory is bent enough by gravity, that it collides with the surface.

We will review the basic principles of General Relativity, based on the excellent treatment of the subject by [12]. The dynamics of systems are discussed, and gravitational waves introduced. We conclude by presenting the Post Minkowskian (PM) expansion of GR, appropriate for scattering. Scattering discussed throughout this thesis, pertain to this PM expansion.

Based on the idea that all objects fall at the same rate, Einstein formulated the Equivalence Principle

In small enough regions, and small enough time durations, the laws of physics reduce to those of Special Relativity. Hence, it is impossible to detect the existence of a gravitational field by means of local experiments.

This statement says that a person in a box freely falling by gravity is identical to a person in a box experiencing no force at all. But the equivalence only holds locally, ie. for a closed box - as soon

1. *An object will either remain at rest or continue moving at constant velocity if not acted upon by a force*
2. *The force on a body is equal to its (inertial)* [3] *mass times its acceleration ($F = ma$)*
3. *Any object exerting a force on another object, feels an equal and opposite force itself*

[4]Modern physics has a new problem. General relativity, although well in agreement with observations, is not reconcilable with quantum field theory. This theory describes elementary particles. Thus General Relativity is not thought to hold on small scales. Seeking a common theory to describe both elementary particles and gravity, many theorists today seek a correction to General Relativity. We will not discuss further such efforts, and stick to ordinary General Relativity throughout this thesis

as we look outside it, we see a planet approaching rapidly! General Relativity has an intimate connection with Special Relativity. Specifically, special relativity shows that frames of reference traveling at different relative speed, experience different ideas of time. This notion is generalized by the Equivalence Principle - not only time, but now also space is only a local notion. What one observer experiences as time, another experiences as space, and vice versa. As Special Relativity predicts, the speed of light c is still the absolute speed limit at which objects of mass can travel. [5]

Following his Equivalence Principle, Einstein conjectured that gravity is a consequence not of a force, but of the nature of space around us. One can describe the paths of objects affected by gravity as straight lines through bent spacetime. See figure 2. This bending is described by the metric $g_{\mu\nu}$, describing the concept of length ds^2 in General Relativity. The pythagorean theorem in three dimensions states that $x^2 + y^2 + z^2 = r^2$ where r is the total length, x, y, z being individual coordinate measurements. Applicable to Euclidean space, the same idea can be formulated for other, warped spaces. In General Relativity time and space are treated on equal footing, the combination (time+space) being denoted *spacetime*. Say we parametrize this spacetime in some coordinates $x^\mu = (t, x, y, z)$. We can choose any coordinates we like. Defining a vector $dx^\mu = (dt, dx, dy, dz)$ as the difference in coordinates between two infinitesimally close points in spacetime, General Relativity defines the length between them as

$$ds^2 = \sum_{\mu=(t,x,y,z)} g_{\mu\nu}(x) dx^\mu dx^\nu = g_{\mu\nu} dx^\mu dx^\nu \tag{2}$$

where the last equality uses Einsteins summation convention of summing repeated indices without writing summation signs [6]The matrix $g_{\mu\nu}(x)$, possibly varying in space, is a set of numbers that encode how length differences dx^μ are combined to form a valid length ds^2 known as the line-element. Depending on the coordinates used, this metric has different entries. Negative components of $g_{\mu\nu}$ generally signify that the corresponding coordinate is interpreted as time. The positive components are interpreted as a spatial direction. Of the coordinates x^μ used, exactly a single is ever interpreted as time. In the limit of no gravity, the metric $g_{\mu\nu}$ reduces to the Minkowski metric in special relativity,

$$\eta_{\mu\nu} = \begin{pmatrix} -1 & 0 & 0 & 0 \\ 0 & 1 & 0 & 0 \\ 0 & 0 & 1 & 0 \\ 0 & 0 & 0 & 1 \end{pmatrix} \tag{3}$$

written here in cartesian coordinates. Writing the same spacetime in different coordinates yields

[5]Throughout this section, we will implicitly adopt natural units of $c = 1$, due to many appearances of this quantity. It can be reinstated by dimensional analysis.

[6]The object $g_{\mu\nu}$ can be interpreted a 4x4 matrix and dx^μ a vector. The last equation then denotes matrix multiplication.

a different structure. As an example, spherical coordinates $x^\mu = (t, r, \theta, \phi)$ yield

$$\eta_{\mu\nu} = \begin{pmatrix} -1 & 0 & 0 & 0 \\ 0 & 1 & 0 & 0 \\ 0 & 0 & r^2 & 0 \\ 0 & 0 & 0 & r^2 sin^2\theta \end{pmatrix} \tag{4}$$

with line-element $ds^2 = -dt^2 + dr^2 + r^2 d\theta^2 + sin^2\theta r^2 d\phi^2$.

In eq. (2), ds^2 is specifically constructed to be invariant under rotations, translations and coordinate reparametrisations, just like an everyday length. Generally, all kinds of coordinates may be used to describe points in spacetime, and formulate the theory. ds^2 can however be negative, depending on what points you choose to measure length between. Say you have two points with coordinate difference $dx^\mu = x_2^\mu - x_1^\mu$. Denote these points x_1 and x_2 for short. Compute their distance apart by eq. (2). Depending on the sign of ds^2,

$ds^2 < 0$: Points x_1 and x_2 are connected by a spacelike curve. They are not causally connected, meaning no physical influence from x_1 can reach x_2 or vice versa

$ds^2 = 0$: Points x_1 and x_2 are connected by a lightlike curve. Only light can reach x_2 from x_1 or vice versa

$ds^2 \equiv d\tau > 0$: Points x_1 and x_2 are connected by a timelike curve. Influences such as a beam of light or a plane can in principle reach x_1 from x_2 or vice versa. In this case, ds^2 is also called the proper time between events.

Turning back to $g_{\mu\nu}$, in order for it to keep the interpretation as describing curvature, it has special properties under coordinate transformations. Specifically, under a transformation $x^\mu \to \tilde{x}^\mu$, we have

$$\tilde{g}_{\mu\nu}(\tilde{x}) = \frac{dx^\rho}{d\tilde{x}^\mu}\frac{dx^\sigma}{d\tilde{x}^\nu} g_{\rho\sigma}(x) \tag{5}$$

Formally, we say that $g_{\mu\nu}$ is a rank-2 oneform. One can generally construct quantities which transform in ways such as to preserve their interpretation. They are generally called tensors and include vectors V^μ, oneforms A_μ and scalars ϕ. They transform like

$$\tilde{V}^\mu(\tilde{x}) = \frac{d\tilde{x}^\mu}{dx^\rho} V^\rho(x) \quad \tilde{A}_\mu(\tilde{x}) = \frac{dx^\rho}{d\tilde{x}^\mu} A_\rho(x) \quad \tilde{\phi}(\tilde{x}) = \phi(x) \tag{6}$$

An example of a tensor is 4-velocity. They are generally denoted with upper, lower and no indices. Contracting indices of a vector and a oneform, yields a scalar $V^\mu A_\mu \to$ transforms like a scalar. This notation makes it clear in eq. (2) that the line-element is invariant under coordinate transformations. A common operation is that of 'lowering/raising the index' of a vector/oneform. It is defined as $V_\mu = g_{\mu\nu} V^\nu$ for lowering and $A^\mu = g^{\mu\nu} A_\nu$ for raising. The object $g^{\mu\nu}$ is the inverse metric defined by $g_{\mu\nu} g^{\mu\rho} = \delta^\rho_\nu$.

There are now two questions: How do we know what metric to use? Given a metric, what are the paths of objects herein?

1.2.1 Geodesic paths

Lets first consider how we get dynamical paths from a metric. This will serve as a direct connection to the Newtonian theory. Suppose we know the metric $g_{\mu\nu}$ corresponding to some big star or other large object [7], around which a small planet (or particle) orbits. How are we to find the motion of the probe? We return to Einsteins Equivalence Principle: Objects affected by gravity are not accelerated.

Thus one needs a notion of acceleration in a metric and set that equal to zero. This gives the equations of motion of General Relativity. Another way to formulate this, is by an old principle of mechanics,

Non-accelerated objects follow trajectories which minimize proper time

Given points A and B, an unaccelerated object will take the fastest route between these. In a flat space, it is simply a straight line. In curved space, one could imagine it being something different.

What is the 'proper time' between two events in General Relativity? It is nothing more than $\sqrt{ds^2}$. One may write the total proper time of a trajectory $x^\mu[\lambda]$, parametrized by some arbitrary parameter $\lambda \in [0,1]$ as

$$\Delta\tau = \int_{\mathcal{P}} d\tau = \int_{\mathcal{P}} \sqrt{g_{\mu\nu} dx^\mu dx^\nu} = \int_0^1 d\lambda \sqrt{g_{\mu\nu} \frac{dx^\mu[\lambda]}{d\lambda} \frac{dx^\nu[\lambda]}{d^\lambda}} \tag{7}$$

This equation holds for all imaginable trajectories $\mathcal{P}$ of the particle. Integrals are taken along this trajectory. The *actual physical* path is found by minimizing the expression. This can be done by a variational principle, often used in Lagrangian theory.

One finds that the minimum of proper time is reached, when the path x^μ satisfies the geodesic equation

$$\frac{d^2x^\mu}{d\tau^2} + \Gamma^\mu_{\nu\rho} \frac{dx^\nu}{d\tau} \frac{dx^\rho}{d\tau} = 0, \qquad \Gamma^\mu_{\nu\rho} = \frac{1}{2} g^{\mu\rho} \left(\frac{\partial g_{\nu\sigma}}{\partial x^\rho} + \frac{\partial g_{\rho\sigma}}{\partial x^\nu} - \frac{\partial g_{\nu\rho}}{\partial x^\sigma} \right) \tag{8}$$

where τ denotes the time as measured by a clock following the trajectory. This is called proper time. The appearance of the metric hides in the object $\Gamma^\mu_{\nu\rho}$, known as a Cristoffel symbol. Coming back to our earlier interpretation, we can now identify the LHS as acceleration in gravity. Specifically, setting $\Gamma = 0$, corresponding to flat space without gravity (as we shall see), one finds the familiar expression $a = \frac{d^2x}{d^2\tau} = 0$ describing straight line motion.

1.2.2 Determining the metric

Having figured out a way to describe trajectories of small objects (formally test particles or probes) in a general metric, we can turn to the problem of actually determining the metric from a system sourcing gravity. Lets start with the basic question: what sources gravity?

As can be imagined, the bending of spacetime happens because of the presence of massive objects. After all, we are looking for a theory of gravity. In fact, all as stated by Einsteins equivalence of mass and energy

$$E = mc^2 \tag{9}$$

[7] How and what sourced a metric is treated in section 1.2.2

we expect the curvature to come from the presence of energy. Specifically, one introduces the energy momentum tensor $T^{\mu\nu}$ which describes both energy densities (00 component), momentum densities (i0 components) and internal forces (ij components) in the system sourcing gravity. $T_{\mu\nu}$ satisfies the conservation equation $\nabla T_{\mu\nu} = 0$ which says that energy cannot be created or destroyed.

This energy momentum tensor has to curve space. The curvature can be described very precisely in two objects: The Ricci tensor $R^{\mu\nu}$ and scalar R,

$$R = R_{\mu\nu}g^{\mu\nu}, \quad R_{\mu\nu} = R^{\rho}_{\mu\rho\nu}, \qquad R^{\rho}_{\mu\sigma\nu} = \partial_\sigma\Gamma^{\rho}_{\nu\mu} - \partial_\nu\Gamma^{\rho}_{\sigma\mu} + \Gamma^{\rho}_{\alpha\sigma}\Gamma^{\alpha}_{\nu\mu} - \Gamma^{\rho}_{\alpha\nu}\Gamma^{\alpha}_{\sigma\mu} \tag{10}$$

They both have the interpretation of containing curvature through its dependence only on $g_{\mu\nu}$ and derivatives of Γ.

We also know that the theory has to produce the same geodesics as Newtonian gravity, when small speeds and weak gravity (the Newtonian limit) is considered. To this extent we can consider a Newtonian limit of gravitation where we write $g_{\mu\nu} = \eta_{\mu\nu} + h_{\mu\nu}$ where $h \ll 1$ and $\eta_{\mu\nu}$ is Minkowski (flat) spacetime from special relativity. The Minkowskian metric describes the absence of gravitational effects.

Based on the knowledge that

1. the energy momentum tensor should 'replace' the notion of mass density in Newtonian theory.

2. the energy momentum tensor should only be a function of R, $R_{\mu\nu}$ and $g_{\mu\nu}$ only.

3. the energy momentum tensor should satisfy the conservation equation $\nabla T_{\mu\nu} = 0$.

4. the equation for $g_{\mu\nu}$ should reduce $g_{\mu\nu}$ to the form $\eta_{\mu\nu} + h_{\mu\nu}$ in the Newtonian limit with $h_{00} = -2\phi$ where ϕ is the gravitational potential

One can produce the anzats $R_{\mu\nu} - \alpha g_{\mu\nu}R = \beta T_{\mu\nu}$ which has consistent indices and relates the energy momentum tensor directly to curvature and the metric.

One finds $\alpha = 1/2$ by imposing the continuity equation and using a relation for the Ricci tensor known as the Bianchi identity. Similarly, by imposing the newtonian limit $g_{\mu\nu} = \eta_{\mu\nu} + h_{\mu\nu}$ with $h \ll 1$ and $h_{00} = -2\phi$, one can determine $\beta = 8\pi G$.

The result is known as Einsteins equations

$$R_{\mu\nu} - \frac{1}{2}g_{\mu\nu}R = 8\pi G T_{\mu\nu} \tag{11}$$

These equations, with the geodesic equations (8), define the Theory of General Relativity. They apply to all dynamics of all macroscopic gravitational systems in the Universe. Given a many-body problem with multiple stars rotating around each other, Einsteins equations yield the metric and the geodesics tell how objects are affected by these. The full dynamics of GR can be cast into an action formalism

$$S = \int \sqrt{-g}\left[\frac{R}{16\pi G} - g^{\mu\nu}T_{\mu\nu}\right] d^4x \tag{12}$$

[8]

[8] or in terms of a Lagrangian, $S = \int dx^4[\mathcal{L}_{GR} + \mathcal{L}_{matter}]$ where $T_{\mu\nu} = -2\frac{\delta\mathcal{L}_{matter}}{\delta g_{\mu\nu}}$

Einsteins equations are found by a variational principle in the field $g_{\mu\nu}$ and the equations of motion follow by a variational principle of dynamical quantities related to the source in $T_{\mu\nu}$.

Getting full dynamics of systems, however often proves difficult. One cannot simultaneously solve Einsteins equations and the geodesics. Instead, approximations are used. The PN approximation, covered in section 1.2.5, is widely applied. Recent methods also include the Post Minkowskian approximation, covered in section 1.2.7, which interprets eq. (12) from a quantum field theory perspective.

Einsteins equations are exceedingly non-linear. In practice they are too difficult to solve exactly, and approximations are necessary. However, metrics of large central objects with small, negligible mass probes flying around them, can be found. We refer to this as the *test particle* limit of binary motion. It will be the main regime considered by the thesis.

The following sections describe two stationary solutions to Einsteins equations, around which such test particles can orbit. They are instrumental to the thesis.

1.2.3 Schwarzschild metric and black holes

First treated by Karl Schwarzschild in 1916, the simplest case to consider is the metric of a spherically symmetric mass M. It is the first ever solution found to Einsteins equations (except the Minkowski spacetime). For such a simple configuration, considering an appropriate ansatz for the metric, Einsteins equations can be solved exactly. The dynamics of probe particles with small mass, negligent in their contribution to the energy momentum tensor, can then be found.

Specifically, we assume a spherically symmetric metric of the form

$$ds^2 = -e^{2\alpha(r)}dt^2 + e^{2\beta(r)}dr^2 + r^2 d\Omega^2 \tag{13}$$

where $d\Omega^2 = d\theta^2 + sin^2\theta d\phi^2$ is the line element of a unit sphere. Assume it drops off to Minkowski spacetime in spherical coordinates (t, r, θ, ϕ) when $r \to \infty$, under the assumption that gravitational interactions are negligent in that limit. Coordinate choices will play an important role for the results in this thesis. We will briefly review coordinate properties both in the bullet points below and in the next treatment on the Kerr metric.

We are only interested in the solution to $g_{\mu\nu}$ outside the mass M. We can thus set $T_{\mu\nu} = 0$, which corresponds to $R_{\mu\nu} = 0$. Readily computing $R_{\mu\nu}$ and its associated Cristoffel symbols, yields

$$ds^2 = -\left(1 - \frac{r_s}{r}\right)dt^2 + \frac{dr^2}{1 - \frac{r_s}{r}} + r^2(d\theta^2 + sin^2\theta d\phi^2) \tag{14}$$

which is known as the *Schwarzschild metric* in Schwarzschild coordinates. It describes the geometry of spacetime outside any spherical mass M that does not rotate - stars, planets, moons, all have gravitational pulls approximately described by this metric (neglecting rotation). The constant $r_s = 2GM$ has units of length and is known as the Schwarzschild radius. The Schwarzschild metric has some crucial properties relevant for this thesis,

- The metric is only a function of r. It is spherically symmetric.
- The metric is diagonal. Each direction is just stretched relative to pure flat space in spherical coordinates. Coordinates (t, r, ϕ, θ) thus have general interpretations as warped spherical

coordinates.

- The metric becomes the Minkowskian spacetime when $r \to \infty$. This is because gravitational interactions vanish in the limit.

- Similarly, turning off gravity by setting $G \to 0$, recovers also the Minkowskian spacetime in spherical coordinates. This is natural: no gravity corresponds to flat spacetime. The two limits $r \to \infty$ and $G \to 0$ are not generally identical, as the parametrization of Minkowski spacetime need not automatically yield spherical coordinates. We will see how when treating the Kerr metric.

- Last, and most importantly, consider the case when the mass M is compressed enough to allow trajectories below $r = r_s$. For $r \to r_s$ the g_{00} metric component has a pole. This singularity is purely an artifact of the coordinates used, and can be removed by a coordinate transformation. Nevertheless, it signifies an important consequence: For $r < r_m$, the coordinate t has $g_{00} > 0$ and coordinate r has $g_{11} < 0$. A time-like coordinate has turned spacelike and a spacelike coordinate has turned timelike. The effects of this can be seen by considering a radial beam of light for $r < r_m$. For two infinitesimal points on its trajectory, consider a radial outgoing light ray within the black hole. Considering two infinitesimally close points on its trajectory, we find by combining eqs. (2) and (14)

$$0 = -(1 - \frac{r_s}{r})dt^2 + \frac{1}{1 - \frac{r_s}{r}}dr^2 \quad \Rightarrow \quad \frac{dr}{dt} = \left|1 - \frac{r_s}{r}\right| \tag{15}$$

  where $dr/dt \geqslant 0$ has been imposed for outgoing light rays. This shows that $dr/dt = 0$ when the light ray reaches $r = r_s$. Light cannot escape the Schwarzschild radius, and because nothing travels faster than light, neither can anything else. Instead, everything will be pulled to $r = 0$ until crunched up in a singular point.

  The Schwarzschild metric describes a *black hole* and $r = r_s$ is its event horizon.

Geodesics in the Schwarzschild metric are fully understood. Since the metric is spherically symmetry, any orbit will be confined to a plane, say the plane $\theta = \pi/2$. Simply invoking the geodesic equations, one can formulate the evolution of (inverse) r in terms of ϕ,

$$\frac{d^2X}{d^2\tau} + X - 3X^2 = \frac{(GM)^2}{L^2} \tag{16}$$

where $X = GM/r$, $L = r^2\dot{\phi}$ is angular momentum of a particle of negligible mass orbiting in the metric and $E = \dot{t}(1 - \frac{r_s}{r})$ is its energy. Dots denote derivatives with respect to proper time τ.

1.2.4 Kerr metric

Another exact solution to Einsteins equations first followed 1963, 57 years after the discovery of the Schwarzschild solution. Named the *Kerr metric*, after its discoverer Roy Kerr [13], written in

Boyer-Lindquist coordinates it reads

$$-\left(1-\frac{r_s r}{\Sigma}\right)dt^2+\frac{\Sigma}{\Delta}dr^2+\Sigma d\theta^2+\left(r^2+a^2+\frac{r_s r a^2}{\Sigma}sin^2\theta\right)sin^2\theta d\phi^2-\frac{2r_s r a sin^2\theta}{\Sigma}dtd\phi \tag{17}$$
$$\Delta=r^2+a^2-r_s r, \qquad \Sigma=r^2+a^2cos^2\theta$$

It describes an intrinsically spinning black hole, with spin parameter $0 \leqslant a \leqslant r_s/2$. Setting $a = 0$ recovers the Schwarzschild solution with Schwarzschild radius r_s. Interestingly, the Kerr metric can be generated from the Schwarzschild solution by a procedure known as the Newman Janis Algorithm (NJA). See section D. Note that the Kerr metric is rotationally symmetric in any plane, except that with $\theta = \pi/2$. This has implications later. Notice further a difference with Schwarzschild. Consider the $\theta = \pi/2$ plane. Note the difference between letting $r \to \infty$ and $G \to 0$ in the metric. For Schwarzschild, they yield the same Minkowski metric in spherical coordinates. However for Kerr, we find

$$\begin{aligned} g_{\mu\nu} &\xrightarrow{r\to\infty} \begin{pmatrix} -1 & 0 & 0 \\ 0 & 1 & 0 \\ 0 & 0 & r^2 \end{pmatrix} \\ g_{\mu\nu} &\xrightarrow{G\to 0} \begin{pmatrix} -1 & 0 & 0 \\ 0 & \frac{r^2}{r^2+a^2} & 0 \\ 0 & 0 & r^2+a^2 \end{pmatrix} \end{aligned} \tag{18}$$

Letting $G \to 0$ does not recover the Minkowski metric in spherical coordinates. However, the metric still describes flat space, which can be rendered in a Minkowski form simply by a coordinate transformation

$$r^2 \to \rho^2 = r^2 + a^2 \tag{19}$$

The same behavior can be expected for any metric: Letting $G \to 0$ should recover flat space, however it might not be expressed readily in spherical coordinates. This behavior plays a prominent role later.

Like the Schwarzschild solution, the Kerr black hole has again a singular radius, beyond which all trajectories tend to the centre. This justifies the 'black hole' designation. However, the Kerr black hole has two interesting radii. The inner, event horizon, behaves just like the Schwarzschild event horizon. It is located at

$$r_+ = \frac{r_s}{2}+\frac{r_s}{2}\sqrt{1-\frac{4a^2}{r_s^2}} \tag{20}$$

at which $g_{rr} \to \infty$. This singularity is fake, just like the Schwarzschild event horizon. It is an event horizon because light rays cannot escape the horizon from within. This might be shown by an argument similar to that of the Schwarzschild metric.

The other interesting horizon is found by solving $g_{tt} = 0$. One finds two solutions, the larger of which is of interest. It is

$$r_{ergo} = \frac{r_s}{2}+\frac{r_s}{2}\sqrt{1-\frac{4a^2}{r_s^2}cos^2\theta} \tag{21}$$

It can be seen that $r_+ \leqslant r_{ergo}$ and that they meet up at $\theta = 0, \pi$, meaning perpendicular to the

equatorial plane. When $r_+ < r < r_{ergo}$, denoted the ergo region, something interesting happens. Computing $d\phi/dt$ of an arbitrary path inside the region, one finds

$$\frac{-g_{t\phi} - sin\theta\sqrt{\Delta}}{g_{\phi\phi}} \leqslant \frac{d\phi}{dt} \leqslant \frac{-g_{t\phi} + sin\theta\sqrt{\Delta}}{g_{\phi\phi}} \tag{22}$$

But we have $g_{tt} > 0$, $g_{\phi t} < 0$ and $g_{\phi\phi} > 0$, thus both solutions are positive. The conclusion: Inside the ergo-region, both massive and light trajectories can only move around the black hole in a single rotational direction. No counter-rotational movement is possible - however hard you try. For this reason, the Kerr metric is interpreted as having spin. In fact, this spin effect comes precisely from the non-diagonal $dtd\phi$ term in the line-element. Dividing the line element eq. (17) by dt^2 creates a term linear in $d\phi/dt$. The sign hereof is thus important, which is reflected by the inequality.

Some advanced theories of gravitation go further in this notion. They propose black holes as elementary particles, much like those of quantum field theory. [14] We will incorporate other quantum field theory aspects in gravity shortly.

Other black hole solutions have also been uncovered. A charged, non-spinning black hole, the Reissner Nordstroem solution, was discovered between 1916 and 1921 by Hans Reissner, Herman Weyl, Gunnar Nordstroem and George Barker Jeffrey independently [15]. They have interesting properties, involving the possibility of arranging multiple black holes in adiabatically moving configurations through equalizing of charge repulsion and gravitational attraction.

The solution combining spin and charge, originated in 1965 [16], is the Kerr-Newman metric.

1.2.5 Post Newtonian approximation of General Relativity and Effective One-Body theory - an example of finding dynamics

As mentioned Einsteins equations are practically impossible to solve exactly. We focus on finding the dynamics of general binary systems, with general masses and rotation. This covers planets, stars, black holes, and neutron stars. To tackle such a problem, one uses a plethora of approximation techniques. One such technique, the assumption of weak fields, is central to this thesis. Just assuming weak fields yields the Post Minkowskian expansion. Additionally imposing small velocities, results in the Post Newtonian expansion. These techniques form the basis of many groundbreaking modern results in gravitational physics.

We will first discuss the Post Newtonian (PN) approximation, including its applications. It primarily concerns dynamics of bound orbits. Scattering orbits are treated in section 1.2.7, with the Post Minkowskian expansion.

The Post Newtonian expansion was among the first approximation methods used in General Relativity. It consists of an expansion in both velocities and weak gravity. Small velocities are imposed by $v/c \ll 1$. Weak fields means writing the metric $g_{\mu\nu}$ as

$$g_{\mu\nu} = \eta_{\mu\nu} + h_{\mu\nu} \tag{23}$$

where $h \equiv h_{\mu\nu}\eta^{\mu\nu} \ll 1$. In the complete classical Newtonian limit, one has $h_{00} = -2\phi$ where ϕ is the Newtonian gravitational potential.

In principle the Post Newtonian expansion is an iterative approach, only conceptually sketched out here. It starts with $g_{\mu\nu}$ from above in the Newtonian limit. Dynamics are found from the metric, from which a corresponding energy momentum tensor is constructed. This energy momentum tensor is plugged into Einsteins Equations, assuming low velocities, which produces a modified metric. This is the 1PN correction to the metric.

To find higher PN orders, one iteratively finds the dynamics in $g_{\mu\nu}$ to correct the low-velocity energy momentum tensor, which then yields a corrected metric and so on. The end product is often a Hamiltonian which encodes the equations of motion. This is just a conceptual sketch and many intricacies exist. To see some of these difficulties, see eg. [17, 18]. One finds perturbatively better and better solutions, around a Newtonian starting point. By this idea, although from a point-particle point of view, corrections to the precession of Mercury were found in almost perfect agreement with theory [10]. This calculation we will consider next.

We first consider the Post Newtonian correction to a probe orbiting the Schwarzschild metric. It is easiest to consider directly eq. (16) for the full Schwarzschild geodesic equations. Plugging the ansatz $X = X_{newton} + X_{GR}$ where $X_{GR} \ll 1$, into eq. (16), using that X_{newton} parametrizes an ellipse, one finds directly a solution for the general relativistic correction X_{GR},

$$X_{GR}(\phi) = \frac{(GM)^4}{L^4}\left(3 + \frac{2e^2}{2} - \frac{e^2}{2}cos\phi + 3e\phi sin\phi\right) \tag{24}$$

where e is the eccentricity of the Newtonian elliptic orbit. The important part of this equation is the appearance of a non-periodic term $\sim \phi sin\phi$. It is not present in Newtons theory, and is responsible for a non-periodic precession of the orbit. It induces an angular shifting of the periastron [9] between rotations. Defining the first periastron to be at $\phi = 0$, the next should be at $\phi = 2\pi + \Delta\phi$, where $\Delta\phi$ is the periastron shift

$$\left.\frac{dX}{d\phi}\right|_{\phi=2\pi+\Delta\phi} \quad \Rightarrow \quad \Delta\phi = \frac{6\pi GM}{(1-e^2)ac^2} \tag{25}$$

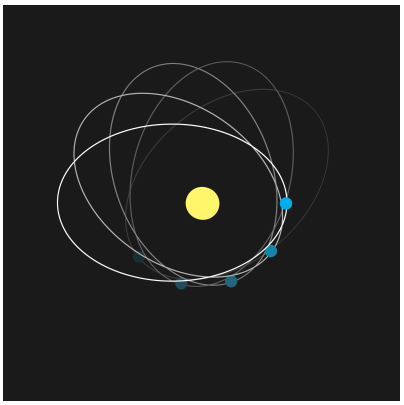

Figure 3: Precession of mercury (blue) in its orbit around the Run (yellow). Notice how the point of closest approach, or periapsis, changes from orbit to orbit. The shift in angle per orbit is the periastronshift, given by eq. (25).

For Mercury, this fills in *exactly* the $43 rad/orbit$ discrepancy between Newtons prediction and observations. It constitutes one of the very earliest successes of General Relativity.

One of the modern applications to the Post Newtonian expansion, is computing geodesics of many-body systems. Thibault Damour has been a pioneer in this field, contributing to the technique for more than 37 years [19].

[9] the highest furthest point Mercury reaches from the Sun

Consider a binary system, eg. of black holes. A 5PN Hamiltonian [10] for such a system has been found [20]. Even though the dynamics are technically obtainable from such an object, the non-linearity of the problem often proves too much to handle.

One promising analytical way of addressing this problem is that of the Effective One-Body Theory (EOB), presented by Thibault Damour [21, 22, 23, 24]. The idea is to map the full dynamics of a binary system, ie. two black holes with masses m_1 and m_2, to an effective test particle of reduced mass $\mu = m_1 m_2/(m_1 + m_2)$ orbiting in some effective EOB metric $g^{eff}_{\mu\nu}$. Calculations in this effective formalism are much easier than the general problem. The idea is, that knowing dynamics in the effective formalism, the dynamics in the real formalism can be found. This is achieved through relating energy, angular momentum as well as coordinates used in each formalism. A set of equations known as an EOB mapping define this map.

One effectively encodes the Hamiltonian of the full system in the EOB metric $g^{eff}_{\mu\nu}$.

Thibault Damour first pioneered the formalism. $g^{eff}_{\mu\nu}$ is determined order by order in center of mass (CM) velocities v [21]. The full energy of each formalism is given by the Hamiltonian encoded in eq. (12) [11]. The energy mapping was made based on quantum mechanical considerations and the ansatz effective metric was supposed isotropic in form. PN expanded dynamics were thus found. The EOB formalism has been tested against numerical methods for colliding black holes (see section 1.2.6). Results provide both predictions and are in agreement with numerical simulations of the problem [25, 26, 27, 28, 29, 30, 31, 32, 33, 34, 35, 36, 37]. However, the natural small velocity restriction of a PN formalism limits its applicability to slow moving events. For the very final parts of black hole collision, one needs fully relativistic results.

To this extent, recent developments have been made towards an EOB approach based on expansions only in $h_{\mu\nu}$, equivalent to expansions in G. This is called a Post Minkowskian (PM) expansion. It still assumes weak gravity, but is fully relativistic. Further details will be provided in sections 1.2.7, 6.1 and C

We now discuss one of the main driving forces behind the modern need of precision dynamics of binary systems: Gravitational waves.

1.2.6 Gravitational waves

Gravitational waves, first mentioned by Einstein in 1916 [38][12], are small ripples in spacetime propagating at the speed of light. They are unique to Einsteins theory of gravity, and do not appear in that of Newton. They originate from heavy, accelerating objects, according to the quadrupole formula

$$\bar{h}_{ij} = \frac{2}{r}\partial_t^2 I_{ij}\Big|_{t=t_r} \qquad [13] \tag{26}$$

[10] corresponding to $(v/c)^{10}$

[11] We will not further investigate the Hamiltonian here, however details necessary later will be presented in section 2

[12] Einstein originally said, gravitational waves did not exsist, but changed his views multiple times during the next 40 years. Finally, around 1960, they were proven a real phenomenon by, among others, Felix Pirani. [38, 39, 40]

[13] Here $h_{\mu\nu} = \bar{h}_{\mu\nu} - 1/2\eta_{\mu\nu}Tr[\bar{h}]$. The time and radial coordinats t, r are spherical Minkowski coordinates. The evaluation in retarded time $t_r = t - r$ shows that the waves always travel at the speed of light.

which says that an acceleration of matter (quadrupole $I_{\mu\nu}$) induces a wavelike perturbation ($h_{\mu\nu}$) such that initially flat spacetime becomes $g_{\mu\nu} = \eta_{\mu\nu} + h_{\mu\nu}$. For rotating systems, these waves will have twice the orbital frequency.

All accelerated matter will emit gravitational waves. Subsequently, energy is carried away by the waves. Thus a binary system of, say, two black holes will produce gravitational waves, and will slowly spiral toward each other as they lose energy - eventually they will collide. Even though many systems emit gravitational waves, only very violent events produce waves large enough for observation. A collision between black holes is a good candidate.

Gravitational waves are very different from electromagnetic ones. Foremost, each wave contains very detailed information about the source. Its shape, or waveform, directly reflects highly-relativistic effects unique to General Relativity. Observation of such waves yields direct tests of General Relativity.

Indirect effects were measured back in 1974 from the first discovery of a neutron star binary [41, 42]. However gravitational waves themselves were only first observed in 2015 by the Laser Interferometer Gravitational-wave Observatory (LIGO) [5]. This happened almost 100 years after first predicted. LIGO observes the collision of very heavy objects, typically (spinning) black holes, producing large gravitational waves. This is called a *merger* (see figure 6). More detail follows below. First a discussion of LIGOs method.

LIGO did the following. The warping of spacetime can be measured as a change in proper time of a trajectory. LIGO achieved this by measuring the relative difference in arrival of laserbeams along two perpendicular arms (see figure 4) [43]. The beams are sent out, from a common point of origin, back and forth through one arm each. When they return, differences in their arrival time can be inferred from the interference pattern created between beams. The LIGO setup is called a Dual Recycled, Fabry Perot Michelson interferometer. An initially 20W beam of light enters the detector. It hits first a Power Recycling Mirror, which magnifies the beam to 750kW. The beam is then split by a beamsplitter, into two beams. The beams then enter one arm each, which are constructed as a Fabry Perot cavities. They consist of one mirror at each end. The beam is thus reflected back and forth in the arm about 300 times. When it leaves the arm, the beams are merged and create an interference pattern in the detector. Furthermore, the mirrors at the far end of the arms are suspended by a very complicated system of dampened wires so as to isolate them from any external oscillation transmitted through the ground (something like a person walking in the nearby town).

Such an elaborate setup is needed in order to achieve enormous sensitivity. LIGO is currently capable of resolving differences in traveltime corresponding to the width of a human hair relative to the distance between earth and its nearest star (4.2 light years). [44]

On the 14th of September 2015 LIGO observed the first gravitational wave (see figure 5). It was named GW150914 after its date of observation. LIGO measured a time difference corresponding to about $2 \cdot 10^{-18}$ meters (a relative dilation of 1 in 100.000 billion-billion of the arms [14]). Analysis showed, that it came from two merging black holes with masses $\sim 36 M_\odot$ and $\sim 29 M_\odot$.[15] They merged to a single black hole with mass $\sim 62 M_\odot$. The difference ($(29 + 36 - 62) M_\odot = 3 M_\odot$), was

[14] 100.000 billion-billion = 10^{23}

[15] $M_\odot$ is the mass of the sun.

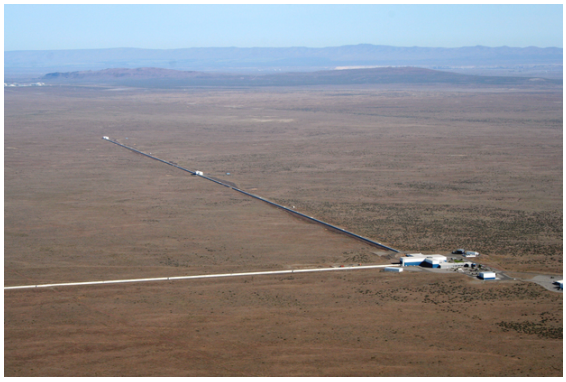

(a) Hanford observatory, a part of LIGO, located in the Nothwest US. LIGO was established in the 1970s and now consists of a collaboration of 4 detectors worldwide: LIGO Livingston (US), LIGO Hanford (US), Virgo (Italy), and KAGRA (Japan). Source: [45]

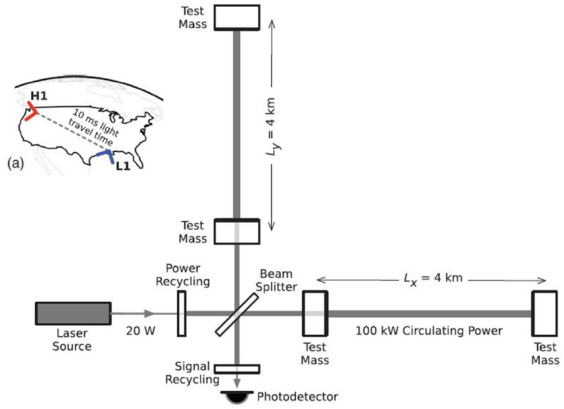

(b) Schematic of the LIGO interferometers. The location and orientation of two American-based LIGO observatories, Livingston and Hanford, can be seen on the top-left insert. Figure adapted from [46]

Figure 4: The Light Interferometer Gravitational-wave Observatory (LIGO) located in Europe and the US. The left figure shows one of the three separate detectors making up the observatory. The figure to the right shows a schematic of a single detector.

in an instant radiated away as gravitational waves [16]. In this instant, the energy radiated was more than all stars in the observable Universe combined!

Since then, numerous observations of gravitational waves have been made [48, 49, 50, 51, 52, 53, 54, 55, 56, 57]. All come from heavy objects like black holes merging. More exotic systems, like the merger of a neutron star with a black hole, have also been observed [57].

Gravitational wave signatures are very sought-after. According to eq. (26), the waveform, ie. the strain of figure 5 which $h_{\mu\nu}$ describes, is entirely defined by the dynamics of its source - the black holes. In the past 5 years, theoretical physicists have gathered from all disciplines of physics to address this problem. Many different techniques of analysing gravitational systems have been proposed. We have already discussed the effective one-body theory as a specific example. It plays a big role in determining waveforms. In fact, different techniques can be employed at different stages of the merger. As indicated by figure 6, a merger can be classified in three stages

- *Inspiral phase*: This is the first phase of a merger. Heavy objects (think black holes) initially rotating steadily around each other lose energy due to their accelerated paths to gravitational waves. Velocities of the black holes are relatively low, and the gravitational waves weak in amplitude, with low frequency.

  They slowly move closer, as energy is radiated away, increasing the gravitational wave amplitude and frequency. As a result, they accelerate. This phase can normally last anything betwen years or days, depending on the system considered. It is the longest lasting phase of the three.

- *Merger phase*: When the objects get closer and closer, their orbital periods become on the

[16] An interesting sidenote, the definition of energy in gravitational waves is much debated. For a recent reference, see [47]

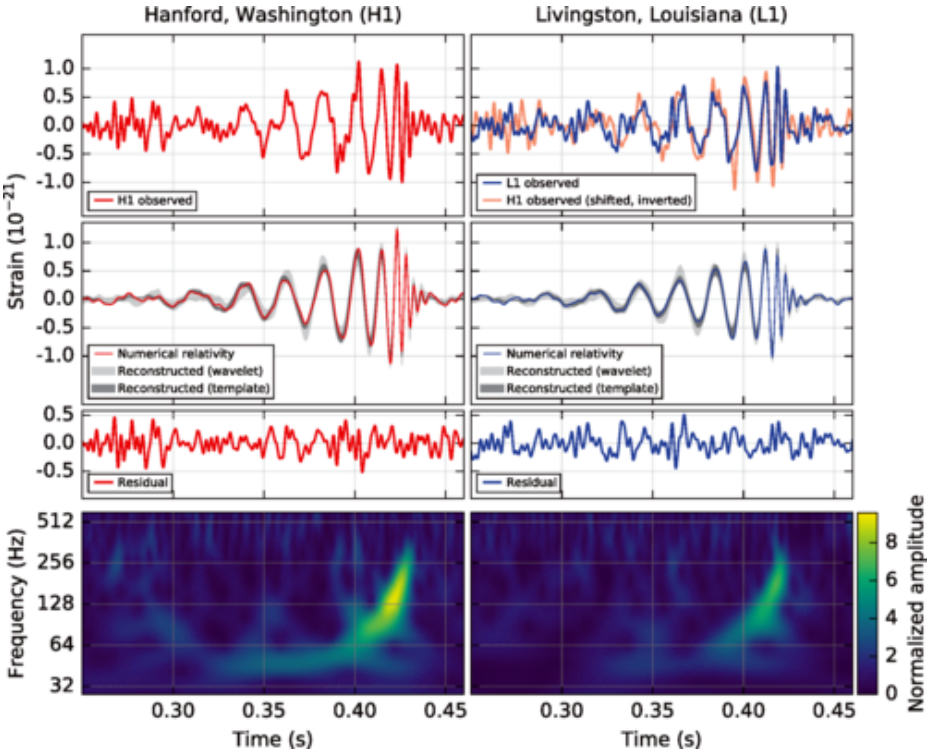

Figure 5: [5] Figure showing the waveform of the first ever observed gravitational wave, GW150914 as obesrved by Hanford (H1, left column) and Livingston (L1, right column). *Top row*: The strain, a measure of the difference in lengths between the arms. An emerging periodic behaviour can be seen (inspiral phase of binary). Then both the frequency and amplitude of the strain increases (larger gravitational waves). At the maximum, the black holes merge (merger phase). In the final 0.05 seconds, the merger has happened, and the gravitational wave signal dies down (ringdown phase) *Second row*: Filtered observed strain (coloured) and predictions by numerical relativity (dark grey). Lightgrey areas show 90% confidence interval of predictions. *Third row*: Residuals between numerical and observed results, after filtering. *Fourth row*: A time-frequency representation of the strain data. It shows an increase (chirp) in the frecuency leading up to the merger.

order of seconds. For black holes several times the size of the sun, speeds become relativistic. The objects collide, merging, within a few seconds. This is a *very* violent event. Often the instantaneous energy radiated is on the order of that radiated by all stars in the Universe!

- *Ringdown*: After collision, the resulting object (typically a larger black hole) does not accelerate because of conservation of momentum. Therefore the gravitational waves experience exponential ringdown, vanishing again within seconds.

Because velocities are low, the inspiral phase, can be considered very accurately in the framework of EOB theory in the PN expansion. [58]

However, when velocities become higher, entering the merger phase, predictions from normal PN expansions collapse. The current state of the art method is to consider numerical simulations of the system, brute forcing the dynamics. Such a method is very accurate through all phases and is only limited by the intrisic numerical uncertainties. It can however take months to generate a single waveform. For a review, see [59]. One also has the opportunity to callibrate the EOB formulation with numerical simulations, thus 'simulating' the missing terms in the EOB expansion [60]. This is denoted an EOBNR waveform, and has been widely used in subsequent analyses of

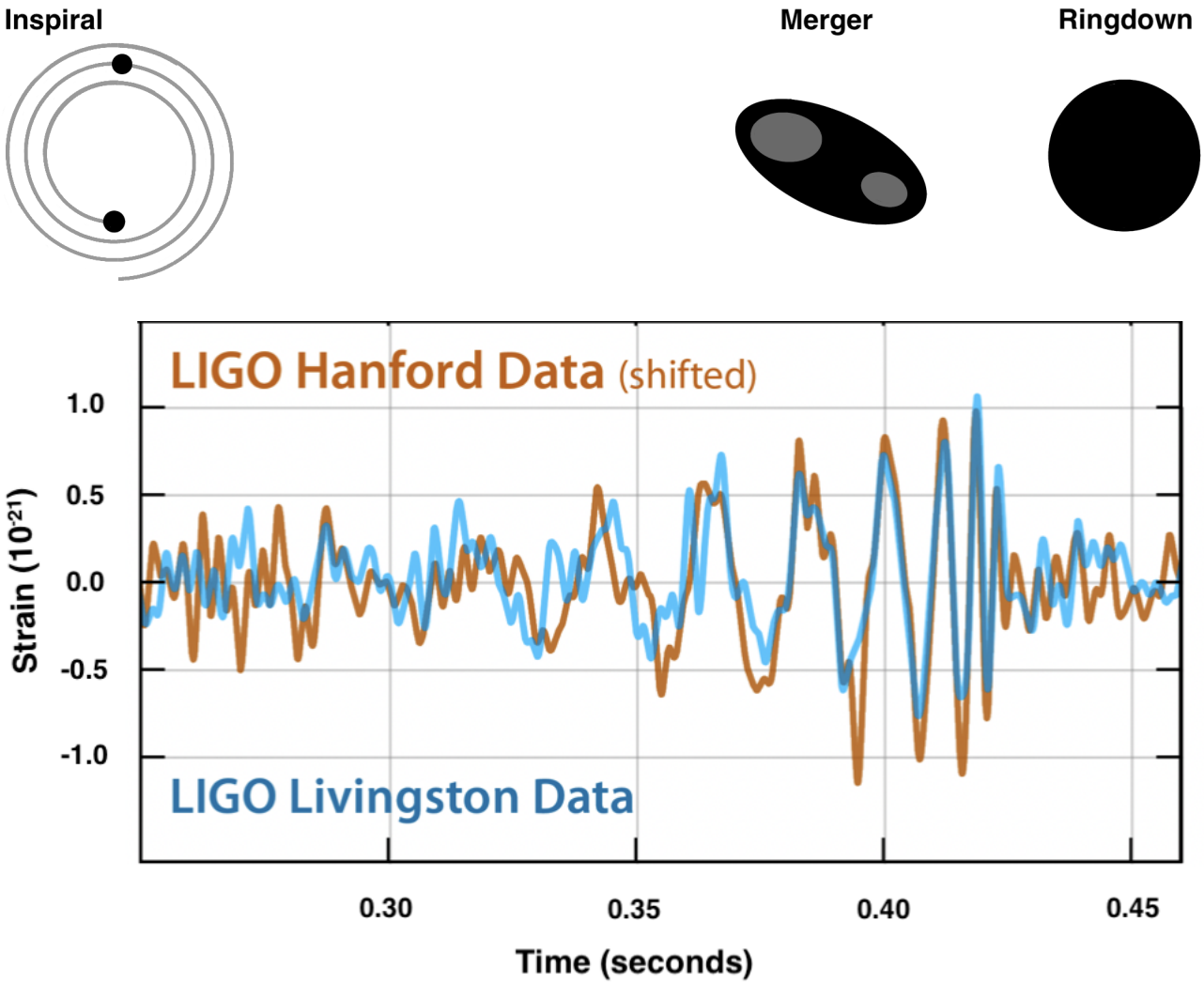

Figure 6: Bottom: Figure showing the GW150914 data from LIGO Livingston and LIGO Hanford. The original signal was received at different times. This shift has been compensated for. Top: A corresponding timeline of the event (top). The event consists of an inspiral, merger and ringdown phase further described in the main text.

the GW150914 data [61, 37].

The ringdown can be modelled from pertubative considerations, modelling the final black hole as a perturbed Kerr solution [62, 63], oscillating slightly with frequencies called quasinormal modes. It encodes interesting properties of the final black hole state. Recent years have seen massive interest to improve purely analytical waveform modelling.

Although numerical relativity is improving with great leaps, the speed of an analytical approach is highly desired.

The next section will discuss a regime to gravity called the Post Minkowskian (PM) expansion. Studying this limit based largely on quantum field theoretical tools, yields important input to both the PN formalism, and itself provides information of complex binary systems. The PM expansion is thus of utmost interest to the study of gravitational waves.

1.2.7 Post Minkowskian expansion - scattering angles

We now introduce the Post Minkowskian expansion, principally used in calculating scattering angles of complex systems in General Relativity. It provides relativistic corrections to the PN expansion, order by order in G. [17]

The PN expansion of gravity, although quite sucessfull in describing dynamics, has two major drawbacks. First, it has natural limitations at high velocities. Second, it becomes very cumbersome at high PN orders. The Hamiltonians on which a mapping is based, have hundreds of terms [20]. Damour proposed in 2016 to construct EOB metrics not in the Post Newtonian expansion, but in the Post Minkowskian expansion (PM). The already established methods in such a framework would provide compact information for such an EOB formalism.

The expansion itself had been known since 1956, first introduced by Bruno Bertotti [65]. It assumes a weak field, however does *not* assume small velocities,

$$g_{\mu\nu} = \eta_{\mu\nu} + h_{\mu\nu}, \qquad \text{(no restriction on velocities)} \tag{27}$$

where $h \equiv \eta^{\mu\nu} h_{\mu\nu} \ll 1$. The PM approximation is constructed as an expansion in G, which modulates the strength of gravity. Its method of constructing PM orders is quite different from the PN method. The assumptions above apply principally to *scattering trajectories* (see figure 1). Accordingly, the main focus of the framework is calculating scattering angles of complicated systems [18] in orders of G. It should be noted, the uses of a Post Minkowskian expansion are far from limited to an EOB approach. Instead the expansion in itself is a vast subject of research, the study of which simplifies certain computations in GR considerably. It is a flourishing field of research. See [64] for a review.

Damour's insight on an PM-based EOB framework was this. Imagine constructing an EOB metric based on scattering angle data. Such a metric encodes the equations of motion of the system. However, these equations of motion are identical for scattering and *bound* orbits. Therefore, no difficulty arises in applying the EOB metric to bound orbits. Section 6.1 and appendix C discusses the formulation of an EOB metric within the PM framework. The rest of the discussion is devoted purely to the PM framework, with no consideration on the EOB formalism.

One can consider Post Minkowskian expansions of testparticle orbits, or the full dynamics of systems. The generic case builds up dynamics from eq. (27), hence the name "Post Minkowskian expansion". In the test particle limit, an ordinary Hamilton-Jacobi theory is sufficient for scattering angle computations (see section 2.2). One simply takes a generic metric, ie. Kerr, compute relevant quantities, and expand those in G assuming weak fields. In this sense, eq. (27) is not used specifically to build up dynamics. The designation "Post Minkowskian" can therefore be debated when considering testparticles, although the assumptions of the theory are the same and results are equal in approriate test particle limits. One can refer to the test particle limit as a "weak field" limit, however we will furthermore refer to both as Post Minkowskian expansions.[19]

Binary objects can generally have spin in arbitrary directions. Depending on spin alignment,

[17] The formalism is not a fully relativistic version of Post Newtonian results in the sense that multiple orders in G contribute to the Newtonian limit [64]. The PM expansion considers a single order in G at a time. However, it provides relativistic corrections to these specific orders.

[18] Binary black holes, neutron stars and the like

[19] See footnote 27 for a further discussion on this fact in light of the thesis

this can yield scattering angles not confined to a single plane. This thesis will focus solely on the test particle case, where scattering happens in a single plane, meaning angular momentum is conserved and spins are aligned. We will briefly discuss the non-spinning, arbitrary mass binary below, before going to the test particle case in the bulk thesis.

Remarkably, studying the PM framework for general systems can succinctly described using quantum field theory (QFT) methods. These are also referred to as amplitude methods (see [64] for a review). The idea is to compute the scattering angle χ, order by order in the PM expansion in G. This is exactly the aim of QFT methods: Compute scattering angles between elementary particles (here our black holes), in perturbative expansions of some coupling constant (here G).

Getting into a bit more detail, consider the case of two interacting arbitrary masses, with no spin. One may couple the action of $g_{\mu\nu}$ (first part of eq. (12)) to two massive non-spinning scalar fields. This represents a non-spinning binary. The formalism may be generalised to a system with spin as discussed by [66]. The associated action is [64, eq. (1)]

$$S = \int d^4x \frac{\sqrt{-g}R}{16\pi G_N} - \frac{1}{2}\int d^4x\sqrt{-g}\sum_{i=1,2}(g^{\mu\nu}\partial_\mu\phi_i\partial_\nu\phi_i + m_i^2\phi_i^2) \tag{28}$$

where $g = det(g_{\mu\nu})$ and we use eq. (27) for $g_{\mu\nu}$ expanded around flat space like $g_{\mu\nu}(x) = \eta_{\mu\nu} + \sqrt{32\pi G}h_{\mu\nu}(x)$. $\phi_i(x)$ are functions of spacetime that describe the exsistence of each black hole (labelled $i = \{1, 2\}$).

This action can be viewed through the glasses of quantum field theory; The fields $h_{\mu\nu}$ and ϕ_i can be considered describing 'quantum fields' of elementary particles known as gravitons ($h_{\mu\nu}$) and point particles (ϕ_i). The first term in (28) describes the propagation of gravitons (dynamics of $h_{\mu\nu}$). The last term describes free propagation of masses in such a gravitational field - it encodes interactions between gravitons and masses. It is closely related to the energy momentum tensor $T_{\mu\nu}$ through eq. (12).

Masses ϕ_i thus scatter off each other through the exchange of gravitons (see figure 7). The action (28) can be considered quantum mechanical and all methods of QFT may be applied to compute the binary scattering angle.

One may construct a dictionary of Feynman rules of the field content $\{\phi_i, h_{\mu\nu}\}$ to calculate the classical scattering amplitude order by order in Newtons gravitational constant G. From the scattering amplitude, one can go to scattering angles by use of the impetus equation or the eikonal formalism [67]. More details on the impetus equations are contained in sections 3.2

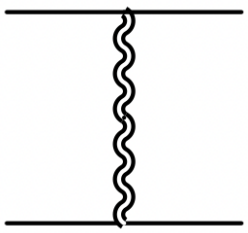

Figure 7: Single graviton exchange between two scalar particles. The squiggly line represents the graviton, and the horizontal lines are the particles. Such a diagram will go like $\mathcal{O}(G)$. Figure adapted from [64].

The PM expansion has seen vast interest in the past few years. Providing a rigorous way of obtaining dynamics of systems, it is a focal point of the gravitational wave community. We provide an overview of recent developments. Binaries without spin have been treated extensively. Scattering angles up to 3PM of a wide range of binary systems are fully understood and work is being done at 4PM, and 5PM in the probe limit [68, 69]. Binary systems consisting of both black holes and neutron stars have been investigated [70]. A worldline approach is also developed with considerable success [71, 72, 73, 74]. Connections between PM scattering and gravitational wave-forms have been established only for non-spinning bodies [3, 75].

Adding spin to binaries has been a major difficulty. There exist spin-spin couplings which distort the motion. Trajectories are only confined to a plane, when all spins are aligned with the angular momentum vector. This regime has thus received major attention. The direct connection with wave-forms is still in its infancy. First Post-Minkowskian results have been established by Justin Vines at all orders in spin from solving Einsteins field equations directly [76]. Additionally, amplitude and worldline based approaches have contributed to various Post Minkowskian results [77, 70].

1.3 Outline of Research in this Thesis

This thesis considers the Post Minkowskian expansion of General Relativity in the probe limit. In this limit, we can employ the Hamilton-Jacobi formulation of GR (see section 2.2). We derive a closed-form expression of the scattering angle of a, possibly spinning, probe in a general metric $g_{\mu\nu}$, in an expanded PM form to arbitrary high orders in G. The formalism treats cases where the probe is confined to a single scattering plane.[20] Our calculation generalises a previous result [1] to a much wider range of systems. The aim is to provide insight and checks to amplitude calculations, which often have nothing to compare with. The Schwarzschild and Kerr black holes are treated specifically, the latter constrained to a $\theta = \pi/2$ plane in Boyer-Lindquist coordinates.

We first present scattering angles of non-spinning probes. Scattering angles are calculated for the Schwarzschild metric up to 10PM and for Kerr up to 6PM for non-spinning probes. Higher PM orders can readily be treated, but for brevity we have truncated at the chosen limits. Kerr angles are naturally all order in Kerr spin a. We provide both results encompassed in literature, and PM orders beyond that previously calculated. Literature on the probe-limit was found to be primarily focused on light bending angles, given as an expansion in Kerr spin and G (see [78] with references therein). To general order in Kerr spin, angles are compared to amplitude results of which the probe limit is taken. [76] gives the 1PM scattering angle of two spinning black holes, nicely structured to all orders in black hole spin. We show this structural dependence on Kerr-spin is reproduced for non-spinning probes at higher PM orders. This might give input to higher PM amplitude calculations involving aligned spinning binaries. Amplitude calculations are currently perturbative in spin. All results are consistent with literature [66, 70, 78]. To the best of our knowledge, orders beyond 4PM are not found in literature for non-spinning probes.

Adding spin to the probe is a considerable theoretical difficulty. Nevertheless, the scattering angle formula readily encompasses this complexity, provided the probe stays in a fixed scattering

[20] This holds when spins are aligned and the metric is rotationally symmetric in this scattering plane.

plane. We provide results up to 5PM and $\mathcal{O}(S^2)$ in probe spin, in a Kerr metric with the spins aligned. Higher PM orders can readily be found. Existing literature goes up to 3PM, as a probe limit of the full binary scattering angle of two spinning black holes with aligned spin [70]. Our results are fully consistent with literature [76, 66, 70]. Finally, we assume natural units with $c = 1$, unless otherwise specified.

Section 2 starts by discussing the types of scattering situations to which the results of this thesis apply. A discussion of the application of a Post Minkowksian expansion and its validity follows. Furthermore, all necessary background Hamilton-Jacobi theory underlying the calculation of the scattering angle will be presented and justified, both for non-spinning and spinning test particles.

Section 3 discusses existing scattering angle calculation schemes, including the method of partie finie introduced by Jacques Hadamard in 1924. A more modern method, due to [1], will also be presented. The scattering angle formula presented in this thesis is a generalisation hereof, and the derivation is very similar.

Section 4 derives the scattering angle formula presented in this thesis. The derivation is presented in full detail and parallels with [1] are pointed out.

Section 5 applies the scattering angle formula to the Kerr and Schwarzschild metrics with (non)-spinning probes. Discussions of the results and structure herein is also presented. Validity beyond the considered orders in test particle spin is postulated.

Section 6 considers further possible applications of the formalism. This includes, but is not limited to, the Effective One Body formalism of binary motion and the possibility of a resummed scattering angle valid to all PM orders.

2 Theory of Post-Minkowskian Scattering

This section sets the scene for the scattering angle calculation presented in section 4. First we will present the very general scattering system considered in this thesis and present the general framework of Hamilton-Jacobi theory. Scattering angle formulae derived from Hamilton-Jacobi theory for both scalar and spinning test particles will be presented last, and the general form of the scattering angle discussed. This will provide all necessary setup to do scattering angle computations in the sections below.

2.1 Scattering in Post-Minkowskian expansion

Assumptions presented here are used without further reference in all chapters below.
Setting the scene for the rest of the thesis, we consider a two-body problem consisting of a test particle of mass m orbiting in a plane around a large central body of mass M. The gravitational interaction is assumed small such that a Post-Minkowskian (PM) expansion is possible. Denoting by $U(r)$ the radial 'gravitational potential' defined in eq. (35), one has

$$\left|\frac{U(r)}{p_\infty^2}\right| \ll 1 \tag{29}$$

where p_∞ is the asymptotical momentum of the scattering particle. For typical problems, such as scattering on a Schwarzschild black hole, this boils down to

$$\frac{GM}{c^2 r} \ll 1 \tag{30}$$

where r is a typical radial distance and M is a typical quantity of mass related to the bigger body. Choises of r and M may vary depending on the exact problem at hand. Generally, the Post-Minkowskian expansion can be regarded as an expansion in G.

Denote by $g_{\mu\nu}$ the metric of the bigger body. For the scattering probe to be contained in the plane the metric is necessarily symmetric under rotations herein. It is sufficient to consider coordinates (t, r, ϕ) restricted to this plane, thus letting $g_{\mu\nu}$ have $3 \times 3 = 9$ components. For the Kerr metric, it can only be the $\theta = \pi/2$ plane. For Schwarzschild, any plane passing through $r = 0$ can be chosen. We will set $\theta = \pi/2$ for simplicity.

Further, if the test particle has spin, this is perpendicular to the scattering plane, such that no deformations of the orbit outside this plane occur. For the same reason, if the metric discussed is the Kerr metric, we assume all spins are aligned. See figure 8 for a complete illustration of the scattering.

Further general requirements on the behaviour of the scattering system can be made and only a subset of possible coordinates need consideration. Impose the scattering system be localised, such that coordinates reduce to spherical coordinates when $r \to \infty$. Furthermore, assume $g_{r\mu} = g_{\mu r} = 0$, for $\mu \neq r$ (see footnote 23). Because of rotational symmetry, the metric may be expressed only as a function of r.

The particle follows a path starting at $r = \infty$ with momentum $p_\infty = m\gamma v$, velocity v and Lorentz contraction factor $\gamma = (1 - v^2)^{-1/2}$. The particle approaches the black hole, reaches its

minimum $r = r_m$, whereafter it moves away to $r = \infty$ again. It sweeps out the scattering angle χ during this motion. This text applies to all scattering systems which conform to the above description. In summarised form (see also figure 8),

$$\begin{aligned}
&\text{(Coordinates)} \quad \{t, r, \phi\} \begin{cases} \text{describe plane of rotational symmetry of } g_{\mu\nu} \\ \text{when } r \to \infty,\ t \text{ is time and } \{r, \phi\} \text{ are polar coordinates} \end{cases} \\
&\text{(Scattering metric)} \quad g_{\mu\nu} \begin{cases} g_{\mu\nu} \text{ is restricted to a plane } \{t, r, \phi\} \text{ with rotational symmetry} \\ g_{\mu\nu} = g_{\mu\nu}(r) \text{ is a function only of } r \\ g_{r\mu} = g_{\mu r} = 0, \text{ for } \mu \neq r \\ g_{\mu\nu} \text{ is diagonal when } G \to 0 \end{cases}
\end{aligned} \tag{31}$$

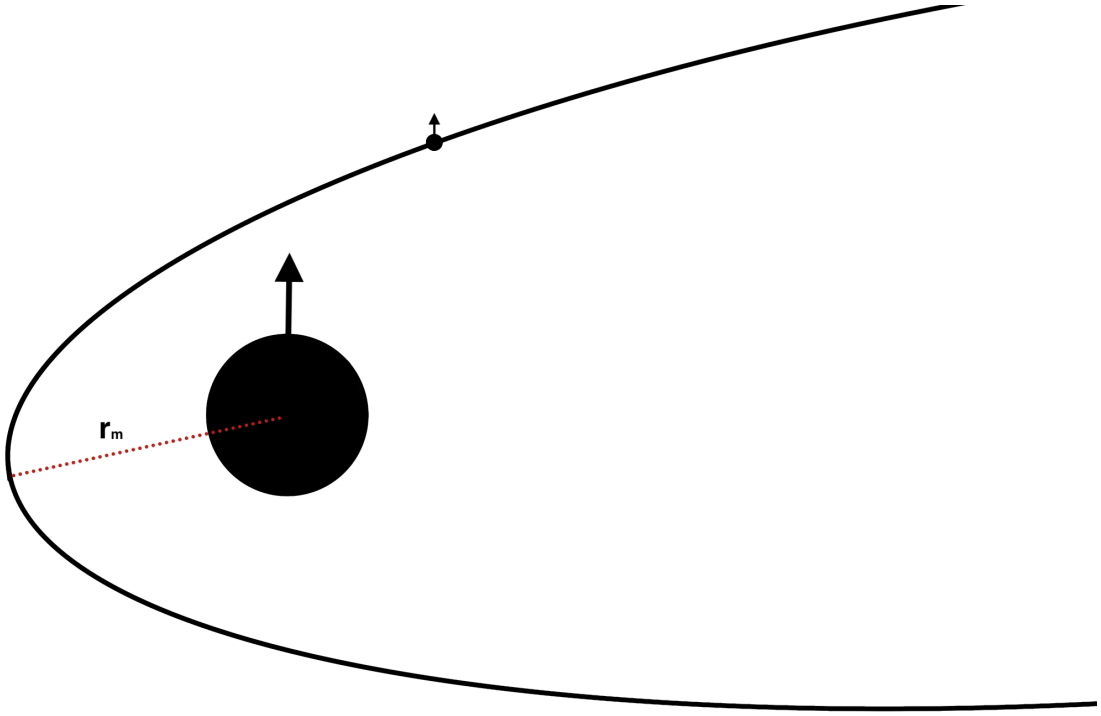

Figure 8: The general scattering setup considered in this thesis. A test particle (small black sphere) follows a planar scattering trajectory around a bigger central object (large black sphere). Both *might* have spin but are not required to (black arrows). Both spins must be perpendicular to the scattering plane, if the particle is to stay herein. *Note that the spins can also be aligned opposite*. The minimum radius $r_m \gg GM$ has also been indicated. The scattering trajectory curve has been exadurated for display purposes. In reality $\chi \ll 1$ following assumptions (29) or (30)

2.2 Hamilton-Jacobi Theory

The scattering angle can be constructed from Hamilton-Jacobi theory, based on ordinary General Relativity. We will present the general principles, starting with a treatment of canonical momenta. Consider the test particle canonical momentum $P_\mu = (-E, p_i)$, with E its energy and p_i the spatial canonical momentum components. It transforms as a one-form, as indicated by the subscript index. Canonical momentum reduces to physical momentum $\mathbf{p} = m\mathbf{v}$ only in flat spacetime. Writing out the conserved and coordinate-independent quantity P^2 yields the Hamilton-Jacobi equation for test particles in GR

$$P_\mu P_\nu g^{\mu\nu} = -m^2 \tag{32}$$

If translational symmetries are present, components of P are conserved by Noether's theorem. This gives them physical interpretation. Consider the general metric described in section 2. It has time-translation symmetry and rotational symmetry in the ϕ direction, and thus

$$P_0 = -E, \quad P_\phi = L \tag{33}$$

for an asymptotically flat metric. $L = \sqrt{L_{\mu\nu}L^{\mu\nu}}$ is the invariant angular momentum and $E = m\gamma$ the energy of the test particle with $\gamma = (1 - v^2)^{-1/2}$ its asymptotical Lorentz contraction factor and v its velocity at $r \to \infty$. We can readily set $p_\theta = 0$, since the particle is confined to the $\theta = \pi/2$ plane and the Hamiltonian therefore necessarily is independent of θ.

P_μ may then be written as

$$P_\mu = (-E, p_r(r), L) \tag{34}$$

where p_r is the canonical radial momentum only dependent on r. Solving for p_r^2 and writing the result in G-(in)dependent parts T and U yields

$$p_r^2(r; b, ...) = T(r; b, ..) - U(r; b, ..) \tag{35}$$

introducing the asymptotical impact parameter $b \equiv J/p_\infty$ as measured at infinity where b is the impact parameter measured at $r \to \infty$ and p_∞ is the asymptotical momentum of the particle at $r \to \infty$. The semi-colon separates coordinate dependency of p_r from dependencies on b and any other parameters in the theory (indicated by dots ...). Solving eq. (32) for p_r often leaves the natural structure $p_r = \sqrt{\cdots}$. Therefore considering p_r^2 is often simpler.

As we will see, the scattering angle can be written as an integral over p_r, rendering it a vital component in scattering angle computations.

2.3 Scattering angle from Hamilton-Jacobi Theory

The scattering angle of any, scalar or spinning, test particle can be written as

$$\chi/2 = \int_{r_m}^{\infty} dr \frac{d\phi}{dr} \tag{36}$$

where r_m is the distance of closest approach. If the Hamiltonian of the system H is quadratic in canonical momentum p_r, r_m may be found from $p_r(r_m) = 0$. The requirements of section 2.1

assure this to be the case.

The appearance r_m in eq. (36) on the lower integration boundary is only superficial, since scattering angles don't generally depend on this quantity. State-of-the-art methods for calculating scattering test particle scattering angles will be treated in 3. It is the general motivation of this work, to show how the dependence r_m cancels, expressing χ as simple integrals with well-defined boundaries. The techinque will be very similar to that presented in [1], which is covered in section 3.

2.3.1 Scalar probes

Considering scalar probes first, the scattering angle can be readily constructed from Hamilton-Jacobi theory as presented in [75]. One may construct the *abbreviated action* S_0 for the scattering test particle [21]

$$S_0 = \int_{\mathcal{P}} p_i \, dq_i \tag{37}$$

where p_i, q_i are canonical 3-momenta and position-coordinates of the test particle and indexes i are summed over. The integral runs over a specific paticle-path $\mathcal{P}$. Similarly to Hamiltons principle with action $S = \int_{t_i}^{t_f} L$, Maupertui's principle states

$$\delta S_0 = 0 \tag{38}$$

around the physical path of the particle. Varying S_0 with respect to q_i and p_i as independent variables, as with the modified Hamiltons Principle [22], obtains the shape of the path.

For the scattering system as described in the introduction of 2, the particle trajectory can be written $\mathcal{P} \in \{r = \infty \to r = r_m \to r = \infty\}$, which is symmetric around $r = r_m$ due to rotational symmetry. Furthermore rotational symmetry dictates $p_i = (p_r, p_\phi) = (p_r, L)$ following eq. (34). S_0 can thus be written, considering only half the trajectory, ie. let $\mathcal{P} \in \{r = r_m \to \infty\}$,

$$S_0 = L\chi/2 + \int_{r_m}^{\infty} dr \, p_r \tag{39}$$

implicitly restricted to the actual path followed by the particle by considering L and p_r as the actual angular and radial momenta. Differentiate with respect to $p_\phi = L$ and impose $\delta S_0 = 0$ to obtain

$$\chi/2 = -\frac{\partial}{\partial L}\left(\int_{r_m}^{\infty} p_r \, dr\right) - \pi/2 \qquad (\text{ where } p_r(r_m) = 0 \ ) \tag{40}$$

where $\pi/2$ has been subtracted by convention to produce $\chi = 0$ when no interactions are present. r_m may be found by solving

$$\dot{r}|_{r=r_m} = \frac{\partial H}{\partial p_r} = 0 \Rightarrow p_r(r_m) = 0 \tag{41}$$

marking the periapsis. $H = E$ is the hamiltonian of the system, found from eq. (32). The implication that $p_r(r_m)$ describes the periapsis imposes the metric structure $g_{r\mu} = g_{\mu r} = 0$, for $\mu \neq r$, discussed in section 2 [23]

[21] The abbreviated action may be defined for any system with canonical variables and momenta {q,p}

[22] See "theoretical mechanics of particles and continua" page 177-178

[23] Note that the Hamiltonian H in eq. (41), is just the energy E because $g_{\mu\nu}$, and thus the Lagrangian, carries

Historically the $\frac{\partial}{\partial L}$ differentiation in eq. (40) has been moved inside integration by use of the Leibnitz-integration rule. This is because $\int_{r_m}^{\infty} dr\, p_r$ diverges. We will do the same, writing

$$\chi/2 = \int_{r_m}^{\infty} dr \frac{d\phi}{dr} - \pi/2 = -\int_{r_m}^{\infty} dr \frac{h(r)}{p_r} - \pi/2 \tag{43}$$

where $h(r)$ is defined from $h(r) \equiv p_r \frac{d\phi}{dr}$. $h(r)$ is invariant under radial coordinate transformations. For scalar probes in the Kerr metric written with Boyer-Lindquist coordinates, it is

$$h(r) = -\frac{r(lr - 2G\kappa M)}{\left(a^2 + r(r - 2GM)\right)^2} \tag{44}$$

As another important example, $h(r) = -\frac{L}{r^2}$ in the Schwarzschild metric in isotropic coordinates. The introduction of $h(r)$ hints at a derivative representation of the scattering angle. The introduction of $h(r)$ thus carries information beyond just being a simple rewriting. This is reflected in its benine, non-diverging behaviour in the scattering domain $r \in [r_m, \infty[$. The functional behaviour of $h(r)$ is very important for the viability of the scattering angle formula.

2.3.2 Spinning probe

Remarkably, the structure of eq. (55) can also be recovered for spinning test particles, with a suitable function $h(r)$ appropriate for spin. This section derives its functional form and discusses Hamilton-Jacobi theory with spin. We consider a test particle with spin S treated perturbatively up to $\mathcal{O}(S^2)$. Higher orders can also be dealt with in a similar fashion.

The Hamilton-Jacobi theory with spin presented here is merely a review of an unpublished note by Justin Vines [24]. It will be referred to simply as "Vines". We will see how the calculation above generalises by discussing the identification of canonical momentum and the subsequent construction of the scattering angle for spinning probes.

Suppose we have a spinning probe of mass m and spin S [25] on a Kerr background with total angular momentum J, *including* spin. We will treat the spin pertubatively, yielding expressions up to $\mathcal{O}(S^2)$. Higher orders can be dealt with in a similar fashion. Before we do actual expansions in S, the Hamilton-Jacobi equation in Boyer-Lindquist coordinates, written in terms of canonical momentum $p_\mu = (p_t, p_\phi, p_r)$ is [eq. (244), Vines]

$$\tilde{m}^2 = -p^2 = -g^{\mu\nu} p_\mu p_\nu = \frac{\left[(r^2 + a^2)p_t + a p_\phi\right]^2}{r^2 \Delta} - \frac{(p_\phi + a p_t)^2}{r^2} - \frac{\Delta}{r^2} p_r^2 \tag{45}$$

valid to all orders in S. It has the exact same structure as the result without spin. Note the appearance of what Vines calls "the dynamical mass" $\tilde{m}$. We will talk about this in a moment.

---

no time-dependence. The Hamilton-Jacobi equation (32) provides $H = E$ as a function of p_r. Eq. (41) is satisfied when

$$\dot{r} = \frac{\partial H}{\partial p_r} \propto p_r \tag{42}$$

which is the case for $H = H(p_r^2)$, meaning (32) only contains p_r^2 terms. This is the case when $g_{\mu r} = g_{r\mu} = 0$ for $\mu \neq r$. Denote the periapsis by $r = r_m$. Here $\dot{r}|_{r=r_m} = 0$. Only when eq. (42) holds, does this imply $\dot{r}|_{r=r_m} = 0 \Rightarrow p_r(r = r_m) = 0$.

[24] Accessed from Justin Vines through personal correspondence with Andrés Luna

[25] S/m is the associated Kerr spin parameter, were the test particle a Kerr black hole

Apart from this difference with the non-spinning case, canonical momenta p_t and p_ϕ are no longer just test particle energy and angular momentum but contain spin as well. They can be determined by constructing energy and angular as Dixon constants of motion, involving both p_t, p_ϕ and the Killing vectors t^μ, ϕ^μ

$$\begin{aligned} E &= -p_a t^a - \frac{1}{2} S^{ab} \nabla_a t_b = -p_t + \frac{GMS}{r^3 \tilde{m}} (p_\phi + a p_t) \\ J &= p_a \phi^a + \frac{1}{2} S^{ab} \nabla_a \phi_b = p_\phi + \frac{S}{\tilde{m}} \left[-p_t + \frac{GMa}{r^3} (p_\phi + a p_t) \right] \end{aligned} \tag{46}$$

again valid to all orders in S. Equation (46) can be solved for p_t and p_ϕ as

$$p_t = -\left(E - \frac{GMS}{r^3 \tilde{m}} (J - aE) \right) \left[1 - \frac{GMS^2}{r^3 \tilde{m}^2} \right]^{-1} \tag{47}$$

$$p_\phi = \left(J - \frac{S}{\tilde{m}} \left[E + \frac{GMa}{r^3} (J - aE) \right] \right) \left[1 - \frac{GMS^2}{r^3 \tilde{m}^2} \right]^{-1} \tag{48}$$

Coming back to the dynamical mass, it is listed up to S^3 [eq. (250), Vines]

$$\tilde{m}^2 - m^2 = -\frac{GMS^2}{r^3} \left[1 + 3 \frac{(p_\phi + a p_t)^2}{r^2 \tilde{m}^2} \right] - \frac{GMS^3}{r^5 m} \left[a + \frac{p_\phi + a p_t}{\tilde{m}^2} \left(2 p_t + 5a \frac{p_\phi + a p_t}{r^2} \right) \right] + \mathcal{O}(S^4) \tag{49}$$

On the RHS $\tilde{m}$ only gives $\mathcal{O}(S^4)$ corrections, and one may thus let $\tilde{m} \to m$. Eqs. (47), (48) and (49) determine p_ϕ and p_t in terms of m.

These equations can be solved up to $\mathcal{O}(S^2)$ as follows. [26] Note that $\tilde{m} = m + \mathcal{O}(S^2)$ generally. Up to order S^2, p_t and p_ϕ may thus be written with $\tilde{m} = m$. Expanding to S^2 yields

$$p_t \textbf{ and } p_\phi \textbf{ up to } \mathcal{O}(S^2)\textbf{, all orders in } G$$

$$p_t = -e + \frac{GMS(J - ae)}{mr^3} - \frac{eGMS^2}{m^2 r^3} + \mathcal{O}\left(S^3\right) \tag{50a}$$

$$p_\phi = J - \frac{S\left(\frac{aGM(J-ae)}{r^3} + e \right)}{m} + \frac{GJMS^2}{m^2 r^3} + \mathcal{O}\left(S^3\right) \tag{50b}$$

$\tilde{m}$ however contains p_t and p_ϕ itself. However, since it goes like $\tilde{m} = m + GS^2[...] + \mathcal{O}(S^3)$ with S-independent content in the brackets, $S \to 0$ limits of p_t and p_ϕ can be inserted to produce simply

$$\tilde{m} \textbf{ up to } \mathcal{O}(S^2)\textbf{, all orders in } G$$

$$\tilde{m} = m - \frac{GMS^2 \left(\frac{3(J-ae)^2}{m^2 r^2} + 1 \right)}{2mr^3} + O\left(S^3\right) \tag{51}$$

after expanding the square root appearing in eq. (49).

Having defined the Hamilton-Jacobi equation equivalent for spinning test bodies, we can now construct the scattering angle. Naturally, it is still given by eq. (36). The integrand $\frac{d\phi}{dr}$ can be

[26] This is sufficient for calculating the scattering angle up to order S^2, since p_t, p_ϕ and $\tilde{m}$ all appear linear or quadratic in eq. (45)

written like [Vines, eq. (251)]

$$\dot{x}^{\mu} = \frac{1}{\tilde{m}} g^{\mu\nu} p_{\nu} + \mathcal{O}(S^3) \tag{52}$$

which yields $\frac{d\phi}{dr}$ written in Boyer-Lindquist coordinates

$$\frac{d\phi}{dr} = \frac{\dot{\phi}}{\dot{r}} = \frac{r^2 p_{\phi} - 2GMr(p_{\phi} - a p_t)}{\Delta^2 p_r} + \mathcal{O}(S^3) \tag{53}$$

Importantly, we see that the denominator is proportional to p_r, exactly like eq. (43). We can thus write $\chi/2 = \int_{r_m}^{\infty} dr \frac{d\phi}{dr} = -\int_{r_m}^{\infty} dr \frac{h(r)}{p_r}$ exactly like eq. (43), and identify the function $h(r)$ for spinning particles as

$$h(r) = -\frac{r(lr - 2G\kappa M)}{\left(a^2 + r(r-2GM)\right)^2} + \frac{aG\kappa MS}{mr\left(a^2 + r(r-2GM)\right)^2} - \frac{G\kappa M(r-2GM)S^2}{m^2 r^2 \left(a^2 + r(r-2GM)\right)^2} + \mathcal{O}(S^3) \tag{54}$$

written with Boyer-Lindquist coordinates. Note that the spin-parts of $h(r)$ do not diverge in the domain $r \in [r_m, \infty[$, exactly like the part without spin. Furthermore eq. (54) reduces trivially to eq. (44) when $S \to 0$.

Sections (2.3.1) and (2.3.2), show that the scattering angle for both spinning and scalar test particles can be written like

$$\chi/2 = \int_{r_m}^{\infty} dr \frac{d\phi}{dr} - \pi/2 = -\int_{r_m}^{\infty} dr \frac{h(r)}{p_r} - \pi/2 \tag{55}$$

at least up to second order in test particle spin S. $h(r)$ is a metric dependent function, invariant under radial coordinate transformations. Eq. (54) gives its specific form for the Kerr metric up to $\mathcal{O}(S^2)$. An at first glance trivial result, in fact anticipates a first order derivative representation of χ, like the one in eq. (40). What this derivative representation should be in the case of spin is still unclear. Remarkably, $h(r)$ is well-behaved at least up to $\mathcal{O}(S^2)$, rendering an at first trivial rewriting into a useful tool.

The scattering angle formula derived in section 4 assumes only χ to be written like (55) and $h(r)$ to obey the general conditions of (81). It renders the scattering angle in an order-by-order form, writing $\chi = \sum_{n=1}^{\infty} \chi_n$ as an expansion in Newtons gravitational constant G, a socalled Post-Minkoswkian (PM) expansion. The formula is valid to all orders in G. Due to the very general constraints on $h(r)$, the calculation might generalise to situations beyond those considered in this thesis, conceivably related to other fields of Physics.

3 Existing scattering angle calculation schemes

Having established the necessary theory, we look for ways to evaluate integrals of the form (55). Before presenting out own method, we will discuss other, existing methods. First the traditional Hadamard Regularisation is treated. Then a method approriate for isotropic amplitude calculations is presented. Our derivation, given in section (4) is a direct generalisation of this last method.

3.1 Partie Finie methods presented by Damour

A common problem in physics is that of evaluating improper integrals. As an example the Feynman propagator for a photon in QED includes a regulating $i\epsilon$ term where at the end of the calculation $\epsilon \to 0$.

One particular kind, Hadamard regularisation, may be used to evaluate PM expanded scattering angles. The Hadamard partie finie method regularises divergent integrals, much like the Cauchy principal value [79, 80]. First introduced by Hadamard in 1923 [79], it applies to integrals of the form

$$\int_a^b dx \, \frac{A(x)}{(b-x)^{p+1/2}} \tag{56}$$

where p is a positive integer. $A(x)$ is analytical and admits p derivatives of x in $x = b$. Assume also that $A(x)$ obeys the Lipschitz condition $|A(x) - A(b)| < L|x - b|$ for some constant L and all $x \in \mathbb{R}$.

Such an expression is meaningless, owing to the $p + 1/2$ order pole at $x = b$. Denote the Hadamard partie finie as Pf[...]. For $A(x) = 1$, we may define the Hadamard partie finie as

$$Pf\left[\int_a^b dx \, \frac{1}{(b-x)^{p+1/2}}\right] \equiv \frac{1}{p-1/2}\frac{1}{(b-a)^{p-1/2}} \tag{57}$$

ie. simply throwing away the divergent upper limit, only keeping the lower limit. Note in passing that the $p = 0$ integral is an ordinary improper integral evaluated by $\lim_{y\to b^+} \int_a^y dx \, \frac{1}{(b-x)^{1/2}} = -2\sqrt{a}$. We will see how "throwing away the divergent terms" can be cast into a formal form with some examples below.

To see the procedure, consider general $A(x)$ satisfying the Lebesque condition with $p = 1$. We want to construct a way to get rid of the upper limit, which is consistent with (57). Write $A(x) = A(x) - A(b) + A(b)$. We then find

$$\int_a^b dx \, \frac{A(x)}{(b-x)^{3/2}} = \int_a^b dx \, \frac{[A(x) - A(b)] + A(b)}{(b-x)^{3/2}} \tag{58}$$

The integral of the term in brackets is a well-defined improper integral, because $|A(x) - A(b)| < L|x - b|$. The second $A(b)$ integral may be calculated readily from (57) with $p = 1$,

$$Pf\left[\int_a^b dx \, \frac{A(x)}{(b-x)^{3/2}}\right] = \lim_{y\to b}\left[\int_a^y dx \, \frac{A(x) - A(b)}{(b-x)^{3/2}}\right] + Pf\left[\int_a^b dx \, \frac{A(b)}{(b-x)^{3/2}}\right] \tag{59}$$

Setting $A = 1$ in eq. (59), the first integral is trivially 0 and the procedure is by definition

equivalent to eq. (57).

The formalism can be extended to general $p > 1$ in eq. (56). We write

$$A(x) = [A(x) - \mathcal{T}_{p-1}[A(x)]] + \mathcal{T}_{p-1}[A(x)] \tag{60}$$

where $\mathcal{T}_{p-1}$ denotes the $p-1$'th order taylor expansion about $x = b$. For reference

$$\mathcal{T}_{p-1}[A(x)] = \sum_{n=0}^{p-1} \frac{A^{(p-1)}(b)(b-x)^n}{n!} \tag{61}$$

Assuming $A(x)$ is analytical, the term in brackets goes at least like $(b-x)^p$. Therefore, substituting eq. (60) in eq. (56)

$$\int_a^b dx\, \frac{A(x)}{(b-x)^{p+1/2}} = \int_a^b \frac{A(x) - \mathcal{T}_{p-1}[A(x)]}{(b-x)^{p+1/2}}\, dx + \int_a^b \frac{\mathcal{T}_{p-1}[A(x)]}{(b-x)^{p+1/2}}\, dx \tag{62}$$

the first integral goes like $(b-x)^q$ with $q \geqslant -1/2$. The first integral is thus an ordinary improper integral, calculated by $\int_a^b dx\, \frac{A(x)-\mathcal{T}_{p-1}[A(x)]}{(b-x)^{p+1/2}} = \lim_{y\to b}\left[\int_a^b dx \frac{A(x)-\mathcal{T}_{p-1}[A(x)]}{(b-x)^{p+1/2}}\right]$. The second integral consists only of terms $\sim \frac{1}{(b-x)^{q+1/2}}$ for integer $-1 \leqslant q \leqslant p$ and can be calculated from eq. (57). We may thus write

$$Pf\left[\int_a^b dx\, \frac{A(x)}{(b-x)^{p+1/2}}\right] = \lim_{y\to b}\left[\int_a^y dx\, \frac{A(x) - \mathcal{T}_{p-1}[A(x)]}{(b-x)^{p+1/2}}\right] + Pf\left[\int_a^b dx\, \frac{\mathcal{T}_{p-1}[A(x)]}{(b-x)^{p+1/2}}\right] \tag{63}$$

Note that we could have written eq. (57) as

$$Pf\left[\int_a^b dx\, \frac{1}{(b-x)^{p+1/2}}\right] \equiv \lim_{y\to b}\int_a^y \frac{1}{(b-x)^{p+1/2}}\, dx - \frac{1}{p-1/2}\frac{1}{(b-y)^{p-1/2}} \tag{64}$$

where the last term absorbs all divergence when taking the limit of y in the first integral. We can thus rewrite eq. (63) as

$$\begin{aligned} Pf\left[\int_a^b dx\, \frac{A(x)}{(b-x)^{p+1/2}}\right] &= \lim_{y\to b}\int_a^y \frac{A(x) - \mathcal{T}_{p-1}[A(x)]}{(b-x)^{p+1/2}}\, dx + \int_a^y \frac{\mathcal{T}_{p-1}[A(x)]}{(b-x)^{p+1/2}}\, dx - \frac{B(y)}{(b-y)^{p-1/2}} \\ &= \lim_{y\to b}\int_a^y \frac{A(x)}{(b-x)^{p+1/2}}\, dx - \frac{B(y)}{(b-y)^{p-1/2}} \end{aligned} \tag{65}$$

with $B(x) = \frac{A(b)}{(p-1/2)(b-x)^{p-1/2}} - \frac{A'(b)}{(p-3/2)(b-x)^{p-3/2}} + \cdots + \frac{(-1)^{p-1}}{(p-1)!}\frac{A^{(p-1)}(b)}{\frac{1}{2}(b-x)^{1/2}}$. The function of $B(x)$ is just to ensure divergencies are cancelled.

A similar method may be used to find partie finie expressions for other types of functions [79], including $\int_a^b \frac{A(x)}{(b-x)^q}$ where q is integer. We will not need such expressions in the present.

Although being mathematically interpreted as a memoprphic continuation of a convergent integral [81], the Hadamard partie finie method can be considered an arbitrary way of obtaining a finite limit of an otherwise ill-defined integral.

A particular use hereof, the partie finie of a scattering angle integral turns out to reproduce

the correct result [82]. Damour and Schaefer considered integrals of the type

$$\chi = \partial_L \int_{r_m}^{\infty} dr\, p_r \tag{66}$$

in a Post Newtonian expansion. Define $\epsilon = v/c$ and expand perturbatively in ϵ. The integral above takes the form

$$\int_{r_m}^{\infty} dr \sqrt{A(r) + \frac{2B(r)}{r} + \frac{C(r)}{r^2} + \epsilon \sum_{n=0}^{\infty} \frac{D_n(r)}{r^{n+2}}} \tag{67}$$

in isotropic coordinates, with A, B, C and D being functions of r determined from the dynamics of the theory. $r_m = r_m(\epsilon)$ is a root of the full theory, with ϵ denoting the dependence on velocity.

Formally analytically continuing the integral to the complex plane and contour integrating on contour $\mathcal{C}$ away from r_m, one may directly expand this integral in powers of ϵ which yields terms like

$$\chi \sim \int_{r_m(0)}^{\infty} \frac{dr}{r^m} \left(A + \frac{2B}{r} + \frac{C}{r^2} \right)^{1/2-q} \tag{68}$$

Factorizing $A + \frac{2B}{r} + \frac{C}{r^2} = r^2 \left([r - r_m(0)][r - r^{(-)}] \right)$ in roots $r_m(0)$ and the smaller root $r^{(-)}$,

$$\chi \sim \int_{r_m(0)}^{\infty} \frac{dr}{r^{m+2q-1}} [r - r_m(0)]^{1/2-q} \cdot [r - r^{(-)}]^{1/2-q} \tag{69}$$

we see that an identical expression to eq. (56) arises. Comparing this partie finie result with that of exact contour integration around a contour $\mathcal{C}$ following $[r_m(0), \infty]$ along the real axis and one circular integral around $r = r_m(0)$, indeed shows that the partie finie of eq. (69) is equal to the desired scattering angle.

Similarly, the partie finie method also yields the correct scattering angle in the Post-Minkowskian expansion [83].

3.2 Amplitude calculations of scattering angles - a related problem

In the case of a binary system without spin, a closed form expression can be found for the scattering angle. This section presents such an angle, as found by [1]. The approach is extremely similar to our derivation below, so we will not go into detail, save present some points of interest.

We go back to section 1.2.7, and consider a binary of arbitrary masses m_1, m_2, both without spin, in the center of mass (CM) coordinate system. As discussed there, the scattering angle of such a setup can be found by considering an amplitude approach to General Relativity.

Only a short review will be given here. For more details, see [67, 66, 1]. One can model the interaction of a non-spinning particle in a metric from the Einstein-Hilbert action coupled to a massive scalar field ϕ, eq. (28).

From such a formalism, a classical intuitive way of describing the scattering may be found. One may construct the associated position-space Hamiltonian as

$$H(p, r) = \sqrt{p^2 + m_1^2} + \sqrt{p^2 + m_2^2} + V(p, r) \tag{70}$$

where p is CM momentum and $V(p,r)$ is the potential describing gravitational interaction between the bodies. The potential $V(p,r)$ can be expressed in terms of the position-space $\mathcal{M}(p,r)$ from the Lippmann-Schwinger equation,

$$\mathcal{M}(p,p') = V(p,p') + \int \frac{d^3\mathbf{k}}{(2\pi)^3 4E_1(p)E_2(p)} \frac{V(p',k)\mathcal{M}(k,p)}{E_p - E_k} \tag{71}$$

Provided $V(p,r)$ is quadratic in momentum p, eq. (70) can be solved for p^2 to produce a remarkable result known as the *impetus equation*,

$$p^2 = p_\infty^2 - V_{eff}(r), \quad V_{eff}(r) \equiv 2E_{p_\infty}\varepsilon(p_\infty)\widetilde{\mathcal{M}}(p_\infty, r) \tag{72a}$$

$$\Rightarrow \quad p_r^2 = p_\infty^2 - \frac{L^2}{r^2} - V_{eff}(r) \tag{72b}$$

This is at least valid up to 3PM [3]. L is the total angular momentum of the system, p_r is the radial momentum in center-of-mass coordinates, $E_{p_\infty} = E$ is the total energy of the system, $\widetilde{\mathcal{M}} = \frac{\mathcal{M}}{4E_1(p)E_2(p)}$ is the non-relativistically normalised scattering amplitude and $\varepsilon(p) \equiv \frac{E_1(p)E_2(p)}{E_p^2}$.

Equation (164) is completely identical to the momentum relation of a classical test particle orbiting in some radial potential $V_{eff}(r)$. The scattering angle of the binary can thus be found identically by eq. (40)

$$\chi/2 = -\partial_L \int_{r_m}^{\infty} dr\, p_r \tag{73}$$

where $p_r^2 = p^2 - \frac{L^2}{r^2}$ and r is the distance between the binary objects.

The construction above is only valid for non-spinning objects, ie. black holes. Introducing spin, the fourier transformed amplitude $\mathcal{M}(p,r)$ becomes dependent on the *vector* $\mathbf{r}$ [66]. Thus the potential also carries vector dependence. The potential is no longer rotationally symmetric, and the radial momentum can no longer be isolated directly from (70).

[1] provides a general way of evaluating the integral (73) provided eq. (72b) holds. This thesis generalises the argument to a more general structure of p_r. We will therefore refrain from going into detail of the derivation in [1], suffice to provide the final result and its applications. The scattering angle eq. (73) under the condition (72b) can be written [1]

$$\chi = \sum_{n=1}^{\infty} \int_0^{\infty} du \left(\frac{d}{du^2}\right)^n \frac{2b}{r^2} \frac{V_{eff}^n(r) r^{2n}}{n! p_\infty^{2n}}, \qquad r^2 = u^2 + b^2 \tag{74}$$

where b is the gauge-invariant impact parameter of the system. This form shows explicitly that the scattering angle is independent of r_m. The scattring angle may be calculated perturbatively in G such that it acquires the form $\chi = \sum_{n=1}^{\infty} \chi_n G^n$.

As a special case, consider a potential of the form $V_{eff} = \sum_{n=1}^{\infty} \frac{f_n G_n}{r^n}$. The scattering angle up to 2PM becomes

$$\chi = \frac{b}{p_\infty^2} \int_0^{\infty} du \frac{\partial_r V_{eff}(r)}{r} \tag{75}$$

using $\left(\frac{d}{du^2}\right) V_{eff}(\sqrt{u^2+b^2}) = \frac{1}{r}\partial_r V_{eff}(r)$. Remarkably the 2PM correction from the $n = 2$ term in eq. (74) drops out. As noted in [1] this is the Bohm formula from [84] for the classical, 1PM, bending angle around static massive sources in the non-relativisitic limit. Notably the result is

here shown explicitly to hold up to 2PM and be fully relativistic in nature, facts only previously noticed by accident.

As an example of the special case of two binary non-spinning black holes, one has up to 2PM in isotropic coordinates [3]

$$f_1 = 2(2\gamma^2 - 1)\frac{\mu^2 M}{E}, \qquad f_2 = \frac{3(5\gamma^2 - 1)}{2}\frac{\mu^2 M}{E} \tag{76}$$

where $M = m_1 + m_2$ is the sum of the binary masses, E is the total energy of the system and $\mu = \frac{m_1 m_2}{M}$ is the reduced mass. The appropriate scattering angle from (75) is

$$\chi = 2(2\gamma^2 - 1)\frac{\mu^2 M}{E}\frac{MG}{bp_\infty^2} + \frac{3(5\gamma^2 - 1)\pi}{4}\frac{\mu^2 M}{E}\frac{M^2 G^2}{b^2 p_\infty^2} + \mathcal{O}(G^3) \tag{77}$$

The probe-limit $m_1 \gg m_2 \equiv m \Rightarrow m_1 \to M$, $E \to M$ and $\mu \to m$ recovers the Schwarzschild scattering angle of a probe of mass m orbiting a Schwarzschild black hole of mass M.

We have presented a general formalism for calculating binary scattering angles in isotropic coordinates, where p_r is of some specific form. Equation (73) is identical in structure to a test-particle scattering angle eq. (40). However, for the test-particle case, assumptions of isotropic coordinates do not generally hold. The Kerr metric cannot be brought on isotropic form. Neither can we deal with spinning test particles, because they do not follow eq. (40).

We lift these restrictions below. Considering integrals of the type (55), we can handle both the amplitude calculations as described above *and* testparticle calculations in arbitrary rotationally symmetric metrics. However, we will limit the discussion to test particle angles throughout the thesis.

4 Scattering angle of test particle in arbitrary rotationally symmetric metric

This section derives in full the main result of this thesis: The test particle scattering angle of a rotationally symmetric metric, both for spinning and non-spinning probes. It applies to all situations described in section 2.1. We generalise [1]. The procedure can be summarised as follows:

We work with scattering angles written as eq. (55). Our general goal is to cancel the r_m dependence in a general way, assuming a PM approximation.

- Write p_r like eq. (35) in special coordinates, such that eq. (55) takes a specific form.

- Assume a PM framework, meaning (29) holds. This allows a binomial expansion in potential $U(r)$ from eq. (35).

- The r_m dependence drops out after using $p_r(r_m) = 0$, and rewriting everything as a Taylor-series.

One finds the scattering angle expressed as a sum without any explicit r_m dependence.

The scattering angle of a (spinning) test body orbiting a scattering centre in some metric $g_{\mu\nu}$ is naturally written in terms of canonical radial momentum, as seen in eq. (55). We can choose to write this momentum in *normal coordinates*, meaning that

$$p_r^2 = T(r) - U(r,b), \quad \text{where} \quad T(r) = p_\infty^2 - \frac{L^2}{r^2} \tag{78}$$

and U contains all G-dependence. $U(r,b)$ will generally depend on r, impact parameter $b = \frac{L}{p_\infty}$ and any other quantities related to the metric and test particle and is an analogous to the potential presented in section 3. The defining property of normal coordinates is they reduce to flat spherical coordinates when $G \to 0$

$$\{t, r, \phi\} \text{ are normal if } g_{\mu\nu} \to \begin{pmatrix} -1 & 0 & 0 \\ 0 & 1 & 0 \\ 0 & 0 & r^2 \end{pmatrix} \text{ when } G \to 0 \tag{79}$$

They can be found for any system, by setting $G \to 0$ and transforming the resulting necessarily flat metric to Minkowskian form. An example of the construction of such coordinates will be detailed in section 5. [27]

As described in section 2, in normal coordinates, the scattering angle for (non)-spinning probes can be written on the form

$$\chi/2 = \int_{r_m}^{\infty} dr \frac{d\phi}{dr} - \pi/2 = -\int_{r_m}^{\infty} dr \frac{h(r)}{p_r} - \pi/2, \qquad \frac{d\phi}{dr} \equiv -\frac{h(r)}{p_r} \tag{80}$$

where $h(r)$ is defined from $\frac{d\phi}{dr}$. It is specific to the metric, but invariant under radial coordinate transformations.

The scattering angle calculation presented below is of very general applicability and very similar to [1]. We will consider a scattering angle as in eq. (80), and not use any specific form of $h(r)$, save require

$$\begin{aligned} &h(r) \text{ is analytical for } r \in [r_m, \infty[\\ &h(r) \to 1/r \text{ when } r \to \infty \end{aligned} \tag{81}$$

The final result may therefore conceivably be applicable to other systems beyond a spinning probe in the Kerr metric, whatever they may be.

We start by considering eq. (80) in normal coordinates of eq. (78). It can be written like

$$\chi/2 = \int_{r_m}^{\infty} dr \frac{h(r)}{p_\infty} \left(1 - b^2/r^2 - \frac{U(r,b)}{p_\infty^2}\right)^{-1/2} \tag{82}$$

[27] Note that $U(r,b)/p_\infty \ll 1$ assumed throughout. This expansion gains an explicit interpretation as being "Post Minkowskian", because U is interpreted as a small correction to the Minkowskian radial momentum $p_r^2 = p_\infty^2 - \frac{L^2}{r^2}$.

We may now rewrite b^2/r^2 by imposing $p_r(r_m) = 0$,

$$p_r^2(r_m)/r_m^2 = 1 - b^2/r_m^2 - U(r_m, b)/p_\infty^2 = 0 \quad \Rightarrow \quad b^2/r^2 = r_m^2/r^2 - \frac{r_m^2}{r^2} U(r_m, b)/p_\infty^2 \tag{83}$$

which inserted in eq. (82),

$$\chi/2 = \int_{r_m}^{\infty} dr \frac{h(r)}{p_\infty} \left(1 - r_m^2/r^2 + \frac{r_m^2}{r^2}\frac{U(r_m, b)}{p_\infty^2} - \frac{U(r, b)}{p_\infty^2}\right)^{-1/2} \tag{84a}$$

$$= -\int_{r_m}^{\infty} dr \frac{h(r)}{p_\infty} \left(1 - r_m^2/r^2 - W(r, b)\right)^{-1/2} - \pi/2 \tag{84b}$$

$$W(r, b) = \frac{1}{p_\infty^2}[U(r, b) - \frac{r_m^2}{r^2} U(r_m, b)] \tag{84c}$$

Introducing integration variable u through $r^2 = u^2 + r_m^2 \quad \Rightarrow \quad rdr = udu$, one finds

$$\chi/2 = -\int_0^{\infty} du \frac{r}{u}\frac{h(r)}{p_\infty} \left(1 - r_m^2/r^2 - W(r, b)\right)^{-1/2} - \pi/2 = -\int_0^{\infty} du \frac{h(r)}{p_\infty} \left(1 - \frac{r^2}{u^2} W(r, b)\right)^{-1/2} - \pi/2 \tag{85}$$

after rearranging expresions slightly. This procedure removes the r_m lower integration limit, however r_m dependence still apparently persists through the relation of r with u. If we now assume a scattering regime where $|\frac{U(r,b)}{p_\infty^2}| \ll 1 \Rightarrow -1 < \frac{r^2}{u^2} W(r, b) < 1$ [28], we may consider the binomial expansion

$$(1 + x)^{-1/2} = 1 + \sum_{n=0}^{\infty} \binom{-1/2}{n+1} x^{n+1} = 1 + \sum_{n=0}^{\infty} \frac{(-1)^{n+1}(2n+1)!!}{2^{n+1}(n+1)!} x^{n+1} \tag{86}$$

of eq. (85) with $x = -\frac{r^2}{u^2} W(r, b)$,

$$\chi/2 = F_0(r_m) - \pi/2 - \sum_{n=0}^{\infty} \frac{(2n+1)!!}{2^{n+1}(n+1)!} \int_0^{\infty} du \frac{1}{u^{2(n+1)}} [\frac{h(r)}{p_\infty} r^{2(n+1)} W^{n+1}(r, b)] \tag{87}$$

where

$$F_0(r_m) = -\int_0^{\infty} du\, h(r)/p_\infty, \quad r^2 = u^2 + r_m^2 \qquad \text{which we will deal with later.} \tag{88}$$

Note, because generally $W(r, b) < 0$, a binomial expansion had been impossible, had we not assumed $r \gg G$. Consider the integrand in eq. (87). For $\mathcal{C}^\infty$ functions $f(u)$ which obey $\frac{1}{u^{2n-1}} f(u) \to 0$ at the integration borders, the following identity holds

$$\int_0^{\infty} \frac{du}{u^{2n}} f(u) = \frac{1}{(2n-1)!!} \int_0^{\infty} du \left(\frac{1}{u}\frac{d}{du}\right)^n f(u) = \frac{2^n}{(2n-1)!!} \int_0^{\infty} du \left(\frac{d}{du^2}\right)^n f(u) \tag{89}$$

If $h(r)$ obeys requirements (81), the convergence properties of the integrand in (87) are those

[28] Note that either $W(r, b) < 0$ or $W(r, b) > 0$ for $r \in [r_m, \infty]$ depending on the actual characteristics of $U(r, b)$. $W(r, b) < 0$ when $U(r, b) \sim 1/r$ for $r \to \infty$.

required by eq. (89). Applying (89) to eq. (87) with $f(u) = \frac{h(r)}{p_\infty} r^{2(n+1)} W^{n+1}$ one obtains

$$\chi/2 = F_0(r_m) - \pi/2 - \sum_{n=0}^{\infty} \frac{(2n+1)!!}{2^{n+1}(n+1)!} \frac{2^{n+1}}{(2n+1)!!} \int_0^\infty du \left(\frac{d}{du^2}\right)^{n+1} \frac{h(r)}{p_\infty} r^{2(n+1)} W^{n+1}(r,b) \quad (90a)$$

$$= F_0(r_m) - \pi/2 - \sum_{n=0}^{\infty} \frac{1}{(n+1)!} \int_0^\infty du \left(\frac{d}{du^2}\right)^{n+1} \frac{h(r)}{p_\infty} r^{2(n+1)} W^{n+1}(r,b) \quad (90b)$$

$$= F_0(r_m) - \pi/2 - \sum_{n=0}^{\infty} \Delta_n \quad (90c)$$

$$\Delta_n = \frac{1}{(n+1)!} \int_0^\infty du \left(\frac{d}{du^2}\right)^{n+1} [\frac{h(r)}{p_\infty} r^{2(n+1)} W^{n+1}(r,b)] \quad (90d)$$

where Δ_n has been introduced to simplify notation and introduce an expanded form of the scattering angle. Note the difference with the Δ's defined in [1] - there is only a different function in front of $W(r,b)$.

We now focus on rewriting Δ_n. Write $W(r,b)^{n+1}$ as

$$W^{n+1}(r,b) = \frac{U^{n+1}(r,b)}{p_\infty^{2(n+1)}} (1-x)^{n+1} \quad \text{where} \quad x \equiv -\frac{r_m^2}{r^2} \frac{U(r_m,b)}{U(r,b)} \quad (91)$$

and write $(1-x)^{n+1} = \sum_{k=0}^{n+1} \frac{(n+1)!}{(n-k+1)!k!} x^k$ as a binomial expansion to obtain [29]

$$\Delta_n = \frac{1}{(n+1)!} \int_0^\infty du \left(\frac{d}{du^2}\right)^{n+1} \frac{h(r)}{p_\infty} r^{2(n+1)} \frac{U^{n+1}(r,b)}{p_\infty^{2(n+1)}} \sum_{k=0}^{n+1} \frac{(n+1)!}{(n-k+1)!k!} (-1)^k \frac{r_m^{2k}}{r^{2k}} \frac{U^k(r_m,b)}{U^k(r,b)} \quad (92a)$$

$$= \int_0^\infty du \left(\frac{d}{du^2}\right)^{n+1} \sum_{k=0}^{n+1} \frac{1}{(n-k+1)!k!} \frac{h(r)}{p_\infty} \frac{r^{2(n+1)} U^{n-k+1}(r,b)}{p_\infty^{2(n+1)}} \left[-\frac{r_m^2}{r^2} U(r_m,b)\right]^k \quad (92b)$$

Once again use $p_r(r_m) = 0$ to rewrite the term in square brackets. From eq. (83),

$$-\frac{r_m^2}{r^2} U(r_m,b) = p_\infty^2 \frac{b^2 - r_m^2}{r^2} \quad (93a)$$

$$\begin{aligned} \Delta_n &= \int_0^\infty du \left(\frac{d}{du^2}\right)^{n+1} \sum_{k=0}^{n+1} \frac{1}{(n-k+1)!k!} \frac{h(r)}{p_\infty} \frac{r^{2(n+1)} U^{n-k+1}(r,b)}{p_\infty^{2(n+1)}} \left[p_\infty^2 \frac{b^2 - r_m^2}{r^2}\right]^k \\ &= \sum_{k=0}^{n+1} \frac{(b^2 - r_m^2)^k}{k!} \int_0^\infty du \left(\frac{d}{du^2}\right)^{n+1} \frac{h(r)}{p_\infty} \frac{r^{2(n-k+1)} U^{n-k+1}(r,b)}{(n-k+1)!\, p_\infty^{2(n-k+1)}} \end{aligned} \quad (93b)$$

where in the last equality terms are rearranged slightly, grouping terms in k outside the differentiation, since b nor r_m depend on u. Note furthermore that the only explicit r_m dependence in the integrand occurs in $r = \sqrt{u^2 + r_m^2}$. Since r is symmetric in r_m^2 and u^2, one may exchange

[29] Note that $|x|$ is not necessarily smaller than 1. The exponent $n+1$ is positive and the binomial expansion can be used.

derivatives in u^2 for ones in r_m^2. Specifically, since $k \leqslant n+1$,

$$\left(\frac{d}{du^2}\right)^{n+1} = \left(\frac{d}{du^2}\right)^{k} \left(\frac{d}{du^2}\right)^{n-k+1} = \left(\frac{d}{dr_m^2}\right)^{k} \left(\frac{d}{du^2}\right)^{n-k+1} \tag{94}$$

χ of eq. (90c) can, as a result, be written in terms of a sum over k and n

$$\chi/2 = F_0(r_m) - \pi/2 - \sum_{n=0}^{\infty}\sum_{k=0}^{n+1} \Delta_{n,k}(r_m) \tag{95a}$$

$$\Delta_{n,k} = \frac{(b^2-r_m^2)^k}{k!}\left(\frac{d}{dr_m^2}\right)^k \int_0^\infty du \left(\frac{d}{du^2}\right)^{n-k+1} \frac{h(r)}{p_\infty}\frac{r^{2(n-k+1)}U^{n-k+1}(r,b)}{(n-k+1)!\,p_\infty^{2(n-k+1)}} \tag{95b}$$

We evaluate the $k = n+1$ and $F_0(r_m)$ terms of eq. (90c) separately. Denote them $\zeta_{-1}/2 \equiv F_0(r_m) - \sum_{n=0}^{\infty}\tilde{\Delta}_{n,n+1}$ with a conventional factor $1/2$, for reasons clear in a moment. $\sum_{n=0}^{\infty}\Delta_{n,n+1}$ can be rewritten in terms of the Taylor-expansion of $F_0(r_m)$ about $r_m = b$

$$\begin{aligned}
\sum_{n=0}^{\infty}\Delta_{n,n+1} &= \sum_{n=0}^{\infty}\frac{(b^2-r_m^2)^{n+1}}{(n+1)!}\left(\frac{d}{dr_m^2}\right)^{n+1}\int_0^\infty du\,\frac{h(r)}{p_\infty} \\
&= \left(\sum_{n=0}^{\infty}\frac{(b^2-r_m^2)^{n}}{(n)!}\left(\frac{d}{dr_m^2}\right)^{n}\int_0^\infty du\,\frac{h(r)}{p_\infty}\right) - \int_0^\infty du\frac{h(r)}{p_\infty} \\
&= -F_0(b) + F_0(r_m)
\end{aligned} \tag{96}$$

where the first expression in the third equality is recognised as the Taylor-series $F_0(b) = F_0(r_m = b)$. As a result, ζ_{-1} is purely a function of impact parameter b and the r_m dependence cancels,

$$\zeta_{-1}/2 = F_0(b) \tag{97}$$

We now deal with the $k \leqslant n$ part of the sum in eq. (95a). The scattering angle can be written like

$$\chi - \zeta_{-1} + \pi = -2\sum_{n=0}^{\infty}\sum_{k=0}^{n}\frac{(b^2-r_m^2)^k}{k!}\left(\frac{d}{dr_m^2}\right)^k\int_0^\infty du\left(\frac{d}{du^2}\right)^{n-k+1}\frac{h(r)}{p_\infty}\frac{r^{2(n-k+1)}U^{n-k+1}(r,b)}{(n-k+1)!\,p_\infty^{2(n-k+1)}} \tag{98}$$

This expression can be simplified remarkably. Similar to the previous section, define the function

$$\zeta_n(x) = -2\int_0^\infty du\left(\frac{d}{du^2}\right)^{n+1}\frac{h(r)}{p_\infty}\frac{r^{2(n+1)}U^{n+1}(r,b)}{(n+1)!p_\infty^{2(n+1)}}, \qquad r^2 = u^2+x^2 \tag{99}$$

where $x \in \mathbb{R}$. Consider $\zeta_n(x)$ as a *definition* of a function for arbitrary x. To be clear, r in eq. (99) should be understood as nothing more than a placeholder for u^2+x^2. It is only the actual radial coordinate from the metric when $x = r_m$, not otherwise.

The scattering angle now becomes

$$\chi = \sum_{n=0}^{\infty}\sum_{k=0}^{n}\frac{(b^2-r_m^2)^k}{k!}\left(\frac{d}{dr_m^2}\right)^k\zeta_{n-k}(r_m) \tag{100}$$

Consider the double sum. Defining $\tilde{n} = n - k$ writes,

$$\chi = \sum_{n=0}^{\infty} \sum_{\tilde{n}=0}^{n} \frac{(b^2 - r_m^2)^{n-\tilde{n}}}{(n-\tilde{n})!} \left(\frac{d}{dr_m^2}\right)^{n-\tilde{n}} \zeta_{\tilde{n}}(r_m) \tag{101}$$

Label the terms in this sum *uniquely* by $(n, \tilde{n})$. Now consider grouping the terms with $\tilde{n}$ fixed. Letting $\tilde{n} \in [0, \infty[$, one can write the double sum as

$$\chi = \sum_{\tilde{n}=0}^{\infty} \sum_{n=\tilde{n}}^{\infty} \frac{(b^2 - r_m^2)^{n-\tilde{n}}}{(n-\tilde{n})!} \left(\frac{d}{dr_m^2}\right)^{n-\tilde{n}} \zeta_{\tilde{n}}(r_m) \tag{102}$$

with the sums over n and $\tilde{n}$ flipped in order. Defining $m = n - \tilde{n}$, decouples the sum

$$\chi = \sum_{\tilde{n}=0}^{\infty} \sum_{m=0}^{\infty} \frac{(b^2 - r_m^2)^{m}}{m!} \left(\frac{d}{dr_m^2}\right)^{m} \zeta_{\tilde{n}}(r_m) \tag{103}$$

The above is easily recognised as the Taylor-expansion of $\zeta_{\tilde{n}}(\sqrt{r_m^2})$ about $r_m^2 = b^2$. Remarkably, this removes all r_m dependence in χ.

One therefore can simply write, letting $\tilde{n} \to n$ to alleviate notation

$$\chi + \pi = \sum_{n=0}^{\infty} \zeta_n(b) + \zeta_{-1} = \sum_{n=-1}^{\infty} \zeta_n(b) = \sum_{n=-1}^{\infty} -2 \int_0^{\infty} du \left(\frac{d}{du^2}\right)^{n+1} h(r) \frac{r^{2(n+1)} U^{n+1}(r,b)}{(n+1)! p_\infty^{2(n+2)-1}}, \qquad r^2 = u^2 + b^2 \tag{104}$$

As indicated by the second equality ζ_{-1} from eq. (97) is simply eq. (99) with $n = -1$ and $r^2 = u^2 + b^2$, ie. $\zeta_{-1} = \zeta_{-1}(b)$. This explains the notation in eq. (97). Simply shifting the sum from $n \in [-1, \infty]$ to $n \in [0, \infty]$ recovers a very concise form of the scattering angle, independent of r_m,

$$\chi + \pi = -2 \sum_{n=0}^{\infty} \int_0^{\infty} du \left(\frac{d}{du^2}\right)^{n} h(r) \frac{r^{2n} U^{n}(r,b)}{n! p_\infty^{2(n+1)-1}}, \qquad r^2 = u^2 + b^2 \tag{105}$$

Equation (105) holds whenever χ can be written like eq. (80) where $h(r)$ obeys eq. (81). It it loosly interpreted as an infinite sum over $\sim \frac{r^2}{u^2}\frac{U}{p_\infty^2} \ll 1$ [30], after noticing $\frac{d}{du^2} \sim \frac{1}{u^2}$ from pure dimensional arguments.

As such the derivation does not *only* apply to test particle scattering, but also to the full isotropic binary problem formulated in eq. [1]. Other possible uses are discussed in 6.

Indeed, the [1] calculation is easily recovered as a special case of (105) where $\zeta_{-1} = \pi$ and $h(r) = -bp_\infty/r^2$. In that case ζ_{-1} cancels the π on the LHS, and the rest reduces to the result found in [1].

Remarkably, this result can be applied to both spinning and non-spinning probes for rotationally symmetric metrics described in section 2.1. $h(r)$ is seen to obey the requirements of (81), at least up to $\mathcal{O}(S^2)$ in test particle spin. Interestingly, specifically for probes with and without spin, further rewriting of eq. (105) is possible to an operator-form not involving $h(r)$ directly.

[30] This is the quantity we assume is small when performing the binomial expansion of (85)

4.1 Scattering angle formula of a scalar test particle

This section derives an operator form of eq. (105) for a non-spinning test particle in an arbitrary metric.

$h(r)$ for a (non)-spinning test particle explicitly obeys eq. (81) to $\mathcal{O}(S^2)$ per eq. (54). As such, eq. (105) can be directly used to calculate the approriate scattering angle. However, eq. (105) can be rewritten using operators in neat way. In this context, we will first derive a special case of eq. (105) for scalar particles, then continue to the case of a spinning probe.

Setting $S = 0$, $h(r)$ from eq. (54) can be rewritten by using

$$\frac{d\phi}{dr} = -\frac{\partial}{\partial J}p_r \quad \Rightarrow \quad h(r) = -\left(\frac{bp_\infty}{r^2} + \frac{1}{2p_\infty}\partial_b U(r,b)\right) \tag{106}$$

We keep $r^2 \to u^2 + b^2$ implicit. ∂_b does *not* act on the b dependence in r. Inserting in eq. (105),

$$\begin{aligned}\chi + \pi &= 2\sum_{n=0}^{\infty}\int_0^\infty du\,\left(\frac{d}{du^2}\right)^n [\frac{bp_\infty}{r^2} + \frac{1}{2p_\infty}\partial_b U(r,b)]\frac{r^{2n}U^n(r,b)}{n!p_\infty^{2(n+1)-1}} \\ &= \pi + 2b\sum_{n=0}^{\infty}\int_0^\infty du\,\left(\frac{d}{du^2}\right)^{n+1}\frac{r^{2n}U^{n+1}(r,b)}{(n+1)!p_\infty^{2(n+1)}} \\ &+ \sum_{n=0}^{\infty}\int_0^\infty du\,\left(\frac{d}{du^2}\right)^n \partial_b[U(r,b)]\frac{r^{2n}U^n(r,b)}{n!p_\infty^{2(n+1)}}\end{aligned} \tag{107}$$

The π in the last equality comes from the $n = 0$ term of the $\frac{bp_\infty}{r^2}$ part. As in [1] this term is responsible for a vanishing zeroth order scattering angle. The last line can be rewritten significantly. Denoting $g(r,b) \equiv r^{2n}U^{n+1}(r,b)$,

$$r^{2n}U^n\partial_b U(r,b) = \frac{1}{n+1}\partial_b g(r,b) \tag{108}$$

which, in turn, can be rewritten in terms of the total derivative $\frac{d}{db}g(r,b) = \partial_b g(r,b) + \partial_r g(r,b)\frac{dr}{db}$ where $\frac{dr}{db} = \frac{d\sqrt{u^2+b^2}}{db} = \frac{b}{r}$,

$$r^{2n}U^n\partial_b U(r,b) = \frac{1}{n+1}(\frac{dg(r,b)}{db} - \frac{\partial g(r,b)}{\partial r}\frac{b}{r}) = \frac{1}{n+1}(\frac{dg(r,b)}{db} - 2b\frac{\partial g(r,b)}{\partial r^2}) \tag{109}$$

where d/db denotes the full derivative of $g(r,b)$ with b, including b dependence in $r^2 = u^2 + b^2$. Inserting (109) in (107), an important cancellation happens

$$\begin{aligned}\chi &= 2b\sum_{n=0}^{\infty}\int_0^\infty du\,\left(\frac{d}{du^2}\right)^{n+1}\frac{r^{2n}U^{n+1}(r,b)}{(n+1)!p_\infty^{2(n+1)}} \\ &+ \sum_{n=0}^{\infty}\int_0^\infty du\,\left(\frac{d}{du^2}\right)^n\left[\frac{d}{db}\left[\frac{r^{2n}U^{n+1}(r,b)}{(n+1)!p_\infty^{2(n+1)}}\right] - 2b\frac{d}{dr^2}\frac{r^{2n}U^{n+1}(r,b)}{(n+1)!p_\infty^{2(n+1)}}\right]\end{aligned} \tag{110}$$

The first line cancels the last term in the second line, after noticing $\frac{d}{dr^2} = \frac{d}{du^2}$ for a function only of r. The derivative $\frac{d}{db}$ acts on *both* the explicit b dependence in U, and the implicit b dependence

in $r = \sqrt{u^2 + b^2}$. One therefore simply finds,

$$\chi = \sum_{n=0}^{\infty} \int_0^{\infty} du \left(\frac{d}{du^2}\right)^n \frac{d}{db}\left[\frac{r^{2n} U^{n+1}(r,b)}{(n+1)! p_\infty^{2(n+1)}}\right], \qquad r^2 = u^2 + b^2 \tag{111}$$

Equation (111) only requires specifying $U(r,b)$ in the chosen normal coordinate system, as opposed to knowing both $h(r)$ and $U(r,b)$ with eq. (105). Because of the easy determination of $U(r,b)$ from the metric, we have used eq. (111) specifically to compute scalar scattering angles below.

4.2 Scattering angle formula for a spinning test particle up to $\mathcal{O}(S^2)$

This section derives an operator form of eq. (105) for a spinning test particle with spin S up to $\mathcal{O}(S^2)$, scattering in an arbitrary metric.

As seen from eq. (54), eq. (105) equally applies to a spinning test particle with spin-parameter S. As with the non-spinning case, equation (105) including test particle spin can be rewritten to an operator form.

To second order in S, one can modify the operator $\partial_L \to \frac{\mathcal{D}}{p_\infty}$ in eq. (40),

$$\begin{aligned} &\frac{d\phi}{dr} \equiv \frac{\mathcal{D}[p_r]}{p_\infty}, \quad \mathcal{D} = \partial_b + f_S(r)\partial_S \\ \Rightarrow \quad &h(r) = -\left(\frac{b p_\infty}{r^2} + \frac{1}{2p_\infty}\partial_b U(r,b,S) + \frac{f_S(r)}{2p_\infty}\partial_S U(r,b,S)\right) \end{aligned} \tag{112}$$

To higher orders, the same structure, with a non-diverging $h(r)$ is expected. $f_S(r)$ is determined order by order in S, by imposing eq. (112). It is, to second order in S

$$f_S(r) = \frac{p_\infty S}{m\kappa} + \frac{p_\infty\left(a^2 r + 2GM\left(\kappa^2 - r^2\right) - \kappa l r + r^3\right) S^2}{m^2\kappa^2\left(\gamma r^3 - a\kappa r\right)} + \mathcal{O}(S^3) \tag{113}$$

As in eq. (54), $\kappa = l - \gamma a$, $\gamma = E/m$ and $l = L/m$.

The first two terms have already been dealt with above. For the part with ∂_S, there is no subtlety with extra b-dependence on r. We thus simply find

$$f_S(r) r^{2n} U^n \partial_S U(r,b) = \frac{f_S(r)}{n+1}\frac{d}{dS} r^{2n} U^{n+1}(r,b,S) \tag{114}$$

Inserting eqs. (112) and (114) in eq. (105), the part with $\frac{d}{dS}$ becomes

$$2\sum_{n=0}^{\infty}\int_0^{\infty} du \left(\frac{d}{du^2}\right)^n \frac{f_S(r)}{2p_\infty}\partial_S U(r,b,S)\frac{r^{2n}U^n(r,b)}{n! p_\infty^{2(n+1)-1}} = \sum_{n=0}^{\infty}\int_0^{\infty} du \left(\frac{d}{du^2}\right)^n f_S(r)\frac{d}{dS}\frac{r^{2n}U^{n+1}(r,b)}{(n+1)! p_\infty^{2(n+1)}} \tag{115}$$

Combining eqs. (115) and (111), one finds the spinning test particle scattering angle (105) in a useful and very concise form,

$$\chi = \sum_{n=0}^{\infty} \int_0^{\infty} du \left(\frac{d}{du^2}\right)^n \mathcal{D}\left[\frac{r^{2n} U^{n+1}(r,b)}{(n+1)! p_\infty^{2(n+1)}}\right], \qquad r^2 = u^2 + b^2 \tag{116}$$

where, importantly, $\mathcal{D}$ does not commute with $\frac{d}{du^2}$. Matching known expressions of $\frac{d\phi}{dr}$ with eq. (112) provides a general order-by-order method of determining $f_S(r)$. We expect the The above perscription, including the construction of $\mathcal{D}$, only requires eqs. (80) and (81).

5 Scattering angle calculations

All scattering angle calculations are performed using the Mathematica code-files `((official) proper math, optimised) Scattering angle proper math.nb`, `Scattering Angle pure v.nb` for test particle with and without spin respectively. To explain the general procedure, we walk through some examples by hand below. A complete explanation of the code can be found in the *Appendix*. Actual code is included as separately appended files.

5.1 Scattering angle in Schwarzschild metric with Schwarzschild coordinates

As an instructive application of eq. (105), let us find the scattering angle to all PM orders of a test particle in the Schwarzschild metric directly from Schwarzschild coordinates. Typically this is done in isotropic coordinates [1], as this simplifies eq. (105). However, using eq. (105) the calculation is just as easy in Schwarzschild coordinates. Doing the calculation in Schwarzschild coordinates exemplifies that $\{t, r, \phi\}$ for which $T = T_0$ are not unique.

As a reminder the Schwarzschild metric in Schwarzschild coordinates $\{t, r, \theta, \phi\}$ is

$$g_{\mu\nu} = \begin{pmatrix} -(1-\frac{r_s}{r}) & 0 & 0 & 0 \\ 0 & (1-\frac{r_s}{r})^{-1} & 0 & 0 \\ 0 & 0 & r^2 & 0 \\ 0 & 0 & 0 & r^2 sin^2\theta \end{pmatrix} \tag{117}$$

where $r_s = 2GM$ is the Schwarzschild radius with black hole mass M and G is Newtons gravitational constant. Due to spherical symmetry, restrict the orbit to the $\theta = \pi/2$ plane without loss of generality. Solving eq. (32) for the canonical radial momentum p_r of a test particle with mass m yields (to all orders in G)

$$p_r^2 = \frac{(E^2-m^2)r^3 + m^2 r^2 r_s - J^2(r-r_s)}{r(r-r_s)^2} = p_\infty^2 - \frac{J^2}{r^2} - \left(r_s \frac{m^2(r-r_s) - E^2(2r-r_s) + \frac{J^2}{r^2}(r-r_s)}{(r-r_s)^2} \right) \tag{118}$$

The last result writes the G-independent and G-dependent terms separately. The test particle energy relation $E^2 - m^2 = p_\infty^2$ at infinite separation has been used to rewrite the zeroth-order term slightly. One recognises the p_r^2 form of eq. (78). Thus identify

$$U(r,b) = r_s \frac{m^2(r-r_s) - E^2(2r-r_s) + \frac{J^2}{r^2}(r-r_s)}{(r-r_s)^2} \tag{119}$$

where again $b \equiv \frac{J}{p_\infty}$. In order to find χ order-by-order in G from eq. (111), one needs a Taylor-

expansion of $U(r,b)$ in G. The result up to second order in G is listed below **correct sign**

$$U(r,b) = U_1(r,b) + U_2(r,b) + \mathcal{O}(G^3) = -\frac{(2E^2-m^2)r^2 - J^2}{r^3} r_s - \frac{(3E^2-m^2)r^2 - J^2}{r^4} r_s^2 + \mathcal{O}(G^3) \tag{120}$$

The next section walks through the computation of χ up to 2PM explicitly.

5.1.1 1PM Schwarzschild scattering angle

Let's begin by getting the first order Schwarzschild scattering angle, χ_1. Only a single expression contributes in eq. (105), namely the G^1 part of $U(r,b)$ in the $n=0$ term,

$$\chi_1 = \int_0^\infty du \frac{\partial}{\partial b} \frac{1}{p_\infty^2} U_1(r,b) = \frac{2GM(2E^2-m^2)}{bp_\infty^2} = \frac{2(2\gamma^2-1)GMm^2}{bp_\infty^2} \tag{121}$$

where $E^2 = \gamma^2 m^2$ with $\gamma^2 = \frac{1}{1-v^2}$ the asymptotical Lorentz factor of the test particle at infinity where its velocity is v. This result is the same found in literature with literature [1], [3].

5.1.2 2PM Schwarzschild scattering angle

Proceeding to 2PM produces two contributions from the sum over n in eq. (111) $\begin{cases} U_1 \text{ term from } n=1 \\ U_2 \text{ term from } n=0 \end{cases}$.

The 2PM contribution to the scattering angle, χ_2, may thus be written

$$\begin{aligned} \chi_2 &= \int_0^\infty du \frac{\partial}{\partial b}\left(\frac{d}{du^2}\right) \frac{r^2 U_1^2(r,b)}{2p_\infty^4} + \int_0^\infty du \frac{\partial}{\partial b} \frac{U_2(r,b)}{p_\infty^2} \\ &= r_s^2 \left(\frac{\pi(6E^2 - 2m^2 - p_\infty^2)}{4p_\infty^2 b^2} - \frac{\pi(8E^2 - 4m^2 - 3p_\infty^2)}{16 b^2 p_\infty^2} \right) \\ &= 4G^2M^2m^2\pi \left(\frac{5\gamma^2-1}{4p_\infty^2 b^2} - \frac{5\gamma^2-1}{16 p_\infty^2 b^2} \right) = \frac{3G^2M^2m^2\pi(5\gamma^2-1)}{4p_\infty^2 b^2} \end{aligned} \tag{122}$$

using $E^2 - m^2 = p_\infty^2$ and $E^2 = \gamma^2 m^2$ where $\gamma^2 = \frac{1}{1-v^2}$ is the asymptotical Lorentz factor of the test particle at infinity where its velocity is v.

This result is again consistent with [1, 3]. We will discuss general features of these angles in section 5.3.

5.2 Kerr scattering angle in Boyer-Lindquist coordinates in $\theta = \pi/2$ plane

The Kerr metric in Boyer-Lindquist coordinates $x \in \{t, r, \phi\}$, restricted to $\theta = \pi/2$

$$g_{\mu\nu} = \begin{pmatrix} -\left(1 - \frac{r_s}{r}\right) & 0 & -\frac{r_s a}{r} \\ 0 & \frac{r^2}{r^2 - r_s r + a^2} & 0 \\ -\frac{r_s a}{r} & 0 & \frac{(r+r_s)a^2 + r^3}{r} \end{pmatrix} \tag{123}$$

is evidently rotationally symmetric. Letting a test particle orbit in the $\theta = \pi/2$ plane, it will have conserved angular momentum L and stay in that plane. Fundamentally this allows the definition

⩽10PM Schwarzschild scattering angle for a non-spinning test particle

n	$\chi_n/\frac{G^n M^n}{b^n v^{2n}}$
1	$2\left(v^2+1\right)$
2	$(3\pi/4)v^2\left(v^2+4\right)$
3	$(2/3)\left(5v^6+45v^4+15v^2-1\right)$
4	$(105\pi/64)v^4\left(v^4+16v^2+16\right)$
5	$(2/5)\left(21v^{10}+525v^8+1050v^6+210v^4-15v^2+1\right)$
6	$(1155\pi/256)v^6\left(v^6+36v^4+120v^2+64\right)$
7	$(2/35)\left(429v^{14}+21021v^{12}+105105v^{10}+105105v^8+15015v^6-1001v^4+91v^2-5\right)$
8	$(45045\pi/16384)v^8\left(5v^8+320v^6+2240v^4+3584v^2+1280\right)$
9	$(2/63)(2431v^{18}+196911v^{16}+1837836v^{14}+4288284v^{12}$ $+2756754v^{10}+306306v^8-18564v^6+1836v^4-153v^2+7)$
10	$(2909907\pi/65536)v^{10}\left(v^{10}+100v^8+1200v^6+3840v^4+3840v^2+1024\right)$

Table 1: Scattering angle of a test particle in Schwarzschild spacetime up to 10PM, calculated using Schwarzschild coordinates, expressed purely in asymptotical test particle velocity v. χ_n is the G^n-order contribution to scattering angle $\chi=\sum_n \chi_n$. Up to 2PM, full results have been checked with literature. Light-bending angles are checked with [85, eq. (25)] up to and including 6PM.

and calculation of scattering angle χ given by eq. (55).

p_r is computed from eq. (32) to give

$$p_r^2=\frac{r[p_\infty^2 r^3+m^3r^2r_s+(a^2p_\infty^2-L^2)r+r_s(Ea-L)^2]}{(a^2+r^2-r_sr)^2}=T(r)-U(r,L,a) \tag{124a}$$

$$T(r)=\frac{r^2}{r^2+a^2}\left(p_\infty^2-\frac{L^2}{r^2+a^2}\right) \tag{124b}$$

$$\begin{aligned}U(r,L,a)=&-\frac{\left[(2E^2-m^2)r^6+(m^2-E^2)r^5r_s+((4E^2-m^2)a^4-4ELa^3)r^2\right]rr_s}{(a^2+r^2-r_sr)^2(a^2+r^2)^2}\\&-\frac{\left[((5E^2-2m^2)a^2-2ELa-L^2)r^4-r_s((E^2-m^2)a^2-L^2)r^3+a^4(Ea-L)^2\right]rr_s}{(a^2+r^2-r_sr)^2(a^2+r^2)^2}\end{aligned} \tag{124c}$$

which is again written as the sum of a G-independent T term, and G-dependent, U term. However, the coordinates considered here are *not* normal since T does not exhibit the structure of eq. (78). This is exemplified by setting $G=0$ in the Boyer-Lindquist metric eq. (123). One finds

$$g_{\mu\nu}^{(0)}=\begin{pmatrix}-1&0&0\\0&\frac{r^2}{r^2+a^2}&0\\0&0&a^2+r^2\end{pmatrix} \tag{125}$$

which is not the Minkowski metric. However the Minkowski metric can be recovered by the radial coordinate transformation $r\to\rho=\sqrt{r^2-a^2}$. To this purpose, define $\tilde{x}\in\{t,\rho,\phi\}$ in which

$$\tilde{g}_{\mu\nu}^{(0)}=\eta_{\mu\nu}=\begin{pmatrix}-1&0&0\\0&1&0\\0&0&\rho^2\end{pmatrix},\qquad \rho^2=r^2+a^2 \tag{126}$$

From eq. (34), p_r transforms like

$$p_\rho = \frac{dr}{d\rho} p_r \tag{127}$$

for any transformation $\rho(r)$ which only involves radial coordinates. Having made a transformation from Boyer-Lindquist to normal coordinates $r \to \rho$, (111) *does* apply with transformed $\tilde{U}(\rho, L, a) = \left(\frac{dr}{d\rho}\right)^2 U(r, L, a)$

$$\chi = \sum_{n=0}^{\infty} \int_0^\infty du \frac{\partial}{\partial b} \left(\frac{d}{du^2}\right)^n \frac{\rho^{2n} \tilde{U}^{n+1}(\rho, b)}{(n+1)! p_\infty^{2(n+1)}}, \quad \rho^2 = u^2 + b^2 \tag{128}$$

b and L are both coordinate-invariant. Calculating χ to 1PM, exactly like Schwarzschild, produces

$$\chi_1 = \frac{2GM\left(\gamma^2(2b - 2av) - b\right)}{\gamma^2 v^2 \left(b^2 - a^2\right)} \tag{129}$$

v is the asymptotical velocity of the test particle. Simplifications are *very* important to be able to do the integrals.

The result may be shown equivalent to test particle limits of [66] and [76] by rewriting γ in these results in terms of v. The Kerr scattering angle is listed up to 6PM in table 2 below. The results found agree with all literature considered; 1PM [66, 76], 2PM [70] and light-bending angle up to 4PM [78].

$\leqslant 6PM$ Kerr scattering angle of a non-spinning test particle

n	$\chi_n / \frac{G^n M^n}{v^{2n}(b^2-a^2)^{(3n-1)/2}}$
1	$2\big[-2av + b(1+v^2)\big]$
2	$(\pi/2a^2)\Big[(b^2-a^2)^{5/2}v^4 + (a-bv)^3\big[-4a^2v + 3ab + b^2v\big]\Big]$
3	$(2/3)\big[2a^5v\left(3v^4 - 10v^2 - 9\right) - 3a^4b\left(v^6 - 15v^4 - 45v^2 - 5\right) - 4a^3b^2v\left(15v^4 + 70v^2 + 27\right)$ $+2a^2b^3\left(11v^6 + 135v^4 + 105v^2 + 5\right) - 18ab^4v\left(5v^4 + 10v^2 + 1\right) + b^5\left(5v^6 + 45v^4 + 15v^2 - 1\right)\big]$
4	$(3\pi/16a^4)\Big[2(b^2-a^2)^{11/2}v^8 + (a-bv)^5\big[-8a^6v\left(14v^2+5\right) + 5a^5b\left(72v^2+7\right)$ $+a^4b^2v\left(16v^2 - 305\right) - 5a^3b^3\left(11v^2 - 14\right) - a^2b^4v\left(11v^2 - 30\right) + 10ab^5v^2 + 2b^6v^3\big]\Big]$
5	$(2/15)\big[-2a^9v\left(15v^8 - 60v^6 + 378v^4 + 900v^2 + 175\right)$ $+15a^8b\left(v^{10} - 15v^8 + 210v^6 + 1050v^4 + 525v^2 + 21\right) + 8a^7b^2v\left(45v^8 - 780v^6 - 6426v^4 - 6300v^2 - 875\right)$ $-140a^6b^3\left(v^{10} - 45v^8 - 630v^6 - 1050v^4 - 315v^2 - 9\right) - 84a^5b^4v\left(45v^8 + 1020v^6 + 2814v^4 + 1500v^2 + 125\right)$ $+14a^4b^5\left(67v^{10} + 3375v^8 + 15750v^6 + 14070v^4 + 2295v^2 + 27\right) - 1400a^3b^6v\left(9v^8 + 84v^6 + 126v^4 + 36v^2 + 1\right)$ $+36a^2b^7\left(29v^{10} + 875v^8 + 2450v^6 + 1190v^4 + 65v^2 - 1\right) - 50ab^8v\left(63v^8 + 420v^6 + 378v^4 + 36v^2 - 1\right)$ $+3b^9\left(21v^{10} + 525v^8 + 1050v^6 + 210v^4 - 15v^2 + 1\right)\big]$
6	$(5\pi/128a^6)\Big[8(b^2-a^2)^{17/2}v^{12} + (a-bv)^7\big[-4a^{10}v\left(1584v^4 + 1540v^2 + 189\right)$ $+7a^9b\left(5720v^4 + 2808v^2 + 99\right) - a^8b^2v\left(2200v^4 + 85232v^2 + 17829\right) + 14a^7b^3\left(260v^4 + 5391v^2 + 330\right)$ $-2a^6b^4v\left(334v^4 - 1491v^2 + 14070\right) + 21a^5b^5\left(85v^4 - 272v^2 + 176\right) + a^4b^6v\left(255v^4 - 1904v^2 + 1680\right)$ $-28a^3b^7v^2\left(17v^2 - 24\right) - 4a^2b^8v^3\left(17v^2 - 56\right) + 56ab^9v^4 + 8b^{10}v^5\big]\Big]$

Table 2: Scattering angle of a non-spinning test particle in Kerr spacetime up to 6PM.

5.3 Spinning test particle in Kerr metric

The scattering angle of a spinning test particle, up to $\mathcal{O}(S^2)$ in test particle spin, can be written like

$$\chi = \sum_{n=0}^{\infty} \int_0^{\infty} du \, \left(\frac{d}{du^2}\right)^n \mathcal{D}\left[\frac{r^{2n} U^{n+1}(r,b)}{(n+1)! p_\infty^{2(n+1)}}\right], \qquad r^2 = u^2 + b^2 \tag{130}$$

$$\mathcal{D} = \partial_b + f_S(r)\partial_S, \qquad f_S(r) = \frac{p_\infty S}{m\kappa} + \frac{p_\infty \left(a^2 r + 2GM\left(\kappa^2 - r^2\right) - \kappa l r + r^3\right) S^2}{m^2\kappa^2\left(\gamma r^3 - a\kappa r\right)} + \mathcal{O}(S^3) \tag{131}$$

per equation (116) in section 4.2. As such, the method of calculation is exactly the same as that without spin concerning eq. (111).

In Boyer-Lindquist coordinates, one finds the radial momentum p_r from the modified Hamilton-Jacobi equations (45) with p_t and p_ϕ given by eq. (50)

$$p_r^2 = T(r) - U(r,b) \tag{132}$$

where

$$T(r) = \frac{r^2}{r^2 + a^2}\left(p_\infty^2 - \frac{(J - \frac{ES}{m})^2}{r^2 + a^2}\right) \tag{133}$$

$$\begin{aligned}
U(r,b) = \\
&2GMr\Big[\frac{-p_{\text{inf}}^2\left(a^6 + a^4\left(b^2 + 4r^2\right) + a^2 r^3(5r - 2GM) + b^2 r^3(2GM - r) + 2r^5(r - GM)\right)}{\left(a^2 + r^2\right)^2\left(a^2 + r(r - 2GM)\right)^2} \\
&\qquad - \frac{\left(a^2 + r^2\right)^2\left(a^2 m^2 - 2abep_{\text{inf}} + m^2 r^2\right)}{\left(a^2 + r^2\right)^2\left(a^2 + r(r - 2GM)\right)^2}\Big] \\
&- \frac{2GMS\left[a^3 m^2 + a p_{\text{inf}}^2\left(a^2 + b^2 + r^2\right) - 2a^2 bep_{\text{inf}} + am^2 r^2 - ber^2 p_{\text{inf}}\right]}{mr\left(a^2 + r(r - 2GM)\right)^2} \\
&+ GMS^2\Big[\frac{-3a^4 m^2 + 6a^3 bep_{\text{inf}} + a^2 m^2 r(GM - 4r) + p_{\text{inf}}^2\left(-3a^4 + a^2\left(-3b^2 + GMr - 3r^2\right) + b^2 r(GM - r)\right)}{m^2 r^3\left(a^2 + r(r - 2GM)\right)^2} \\
&\qquad + \frac{2aberp_{\text{inf}}(2r - GM) + m^2 r^3(2GM - r)}{m^2 r^3\left(a^2 + r(r - 2GM)\right)^2}\Big] + \mathcal{O}(S^3)
\end{aligned} \tag{134}$$

Notice that $T(r)$ is not of normal form, and has exactly the same structure as eq. (124b). The radial coordinate transformation $r^2 \to \rho^2 = r^2 + a^2$ still brings the Boyer-Lindquist Kerr metric to normal form. This takes care of the $\frac{r^2}{a^2+r^2}$ prefactor of $T(r)$. Denoting the transformed quantity with $\tilde{T}$, whats left is something on the form

$$\tilde{T}(r) = p_\infty^2 - \frac{(J - \frac{ES}{m})^2}{\rho^2} \tag{135}$$

It can be brought to the well-known form of eq. (78) by two arguments. Note that J is the total angular momentum of the probe, including its spin. The orbital angular momentum L appearing in eq. (78) is exactly $J - \frac{ES}{m}$. This can be seen by requiring the $G \to 0$ dynamics of spinning and non-spinning test particles to be equal, ie. straight line motion. This would require the T-terms

to have exactly the same form. One therefore necessarily has the requirement

$$L = J - \frac{ES}{m} \equiv bp_\infty \tag{136}$$

Note how this also fixes the definition of impact parameter. The (134) expression for $U(r, b)$ is found by substituting eq. (136) in (50), solving the modified Hamilton-Jacobi equation (45) and expanding to second order in test particle spin S.

The scattering angle calculation now proceeds as in 5.2, coordinate-transforming $U(r, b) \to \tilde{U}(\rho, b)$ to $\rho^2 = r^2 + a^2$ coordinates and plugging into eq. (116). The full 1PM scattering angle up to $\mathcal{O}(S^2)$ is then

$$\begin{aligned}\chi_1 =& \frac{2GM\left(-2av + bv^2 + b\right)}{v^2\left(b^2 - a^2\right)} + \frac{4GMS\left(v\left(-a^2 - b^2\right) + abv^2 + ab\right)}{mv^2\left(b^2 - a^2\right)^2} \\ &+ \frac{2GMS^2\left(-2v\left(a^3 + 3ab^2\right) + v^2\left(3a^2b + b^3\right) + 3a^2b + b^3\right)}{m^2v^2\left(b^2 - a^2\right)^3} + \mathcal{O}(S^3)\end{aligned} \tag{137}$$

The spin contributions to the scattering angle up to $\mathcal{O}(S^2)$ and $\mathcal{O}(G^5)$ are listed in table 3 below. These have been checked against literature up to $\mathcal{O}(G^3)$ [76, 66, 70]. Orders higher than $3PM$ are new results. Any PM order can readily be found from eq. (116), however we truncate the table at 5PM for brevity. Note how individual components $\chi_{n,k}$ have the general structure

$$\chi_{n,k} \sim \frac{G^n M^n (S/m)^k}{v^{2n}\left(b^2 - a^2\right)^{(2n+2k-1)/2}} \tag{138}$$

and thus diverge when $b \to a$. This divergence is of no practical consequence, since we require $b \gg a$ from the Post Minkowskian assumption (30) implicit in expressions. We expect this relationship to continue to higher orders in S and G, although this is beyond the scope of our current treatment. We expect eq. (105) to be applicable to higher orders in S.

$\leqslant 5PM$ Kerr scattering angle of a spinning test particle up to $\mathcal{O}(S^2)$

(n,k)	$\chi_{n,k}/\frac{G^n M^n (S/m)^k}{v^{2n}(b^2-a^2)^{(3n+2k-1)/2}}$
$(1,1)$	$-4(av-b)(a-bv)$
$(1,2)$	$-4a^3v+6a^2b\left(v^2+1\right)-12ab^2v+2b^3\left(v^2+1\right)$
$(2,1)$	$(3\pi/2)(av-b)(a-bv)\big[a^2\left(-2v^2-3\right)+10abv-b^2\left(3v^2+2\right)\big]$
$(2,2)$	$(3\pi/4)\big[-10a^5v\left(v^2+1\right)+a^4b\left(12v^4+71v^2+12\right)-90a^3b^2v\left(v^2+1\right)$ $+a^2b^3\left(21v^4+128v^2+21\right)-40ab^4v\left(v^2+1\right)+b^5\left(2v^4+11v^2+2\right)\big]$
$(3,1)$	$8(av-b)(a-bv)\big[a^4\left(-v^4-10v^2-5\right)+8a^3bv\left(3v^2+5\right)$ $-2a^2b^2\left(5v^4+38v^2+5\right)+8ab^3v\left(5v^2+3\right)-b^4\left(5v^4+10v^2+1\right)\big]$
$(3,2)$	$4\big[-2a^7v\left(7v^4+30v^2+11\right)+5a^6b\left(3v^6+55v^4+65v^2+5\right)$ $-6a^5b^2v\left(51v^4+190v^2+63\right)+5a^4b^3\left(17v^6+265v^4+275v^2+19\right)$ $-10a^3b^4v\left(53v^4+170v^2+49\right)+3a^2b^5\left(19v^6+255v^4+225v^2+13\right)$ $-10ab^6v\left(11v^4+30v^2+7\right)+b^7\left(3v^6+35v^4+25v^2+1\right)\big]$
$(4,1)$	$(105\pi/16)(av-b)(a-bv)^3\big[a^4\left(-8v^4-20v^2-5\right)+12a^3bv\left(6v^2+5\right)$ $-2a^2b^2\left(10v^4+79v^2+10\right)+12ab^3v\left(5v^2+6\right)-b^4\left(5v^4+20v^2+8\right)\big]$
$(4,2)$	$(15\pi/32)(a-bv)\big[-2a^8v\left(24v^6+320v^4+485v^2+95\right)$ $+7a^7b\left(248v^6+1100v^4+635v^2+30\right)-a^6b^2v\left(760v^6+15808v^4+25345v^2+4980\right)$ $+105a^5b^3\left(92v^6+466v^4+276v^2+13\right)-15a^4b^4v\left(106v^6+2272v^4+3860v^2+769\right)$ $+21a^3b^5\left(405v^6+2050v^4+1258v^2+60\right)-a^2b^6v\left(585v^6+12140v^4+20270v^2+4196\right)$ $+7ab^7\left(160v^6+775v^4+460v^2+24\right)-5b^8v\left(4v^6+79v^4+124v^2+24\right)\big]$
$(5,1)$	$4(av-b)(a-bv)\big[a^8\left(v^8-36v^6-378v^4-420v^2-63\right)$ $+64a^7bv\left(v^6+27v^4+63v^2+21\right)$ $-4a^6b^2\left(9v^8+668v^6+3222v^4+2268v^2+105\right)$ $+64a^5b^3v\left(27v^6+289v^4+405v^2+63\right)$ $-2a^4b^4\left(189v^8+6444v^6+18094v^4+6444v^2+189\right)$ $+64a^3b^5v\left(63v^6+405v^4+289v^2+27\right)$ $-4a^2b^6\left(105v^8+2268v^6+3222v^4+668v^2+9\right)$ $+64ab^7v\left(21v^6+63v^4+27v^2+1\right)$ $-b^8\left(63v^8+420v^6+378v^4+36v^2-1\right)\big]$
$(5,2)$	$-2\big[2a^{11}v\left(11v^8+500v^6+2114v^4+1652v^2+203\right)$ $-7a^{10}b\left(3v^{10}+467v^8+4214v^6+6734v^4+2087v^2+63\right)$ $+2a^9b^2v\left(1665v^8+35036v^6+110726v^4+73052v^2+8001\right)$ $-21a^8b^3\left(51v^{10}+3491v^8+22358v^6+28910v^4+7703v^2+207\right)$ $+12a^7b^4v\left(2845v^8+41836v^6+103726v^4+56812v^2+5341\right)$ $-42a^6b^5\left(133v^{10}+6517v^8+32410v^6+33922v^4+7489v^2+169\right)$ $+84a^5b^6v\left(829v^8+9580v^6+19054v^4+8428v^2+637\right)$ $-6a^4b^7\left(1029v^{10}+40789v^8+164122v^6+137410v^4+23617v^2+393\right)$ $+42a^3b^8v\left(795v^8+7604v^6+12194v^4+4148v^2+219\right)$ $-a^2b^9\left(1449v^{10}+49049v^8+162722v^6+105770v^4+12437v^2+93\right)$ $+14ab^{10}v\left(203v^8+1652v^6+2114v^4+500v^2+11\right)$ $-b^{11}\left(35v^{10}+1043v^8+2870v^6+1358v^4+71v^2-1\right)\big]$

Table 3: Scattering angle of a spinning probe in a Kerr background up to 5th order in G. $\chi_{n,k}$ is the G^nS^k contribution to the full scattering angle $\chi=\sum_{n,k}\chi_{n,k}$.

6 Further Possible Applications

Apart from the direct calculation of scattering angles, eq. (105) provides intriguing possibilities for further insight into other related areas. Any calculation that can be brought on the form of eq. (105), whether it might come from a test particle limit, from amplitudes or someplace else, can be treated by the formalism. The derivation of [1] provided applications not only to the test particle case, but also much wider amplitude calculations.

We discuss here further possible uses of (105). A full treatment of these subjects has been beyond the scope of this project, and so we only conjecture as to the applicability of eq. (105).

6.1 Effective One-Body Theory of Binary Motion

Ever since the observation of gravitational waves (GWs) by LIGO in 2016 [5] and the many subsequent observations [48, 49, 50, 51, 52, 53, 54, 55, 56, 57], detailed trajectories of dynamical systems in General Relativity have been sought after.

The Effective One-Body approach to GR provides a way to achieve this. As an alternative to the traditional PN formalism covered in section 1.2.5, recent developments have been made towards an EOB formalism based on a Post-Minkowskian expansion in Newtons gravitational constant G [75, 86, 83, 3]. First introduced by Thibault Damour [75], one considers a map of not energy, but scattering angles in a PM expansion. The resulting EOB metric, although constructed by considering scattering, can also be used for bound orbits - the metric encodes equations of motion, and these are identical for scattering and bound orbits. A main advantage of the PM expansion over the PN one, is the availability of scattering data from amplitude methods, as described in section 1.2.7.

The case of two arbitrary mass, non-spinning black holes has been studied in detail [3]. Up to 3PM, Damgaard et. al. showed that such a map cast $g^{eff}_{\mu\nu}$ into an energy dependent form [3]. This is thought a natural artifact of the energy and momentum dependent non-linear back-reactions between bodies outside the test body limit. The result was shown to be in agreement with previous methods [75, 83], up to a canonical transformation. For a full treatment of [3], see the Appendix.

For binary objects with aligned spin, a similar procedure might be envisioned. The motion stays in a plane due to the lack of spin-spin interactions which would precess the orbit, and the scattering angle is defined as usual. Scattering angle data for such systems is abundant from amplitude methods [66, 87]. However, the effective side of the picture does need more work. A general method for computing scattering angles in rotationally symmetric (EOB) metrics has not been previously available.

Another difficulty, an ansatz of the EOB metric is not isotropic in form. This follows because the test particle limit of $g^{eff}_{\mu\nu}$, the Kerr metric, cannot be rendered isotropic. A general principle for the structure of the EOB metric does not yet exist. Such a principle might restrict the problem in the way an isotropic form has completely determined the EOB metric without spin. The analysis above lends partial insight to this problem. Imposing eq. (55) the EOB metric must obey eq. (31). This reduces the degrees of freedom of $g^{eff}_{\mu\nu}$ from 6 to 4, setting $g^{eff}_{r\mu} = 0$ for $\mu \neq r$.

Considering the 2 dofs of the isotropic metric, and the single undetermined function $h(r)$ used in [3], this is not enough to fully determine the metric.

Equation (105) gives a tool to construct metrics which reproduce the scattering angle of systems described above as a perturbative expansion in G. An actual EOB interpretation is not made, since such a metric is not unique. Suppose a scattering angle formula is given by amplitudes. This formula should be turned into a potential calculation, like eq. (105), with well-defined potential $V_{eff}(r)$. Specifically, V_{eff} should only depend on radial coordiate r. If this is possible, one can equate scattering angles

$$\chi_{eff} = \chi_{real}, \quad \Rightarrow \quad V_{eff} = U \tag{139}$$

using eq. (105). A way of determining the potential U of the effective metric in eq. (105) is thus established. Such a relation can then be used to determine the underlying EOB metric components. Like [1], given only the single constraint of eq. (139), the metric should only contain a single degree of freedom.

6.2 All order scattering angle in single expression?

The only drawback to eq. (105) is that the sum has to be evaluated manually to each order. Although the procedure is valid to all orders in G, and a computer can readily do computations, these can become quite lengthy.

In the light of this complication, the prospect of obtaining an all-PM order scattering angle eq. (105) is very intriguing. In principle one could envision summing up the contributions from eq. (105), "collapsing the expansion" to a form without summation.

This is however not straight forward. First note that the structure of eq. (105) is somewhat similar to that of eq. (89). One can thus imagine a procedure similar to applying the steps (85)-(90a) in reverse to get a resummed version of eq. (105). However the equivalent of $f(u)$, namely $\frac{(2n-1)!!}{2^n} h(r) \frac{r^{2n} U^n(r,b)}{n! p_\infty^{2(n+1)-1}}$ does not conform to the requirement of $\frac{f(u)}{u^{2n+1}} \to 0$ for $u \to 0, \infty$. Something else is required.

7 Conclusion

We have provided a general Post Minkowskian formula for the evaluation of probe scattering angles found from the Hamilton-Jacobi formula of GR. It generalises the derivation of [1]. Our formula applies to all PM orders, both for spinning and non-spinning probes, provided angular momentum is conserved and all spins aligned. This implies the scattering happens in a single plane and that the metric is rotationally symmetric in this plane. When this is the case, tested explicitly to $\mathcal{O}(S^2)$ in probe spin, the scattering angle can be written

$$\chi/2 = -\int_{r_m}^{\infty} dr \frac{h(r)}{p_r} - \pi/2 \tag{140}$$

p_r is canonical radial momentum, possibly carrying probe spin dependence, but only a function of r. It comes from the Hamilton-Jacobi formulation of section 2. r_m is the minimum distance of approach between probe and scattering centre with $p_r(r_m) = 0$. The formula found requires nothing more than the function $h(r)$ to be well-behaved for $r \in [r_m, \infty[$. The coordinates used to parametrise the problem should reduce to spherical Minkowski coordinates when $G \to 0$, such that $p_r^2 = p_\infty^2 - \frac{L^2}{r^2} - U(r, b)$ with arbitrary 'potential' $U(r, b)$ [31]. Labelled *normal coordinates*, they can be constructed from any metric by setting $G = 0$.

Provided the scattering angle can be written like (140), the infinite sum in (105) yields this angle to all PM orders.

This way, scattering angles of the Schwarzschild metric up to 10PM and of Kerr up to 6PM for non-spinning probes are found. Additional orders are readily treated, but excluded to conserve space. We also present scattering angles of spinning probes up to 5PM and $\mathcal{O}(S^2)$ in probe spin. To the best of our knowledge, literature covers up to 4PM without probe spin and 3PM including probe spin. Excluding lightbending, all literature found provide full arbitrary mass two-body scattering angles. Our results are checked against probe-limits hereof. Scattering of light in the Kerr metric has been covered to 4PM. All scattering angles found in this thesis agree with literature [76, 66, 70, 78].

Consider a spinning probe in a Kerr metric, aligned with the Kerr spin. Denoting by b the asymptotical impact parameter, by S the rescaled probe spin and by a Kerr spin parameter, we generally find a structure like

$$\chi_{n,k} \sim \frac{G^n S^k}{(b^2 - a^2)^{(3n+2k-1)/2}} \tag{141}$$

at order n in G and order k in probe spin S. Additional b and a dependence is present. For $S = 0$, to all calculated PM orders, we reproduce the resummed spin dependence of [76]. We hope this yields insight to future higher PM treatments of the full binary problem with aligned spin. Currently, spin can only be handled perturbatively [70].

Finally, we have noted our derivation is mostly mathematical, presenting an integration technique of the wide class of integrals (140). It naturally also be applies to the full isotropic binary problem stated in [1]. It is thus not unthinkable that the scattering angle formula might be useful for other purposes. We have briefly discussed the possibility of applications within an EOB formulation of GR, and the possibility of a resummed, all order in G scattering angle.

[31] p_∞ is asymptotical momentum and L is angular momentum of the testparticle

Acknowledgements

I would like to sincerely thank my supervisors, Poul and Andrés. Your enthusiasm and support throughout the project has truly been awe-inspiring. Working together, not only on the thesis but also our paper with Justin Vines, your warm, welcoming attitude has made for the most pleasant and productive atmosphere imaginable. I will miss our discussions on everything from bicycle helmets to 'funky vs proper math'. It has been a true pleasure! I wish you both all the best for the future.

Thank you.

8 Appendix

A Special theory of Relativity

First proposed by Albert Einstein in 1905 [6], the special theory of relativity revolutionised the dynamics of kinematics without gravity. The word "special relativity" has only been keyed after the development of General Relativity, of which the former is a special case. Many key ideas are common between the theories. The special theory of relativity does not consider gravitation, but pertains to relations between inertial frames of reference related to each other by a constant velocity. Replacing Newtons idea of absolute time, many implications about the very nature of physics itself, can be derived from the special theory of relativity. Einstein did a famous *Gedankenexperiment*; Consider a person standing on the platform of a trainstation. Consider now the same person sitting in the train travelling at some constant velocity v relative to the platform. Both systems are inertial, meaning not accellerated. Suppose the train has no windows. How would the person know if the train is moving? They cannot. Any experiment he can do locally inside the train, without gravity, produces exactly the same result as were it made on the platform: Standing up feels the same, moving around feels the same. This also applies to the measurement of the speed of light: Its speed as measured on the platform or in the train is *exactly* the same, c. The constant of physical laws between inertial reference frames, is known as the first principle of relativity first formulated by Einstein,

If an intertial system exists in which the physical laws hold in their most basic form, then in any other inertial system related to the first by a relative, constant velocity, the same laws of physics will also hold.

The resulting constant speed of light is in stark contrast to the Galilean point of view adopted by Newtons 3 laws of motion. Newton considered the speed of light considered relative to the emitting object, and can in principle be overtaken exactly like a car on the highway. Newtons fallacy, as we shall see, is that he considered time as absolute. In fact, measurement of time: How many times do I blink my eyes a second etc., can only be defined from a local perspective.

To see this, we turn back to our example of the train and station. We will see how the constancy of speed of light has important implications for the relative experience of time between these reference frames. Consider a set of mirrors in the train, between which a beam of light travels (see figure 9). Each time the light bounces back and forth, a clock ticks in the train. The mirrors are placed vertically a distance d apart. Ask now a deceptively simple question: What is the time taken between the beam hitting mirrors in each reference?
In the train frame of reference, it is an easy question: The light is travelling at speed c, and the mirrors are distance d apart. The time light takes to travel from one mirror to the next is thus $\Delta t_{train} = d/c$.
As viewed from the platform, the situation is quite different. Because the train moves, the distance travelled by the lightbeam between the mirrors is increased. This distance, as shown by figure 9 is $d_{platform} = \sqrt{d^2 + v^2 \Delta t_{platform}^2}$ where $\Delta t_{platform}$ is the time difference measured from the platform. $\Delta t_{platform} = \frac{d_{platform}}{c}$ then follows because the speed of light is invariant between formalisms. The

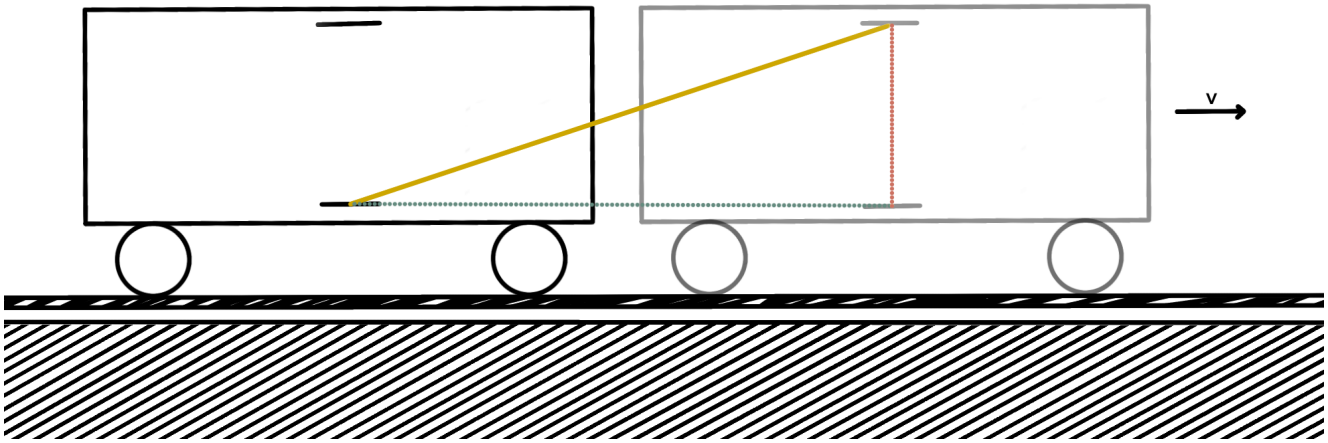

Figure 9: Albert Einsteins famous Gedankenexperiment, of a lightbeam reflecting of mirrors in a moving train. The train moves along the tracks to the right with velocity v, seen from the station platform. It is depicted at two different times (black and grey train). The 'black train' snapshot is taken when the lightbeam (yellow solid line) leaves the bottom mirror. The 'grey train' snapshot is taken when the lightbeam reaches the top mirror. These mirrors are a distance d apart (red dotted line). The time measured from the platform of light passing from one mirror to the next is denoted $\Delta t_{platform}$. Because the train moves as observed from the platform, the lightpath is slanted covering a total distance $d_{platform}$. Knowing that the train moves at velocity v, the horizontal distance (green dotted line) covered between light hitting the mirrors is $v\Delta t_{platform}$. The Pythagorean theorem applied to the right triangle red-green-yellow lines then yields

$$d^2_{platform} = (\text{green dotted line})^2 + (\text{red dotted line})^2 = d^2 + (v\Delta t_{platform})^2$$

time beteween ticks of the clock measured from the platform is then

$$\Delta t_{platform} = \frac{\sqrt{d^2 + v^2 \Delta t^2_{platform}}}{c} \quad \Rightarrow \quad \Delta t_{platform} = \Delta t_{train}\gamma \tag{142}$$

where $\gamma = \frac{1}{\sqrt{1-v^2/c^2}}$ is the Lorentz contraction factor. Every single imaginable clock should tick at the same rate as the light-clock imagined here. Equation (142) then says that

moving clocks run slower than stationary clocks

A different but similar argument of two events happing instantaneously in one reference frame, gives the contraction of lengths in reference frame. If the train length is measured at L in the train reference frame, it will be measured as

$$L_{platform} = \frac{L}{\gamma} \tag{143}$$

in the platform reference frame. The behaviour $\Delta t_{platform} \to \infty$ and $L_{platform} \to 0$ when $v \to c$ signifies the impossibility of massive objects reaching velocities greater than that of light. c is thus the absolute speed limit in the Universe.

A vital interpretation of the theory can be made by considering a coordinate system $x \in \{t, x, y, z\}$ is laid on the platform and a coordinate system $x' \in \{t', x', y', z'\}$ is laid in the train. Consider the difference in Δx and $\Delta x'$ of light hitting the mirrors. Denote the position of the

mirror by subscript 1 and 2 for the lower and upper mirror. Because of the constancy of the speed of light, one may write$-c(t_2-t_1)^2+(x_2-x_1)^2+(y_2-y_1)^2+(z_2-z_1)^2=0=-c(t_2'-t_1')^2+(x_2'-x_1')^2+(y_2'-y_1')^2+(z_2'-z_1')^2$. This relation is completely independent of the velocity between frames of reference and the coordinates. The "difference" $-c^2\delta t^2+\delta x^2+\delta y^2+\delta z^2$ between two events is thus invariant in all possible reference frames. The above relation holds for event on a light trajectory. For general events, on light trajectories or not, the quantity

$$ds^2=-c^2\delta t^2+\delta x^2+\delta y^2+\delta z^2 \tag{144}$$

is still invariant. ds^2 has different sign for different events: $ds^2>0$ for events that can be considered simultaneous in some reference frame. $ds^2<0$ for events that happen at the same spatial spot in some reference frame. $ds^2=0$ for light-like trajectories.

Because of the invariance of ds^2, it reflects the idea of length in the traditional sense - length of objects in Newtonian physics is invariant under rotations and translations. Similarly 'length' between events in special relativity is invariant under Lorentz transformations: rotations, translations and boosts of reference frame velocity. Note that, without the time-term, ds^2 is just the traditional Galilean length. The realm in which this length is measured, time+space, is aptly called spacetime. Note how time enters equally in eq. (144) compared to spatial directions, just like an extra dimension tagged onto Galilean space. The spacetime interpretation of eq. (144) can be made more explicit. Rewrite it like

$$ds^2=\eta_{\mu\nu}dx^\mu dx^\nu,\quad \eta_{\mu\nu}=\begin{pmatrix}-1&0&0&0\\0&1&0&0\\0&0&1&0\\0&0&0&1\end{pmatrix} \tag{145}$$

$dx^\mu=\{dt,dx,dy,dz\}$ denotes the infinitesimal difference in coordinates between two otherwise arbitrary events. $\eta_{\mu\nu}$ is a 4×4 matrix known as the Minkowskian metric. The indices $\mu,\nu\in\{0,1,2,3\}$ indicate coordinates. Repeated indices are implicitly summed over and the above equation thus implicitly $ds^2=\sum_{\mu=0}^3\sum_{\nu=0}^3\eta_{\mu\nu}dx^\mu dx^\nu$. The metric encodes how coordinates enter in the definition of invariant lengths ds^2 between events. As such, the metric encodes the geometry of spacetime in special relativity. Because we consider the case of special relativity, excluding gravity, the Minkowski metric is often associated with flat space. We will make this interpretation more clear in a moment.

Special relativity provided solutions to many problems. Originally conceived to solve the incompatibility of Newtonian mechanics with Maxwells laws of Electrodynamics, it turned out completely in agreement herewith. From the generalisation of conservation of mass, it further provided the perhaps most famous of all physical formulae, the equivalence between energy and mass of particles

$$E=mc^2 \tag{146}$$

As already discussed, it further established relativistic velocity addition, showing that no object with mass can surpass the velocity of light. The relativistic Doppler effect of light was also discovered, with important applications to precision measurements of cosmic Doppler effects.

B Derivation of the dopplershift of light by gravity

We will follow the derivations of [12]. Consider first the case of two accelerating spacecraft a constant distance L apart accelerating at rate a. We will only consider Newtonian mechanics, thus neglecting special relativity for the moment. It is valid if the quantity aL/c^2 is very small and corresponds to both spacecraft being in the same reference frame. In the Newtonian framework, we can consider both spacecraft in the same inertial system. Suppose now we send a lightbeam from one spacecraft to the other. Because they are a distance L apart, observed form both, light takes $\Delta t = L/c$ to reach the other spacecraft. But in this time interval, they have gained the speed $\Delta v = a\Delta t = aL/c$. Viewing the system from the Newtonian point of view [32], an accompanying redhifted of emitted and received wavelengths of light is present,

$$\Delta\lambda \equiv \lambda_r - \lambda_e = \frac{\Delta v}{c}\lambda_e = \frac{La}{c^2}\lambda_e \tag{147}$$

where λ_e and λ_r are the wavelengths emitted and received by the spacecrafts. If light is sent from the front to the back spacecraft, a redshift occurs. The other way around, a blueshift occurs.

Consider now the case of a tower from the top of which a light beam is emitted. Both the top and bottom of the tower experience the force of gravity. According to the Equivalence Principle, the situation is identical to the spaceships considered above. Define h as the height from Earths surface (the bottom of the tower). Writing the gravitational potential as $\phi = hg$, we find

$$\Delta\lambda = \frac{Lg}{c^2}\lambda_e \qquad \Rightarrow \qquad \Delta\lambda/\lambda = \frac{1}{c^2}\Delta\phi \tag{148}$$

where $\Delta\phi$ is the potential difference between received and emitted locations and $\lambda_e \equiv \lambda$ has been renamed. The potential increases with height. Therefore, when a lightray is shot toward Earth, its wavelength decreases. Contrary, when it is shot upward, its wavelength increases. Light experiences red- and blue-shifts in gravitational fields.

C Review of the Effective One-Body approach from a Post-Minkowskian expansion, following [3]

This short sketch seeks to find the effective one-body (EOB) metric of a spinning binary to first Post-Minkowskian (1PM) order. It should be seen solely as a reproduction of the methods and results obtained in [3].

Consider a binary system of pointlike particles (ie. black holes) with arbitrary masses m_1, m_2, scattering on each other in a metric $g_{\mu\nu}$ in their center of mass (cm) frame. The dynamics of such a system may be found by remodelling the binary in an effective one-body formalism. Such a formalism reduces the binary motion to that of an effective testparticle scattering in an effective metric $g^{eff}_{\mu\nu}$. A minimal requirement on the EOB metric may be formulated as

$$(g_{\mu\nu})_{testbody} = (g^{eff}_{\mu\nu})_{testbody} \textit{ in the testbody limit of both} \tag{149}$$

[32] neglecting time-dilation between the frames of reference

The aim of this section is to present a mapping between real and EOB formalisms and find the EOB metric to first Post-Minkowskian order, subsequently checking its consistency.

C.1 discusses the translation (mapping) between variables in effective and real formalisms.
C.2 presents the ansatz for the effective metric $g^{eff}_{\mu\nu}$, parametrised by a single function to be determined by enforcing the mapping.
C.3 calculates the metric up to first Post-Minkowskian order.
C.4 discusses the validity of the result found by computing the testbody limit of the EOB metric. The periastron shift, obtained from the 2PM expansion by [3], is also briefly presented.

Notationally, quantities in the effective formalism will be denoted "eff", while those in the real formalism will not be given extra notation. 4-vectors/oneforms will be given greek indices throughout to distinguish them from their 3-vector counterparts, which don't carry any extra notation nor any special font. This is to conform with notation in [3].

C.1 Effective One-Body mapping

The mapping between effective and real formalisms is crucial for obtaining equivalent results. Every dynamical and physical quantity must be mapped. Among these, the scattering angle map will prove to be the crucial link determining the effective metric. First, let us define the real and effective physical quantities, then map them.

In the real formalism, two objects of mass m_1, m_2, 4-momenta p_1^μ, p_2^μ and total energy $E = E_1 + E_2$ scatter on each other with impact parameter b and total angular momentum J. Denote $M = m_1 + m_2$ for convenience. The system is considered in the center of mass frame in which $p_1 = -p_2$ where they move with relative velocity $v \equiv v_1 - v_2$

The effective formalism particle has mass $\mu = \frac{m_1 m_2}{m_1+m_2}$ (see eg. [75]) and moves at the same velocity v with 4-momentum p^μ_{eff} and angular momentum J_{eff}. This particle scatters with impact parameter b_{eff} on an effective metric $g^{eff}_{\mu\nu}$, the latter of which will be discussed later. Coordinates used in the effective formalism are spherical $\{t, r, \theta, \phi\}$ where t, θ, ϕ are time and angle coordinates and where r is interpreted as the *real-world* particle separation.

Momentum and energy will be mapped first. We will evaluate the mapping in the Minkowskian limit, that is, with infinite particle separation $r = r_1 - r_2 \to \infty$. The resulting mapping is assumed to generalise outside this regime.

For additional reasons made clear in the next section, we will map the effective particle momentum p_{eff} to the center of mass momentum p_∞ of a single particle when $r \to \infty$. In this limit any potential terms in particle energies $(E_1, E_2)_{r\to\infty}$ can be neglected.

The effective particle momentum is given by $p_{eff} = \gamma\mu v$, where $\gamma = \frac{1}{\sqrt{1+v^2}}$ is the lorentz contraction factor. In a flat background, in terms of real-formalism variables evaluated in the CM frame, it is

$$\gamma = \frac{p_1^\mu (p_2)_\mu}{m_1 m_2} = \frac{E^2 - m_1^2 - m_2^2}{2m_1 m_2} \qquad [33] \tag{152}$$

[33]Note that $p_1^\mu(p_2)_\mu$ is covariant. Evaluating it in the restframe $\tilde{S}$ of m_1, using $E_i = \gamma_i m_i$ where i indicates particle index and $\gamma_i = \frac{1}{1-\tilde{v}_i^2}$

$$p_1^\mu (p_2)_\mu = E_1 E_2 - p_1 p_2 = m_1 \gamma_2 m_2 = m_1 m_2 \gamma \tag{151}$$

where E is the CM energy of the real-formalism particles. The energy map may be found from eq. (150) and using $E_{eff} = \mu\gamma$,

(energy map)

$$E = M\sqrt{1 + 2\nu(\gamma - 1)} = M\sqrt{1 + 2\nu\left(\frac{E_{eff}}{\mu} - 1\right)} \tag{153}$$

where $\nu = \mu/M = \frac{m_1 m_2}{M^2}$. This is the *energy map.*

One may now evaluate p_{eff}^2

$$\frac{p_{eff}^2}{\mu^2} = \frac{(E^2 - (m_1 + m_2)^2(E^2 - (m_1^2 - m_2^2))}{4m_1^2 m_2^2} \quad {}^{34} \tag{155}$$

and compare it to p_∞^2

$$p_\infty^2 = \frac{(E^2 - (m_1 + m_2)^2)(E^2 - (m_1^2 - m_2^2))}{4E^2} \quad {}^{35} \tag{160}$$

to obtain

(momentum map)

$$p_{eff} = \frac{\mu E}{m_1 m_2} p_\infty = \frac{E}{M} p_\infty \tag{161}$$

---

since particle 2 in this frame moves at velocity $\tilde{v}_2 = v$. Subscript "tilde" has been used to avoid confusion with CM velocities v_1, v_2.

The second equality follows from calculation of

$$(p_1 + p_2)_\mu (p_1 + p_2)^\mu = E^2 = m_1^2 + m_2^2 + 2p_1^\mu (p_2)_\mu \quad \Rightarrow p_1^\mu (p_2)_\mu = \frac{E^2 - m_1^2 - m_2^2}{2} \tag{152}$$

in the CM frame with total energy E.

[34]This result is readily obtained from

$$p_{eff}^2/\mu^2 = \gamma^2 v^2 = \gamma^2 - 1 = \frac{(E^2 - m_1^2 m_2^2)^2 - 4m_1^2 m_2^2}{4m_1^2 m_2^2} \tag{155}$$

which upon inspection is equal to the expression given.

[35]Let $i = 1, 2$ be particle index. In the CM frame and letting $r_1 - r_2 \to \infty$

$$E_i = \sqrt{m_i^2 + p_\infty^2} \tag{157}$$

Then writing out the square of eq. (150), one finds

$$\frac{(E^2 - m_1^2 - m_2^2)^2}{4} = (p_1^\mu (p_2)_\mu)^2 = (E_1 E_2 + p_\infty^2)^2 = E_1^2 E_2^2 + p_\infty^4 + 2E_1 E_2 p_\infty^2 = (m_1^2 + p_\infty^2)(m_2^2 + p_\infty^2) + p_\infty^2 + 2E_1 E_2 p_\infty^2 \tag{158}$$

which upon inspection may be written as

$$\frac{(E^2 - m_1^2 - m_2^2)^2}{4} = m_1^2 m_2^2 + p_\infty^2 E^2 \tag{159}$$

where $E = E_1 + E_2$ using the exact form above. Some simple rewriting yields

$$p_\infty^2 = \frac{(E^2 - (m_1 + m_2)^2)(E^2 - (m_1 - m_2)^2)}{4E^2} \tag{160}$$

which is the *momentum map*.

Angular momentum and scattering angles are to be mapped next. Working with scattering states, it is natural to assume the scattering angle map

$$\chi_{eff} = \chi \quad \text{(scattering angle map)} \tag{162}$$

as in [75]. As was the case of angular momentum, it is natural to equate impact parameters $b_{eff} = b$, such that

$$\text{(angular momentum map)}$$
$$b_{eff} = b \quad \Rightarrow \quad J/p_\infty = J_{eff}/p_{eff} \quad \Rightarrow \quad J_{eff} = \frac{p_{eff}}{p_\infty} J = \frac{E}{M} J \tag{163}$$

which follows directly from the definition $b \equiv J/p$. Alternatively one could have equated angular momenta directly, as in [75]. The above prescription introduces energy dependence in the EOB metric.

C.2 Real and effective scattering angles and the EOB metric

The real formalism scattering angle χ is known [76] order by order in Newtons gravitational constant G_N. Using eq. (162), one may thus determine the EOB metric order by order in G_N.

The first task is to find expressions for χ and χ_{eff}. First we will show how χ is related to first order to the effective potential $V_{eff}(r, p)$ of the real problem. The effective potential may be defined by the impetus equation, relating center of mass momentum p to its value at infinite separation, p_∞

$$p^2 = p_\infty^2 - V_{eff}(r, E) \tag{164}$$

where V_{eff} may be expressed as an expansion in G_N like

$$V_{eff}(r, E) = -\sum_{n=1}^{\infty} f_n(E) \left(\frac{M G_N}{r} \right)^n \tag{165}$$

where the coeffiecients $f_n(E)$, only depending on energy E, will be related to the scattering angle. The scattering angle χ of the scalar probe is given by eq. (40), which when written out produces

$$\frac{d(\chi/2)}{dr} = \frac{b/r^2}{\sqrt{1 - \frac{V_{eff}(r,E)}{p_\infty^2} - b^2/r^2}} \tag{166}$$

inserting eq. (164) and using $b = J/p_\infty$. One may now compare orders in G_N of eq. (166) with results previously found from amplitude calculations [1, 88], thus finding individual orders $\chi_n(V_{eff})$. This has been achieved to all orders in G_N [1, eq. (4.22)]. Quoting the first-order term from [1, eq. (4.34)]

$$\chi_1 = \frac{M f_1}{L p_\infty} = \frac{E f_1}{L \mu \sqrt{\gamma^2 - 1}} \quad {}^{36} \tag{168}$$

[36] Second rewriting comes from

$$p_\infty = \frac{\nu M^2 \sqrt{\gamma^2 - 1}}{E} \tag{168}$$

note the extra factor of M, corresponding to a different definition used for f_1 in [1, eq. (4.23)] compared to eq. (165). One remarkable fact about the general expansion, evident from [1, eq. (4.29-4.30)], is that powers of G_N and $1/J$ for any single term accompany each other. Expansions in either are thus equivalent. χ to 1PM order is known from auxhilliary calculations [76, eq. (85), no spin],

$$\chi = \chi_1 G_N = \frac{2G_N m_1 m_2}{L} \frac{2\gamma^2 - 1}{\sqrt{\gamma^2 - 1}} = \frac{G_N E}{L\mu\sqrt{\gamma^2 - 1}} \overbrace{\frac{2(2\gamma^2 - 1)\mu^2 M}{E}}^{=f_1 \text{ compared to (167)}} \tag{169}$$

This determines f_1, and thus V_{eff} to first order [3]

$$f_1 = 2(2\gamma^2 - 1)\frac{\mu^2 M}{E} \qquad [37] \tag{172}$$

We now focus on calculating χ_{eff}.

It may be found with eq. (40) directly from the Hamilton-Jacobi equation for the effective particle

$$g^{\mu\nu}_{eff} \partial_\mu S \partial_\nu S = \mu^2 \tag{173}$$

where $\partial_\mu S \equiv p^{eff}_\mu = (E, -p^{eff})$ is defined as the 4-momentum of the scattering particle. [38] Because of spherical symmetry, restricting to $\theta = \pi/2$ orbits, one may write a separated ansatz for S

$$S = E_{\text{eff}}\, t - J_{\text{eff}}\phi - W(r) \quad [39] \tag{174}$$

An ansatz for the metric $g^{eff}_{\mu\nu}$ is also sought after.
Since the interaction potential between particles is spherically symmetric as viewed from the CM frame, one should also expect spherical symmetry of the EOB metric. In isotropic coordinates, one may adopt the general ansatz

$$ds^2 = A(r)dt^2 - B(r)(dr^2 + d\theta^2 + sin^2\theta d\phi^2) \tag{175}$$

---

[37] As a check, inserting eq. (170) in (167) reproduces the 1PM scattering angle found by [76, eq. (85), no spin]. The calculation is a simple check. Suppose eq. (170) and eq. (167) reproduces [76]. Then

$$\frac{2(\gamma^2 - 1)\mu^2 M^2}{L p_\infty E} \stackrel{?}{=} \frac{2(\gamma^2 - 1)\mu M}{L\sqrt{\gamma^2 - 1}} \Rightarrow \frac{p_\infty E}{m_1 m_2} = \sqrt{\gamma^2 - 1} \tag{171}$$

which when using $p_\infty E = p_{eff} m_1 m_2/\mu$ and $E_{eff} = \gamma\mu$ becomes

$$p_{eff}/\mu = \sqrt{E^2_{eff}/\mu^2 - 1} \Rightarrow p^2_{eff} = E^2_{eff} - \mu^2 \tag{172}$$

which just expresses the 4-momentum norm $p^\mu_{eff}(p_{eff})_\mu = \mu^2 = E^2_{eff} - p^2_{eff}$ of the effective particle.

[38] Note that the definition differs in sign compared to [75], because we work in a (+,-,-,-) convention, compared to the (-,+,+,+) convention used there.

[39] Note the different signs compared to [3], [75]. These are immaterial since $W(r)$ and J_{eff} appear as squared quantities in the Hamilton-Jacobi equation (178). The formal $\pm$ solutions of $W(r)$ in (179) reflect this. See the associated footnote for more information.

with $A(r)$ and $B(r)$ parametrised as

$$A(r) = \left(\frac{1-h(r)}{1+h(r)}\right)^2, \quad B(r) = (1+h(r))^4 \tag{176}$$

as a gaugefixing condition. In the test-body limit $\nu \to 0$ one expects $h(r) \to \frac{GM}{2r}$, corresponding to the Schwarzschild metric with mass M in isotropic coordinates [40].

Inserting in eq. (173) yields [41]

$$\frac{E_{eff}^2}{A} - \frac{1}{B}\left(\left(\frac{dW(r)}{dr}\right)^2 + \frac{J_{\text{eff}}^2}{r^2}\right) = \mu^2 \tag{178}$$

from which $\frac{dW(r)}{dr} = p_r^{\text{eff}}$ may be isolated,

$$\frac{dW(r)}{dr} = \sqrt{\frac{B}{A}E_{eff}^2 - B\mu^2 - \frac{J_{eff}^2}{r^2}} \quad [42] \tag{179}$$

from which the scattering angle becomes

$$\frac{d\chi_{eff}}{dr} \equiv -\frac{\partial}{\partial J_{eff}}\left[\frac{dW(r)}{dr}\right] = \frac{J_{eff}/r^2}{\sqrt{\frac{B}{A}E_{eff}^2 - B\mu^2 - \frac{J_{eff}^2}{r^2}}} = \frac{b_{eff}/r^2}{\sqrt{\frac{B}{A}\frac{E_{eff}^2}{p_{eff}^2} - B\frac{\mu^2}{p_{eff}^2} - \frac{b_{eff}^2}{r^2}}} \tag{180}$$

again using $b_{eff} = J_{eff}/p_{eff}$.

C.3 EOB metric $g_{\mu\nu}^{eff}$ to 1PM

$h(r)$ from the EOB metric may be determined by imposing the scattering angle map, $\chi = \chi_{eff}$. From eqs. (166) and (180)

$$\frac{d\chi}{dr} = \frac{d\chi_{eff}}{dr} \Rightarrow \frac{b/r^2}{\sqrt{1 - \frac{V_{eff}(r,E)}{p_\infty^2} - b^2/r^2}} = \frac{b_{eff}/r^2}{\sqrt{\frac{B}{A}\frac{E_{eff}^2}{p_{eff}^2} - B\frac{\mu^2}{p_{eff}^2} - \frac{b_{eff}^2}{r^2}}} \tag{181}$$

which upon imposing mappings (161) and (163) becomes

$$1 - \frac{V_{eff}(r,E)}{p_\infty^2} = \frac{B\mu^2}{p_{eff}^2}\left(\frac{E_{eff}^2}{\mu^2 A} - 1\right) \tag{182}$$

[40] Note that $\nu \to 0$ may be enforced by taking one mass, say, $m_1 \to 0$. Then $M \to m_2$ as expected for a testparticle m_1 orbiting m_2.

[41] The inverse metric is evidently

$$g_{eff}^{\mu\nu} = \frac{1}{A(r)}\delta_\mu^0\delta_\nu^0 - \frac{1}{B(r)}\left(\delta_\mu^1\delta_\nu^1 + \frac{1}{r^2}\delta_\mu^2\delta_\nu^2 + \frac{1}{r^2 sin^2\theta}\delta_\mu^3\delta_\nu^3\right) \tag{177}$$

[42] Here we take the + solution, as a convention. Note that restricting $\chi \to mod_{2\pi}(\chi)$ makes the sign in the definition of $d\chi/dr$, and thus that of $dW(r)/dr$, completely irrelevant.

Employing the 4-momentum norm expression $E_{eff}^2 = \mu^2 + p_{eff}^2 = \gamma^2\mu^2$ yields

$$1 - \frac{V_{eff}(r,E)}{p_\infty^2} = \frac{B}{\gamma^2-1}(\frac{\gamma^2}{A} - 1) \tag{183}$$

and inserting eq. (176) finally produces a 6th order equation in $h(r)$ after multiplying by $(1+h)^2$ and using $p_\infty^2 = \frac{\nu^2 M^4(\gamma^2-1)}{E^2}$ [43]

$$\left(h(r) + \frac{\gamma-1}{\gamma+1}\right)\left(h(r) + \frac{\gamma+1}{\gamma-1}\right)(1+h(r))^4 = (1-h(r))^2\left(1 - \frac{E^2}{(\gamma^2-1)M^2}\frac{V_{eff}(r,E)}{\nu^2M^2}\right) \tag{185}$$

[44]

Writing $h(r) = \sum_{n=1}^{\infty} h_n \left(\frac{G_N M}{r}\right)^n$, this equation may be solved for h_n order by order in G_N. To first order, with f_1 from eq. (165)

$$h_1\left(4 + \frac{\gamma-1}{\gamma+1} + \frac{\gamma+1}{\gamma-1}\right) = \frac{E^2}{(\gamma^2-1)M^4\nu^2}f_1 - 2h_1 \tag{186}$$

and thus

$$h_1 = \frac{E^2}{4M^2(2\gamma^2-1)}\frac{f_1}{\nu^2M^2} = \frac{E}{2M} \tag{187}$$

C.4 Reflection on EOB metric without spin

The full 1PM EOB metric without spin is per eq. (187)

$$ds^2 = \left(\frac{1-\frac{G_N E}{2r}}{1+\frac{G_N E}{2r}}\right)^2 dt^2 + (1+\frac{G_N E}{2r})^4(dr^2 + r^2d\theta^2 + r^2sin^2\theta d\phi^2) \tag{188}$$

In the testbody case $\nu \to 0$ meaning $E \to M$ and $h \to 1/2$, the above reduces to the Schwarzschild metric in isotropic coordinates. This is consistent with requirement (149).

Solving (185), one may find $h_{n\leqslant 3}$, beyond which the impetus equation (164) has not been proven to hold. The energy map (153), which plays no part in finding h, may actually be found from eq. (182). The same is true for the free-particle relation $E_{eff} = p_{eff} + \mu^2$, as shown by [3]. Expanding eq. (182) up to first order in G_N yields

$$-\frac{1}{p_{eff}^2}(E_{eff}^2 - \mu^2 - p_{eff}^2) + \left[\frac{f_1}{p_\infty^2} + \frac{h_1}{p_{eff}^2}(2\mu^2 - 6E_{eff}^2 - 2p_{eff}^2)\right]\frac{G_N M}{r} + \mathcal{O}(G_N^2) = 0 \tag{189}$$

Requiring each order in G_N vanish identically, the 0'th order term yields the free-particle expression for E_{eff},

$$E_{eff}^2 = \mu^2 + p_{eff}^2 \tag{190}$$

[43] follows directly from the momentum map (161)

$$p_\infty^2 = \frac{M^2}{E^2}p_{eff}^2 = \frac{\mu^2M^2(\gamma^2-1)}{E^2} = \frac{\nu^2M^4(\gamma^2-1)}{E^2} \tag{184}$$

where $p_{eff}^2 = E_{eff}^2 - \mu^2 = (\gamma^2-1)\mu^2$ from the 4-momentum norm $p_\mu^{eff}p_{eff}^\mu = \mu^2$

[44] Note the sign difference compared to [3, eq. (30)].

and then the first order term determines the energy mapping

$$\frac{E_{eff}}{\mu} = \sqrt{\frac{f_1 E^2 + 4\mu^2 M^2 h_1}{8\mu^2 M^2 h_1}} = \gamma = \frac{E^2 - m_1^2 - m_2^2}{2m_1 m_2} \qquad [45] \tag{194}$$

which corresponds exactly to eq. (150). Equations (190) and (191) necessarily hold to all orders in G_N. Continuing the calculation to 2PM, [3, eq. (40)] shows that the 2PM periastron shift $\Delta\Phi$ corresponds exactly to expectations. The result will just be quoted here for reference without further discussion,

$$\Delta\Phi = \frac{3\pi G_N^2 M^2 \mu^2}{2J^2} \left(\frac{E}{M}\right) (5\gamma^2 - 1) \tag{195}$$

[45] Inserting eq. (190) in the first order term of (189) yields the requirement

$$\frac{f_1}{p_\infty^2} + 4\frac{h_1 \mu^2}{p_\infty^2}(1 - 2\frac{E_{eff}^2}{\mu^2}) = 0 \tag{192}$$

Then isolating E_{eff}/μ gives

$$E_{eff}/\mu = \sqrt{\frac{f_1 E^2 + 4\mu^2 M^2 h_1}{8\mu^2 M^2 h_1}} \tag{193}$$

which upon inserting $f_1 E^2 = 2(2\gamma^2 - 1)\mu^2 ME = 4(2\gamma^2 - 1)\mu^2 M^2 h_1$ where $h_1 = \frac{E}{2M}$, gives directly

$$E_{eff}/\mu = \gamma = \frac{E^2 - m_1^2 - m_2^2}{2m_1 m_2} \tag{194}$$

where the last equality follows from the last part of eq. (150)

D NJA algorithm

The Newman Jones Algorithm (NJA) is a procedure of introducing spin to a static metric. First introduced by Newman and Janis as a quriosity in 1965 [89], it was shown to produce the Kerr metric from the Schwarzschild solution. Furthermore it also produces the Kerr-Newman metric from the Reissner Nordstroem solution [16]. The procedure is considered ad-hoc, because no formal explanation has been given as to its sucessfulness (see step 3 below) [90, 91].

The algorithm consists of the following. [91]

1. Consider a general spherically symmetric metric and write it in advanced null coordinates

$$ds^2 = e^{2\Phi(r)}du^2 + e^{\Phi(r)+\lambda(r)}dudr - r^2(d\theta^2 + sin^2\theta d\phi^2) \tag{196}$$

The Schwarzschild metric in advanced null coordinates is

$$ds^2 = \left(1 - \frac{r_s}{r}\right)du^2 + 2dudr - r^2\left(d\theta^2 + sin^2\theta d\phi^2\right) \tag{197}$$

2. Express the metric in terms of null-tetrads $Z^\mu_a = (l^\mu, n^\mu, m^\mu, \bar{m}^\mu)$

$$g^{\mu\nu} = l^\mu n^\nu + l^\nu n^\mu - m^\mu \bar{m}^\nu - m^\nu \bar{m}^\mu \tag{198}$$

where

$$l_\mu l^\mu = m^\mu m_\mu = n_\mu n^\mu = 0, l_\mu n^\mu = -m_\mu \bar{m}^\mu = 1, l_\mu m^\mu = n_\mu m^\mu = 0 \tag{199}$$

For the metric (197), the null tetrads are

$$l^\mu = \delta^\mu_1 \tag{200a}$$

$$n^\mu = \delta^\mu_0 - \frac{1}{2}\left(1 - \frac{r_s}{r}\right) \tag{200b}$$

$$m^\mu = \frac{1}{\sqrt{2}r}\left(\delta^\mu_2 + \frac{i}{sin\theta}\delta^\mu_3\right) \tag{200c}$$

3. Define a complex coordinate $\tilde{x}$ and rewrite $Z^\mu_a \in \mathbb{R}$ in such a way that when $\tilde{x} \to x$, the correct form of Z^μ_a is recovered. This procedure is not unique, being generally considered ad-hoc. The correct procedure which recovers Kerr from Schwarzschild lets

$$\begin{aligned} &\frac{1}{r} \to \frac{1}{\tilde{r}} + \frac{1}{\bar{\tilde{r}}}, \qquad \frac{1}{r^2} \to \frac{1}{\tilde{r}\bar{\tilde{r}}} \qquad \text{in } l^\mu \text{ and } n^\mu \\ &r \to \tilde{r} \text{ and } r \to \bar{\tilde{r}} \qquad \text{for } m^\mu \text{ and } \bar{m}^\mu \text{ respectively} \end{aligned} \tag{201}$$

such that eq. (200) becomes

$$l^\mu = \delta^\mu_1 \tag{202a}$$

$$n^\mu = \delta^\mu_0 - \frac{1}{2}\left(1 - \frac{r_s}{2}(\frac{1}{\tilde{r}} + \frac{1}{\bar{\tilde{r}}})\right) \tag{202b}$$

$$m^\mu = \frac{1}{\sqrt{2}r}\left(\delta^\mu_2 + \frac{i}{sin\theta}\delta^\mu_3\right) \tag{202c}$$

4. Now perform a complex coordinate transformation $\tilde{x} \to x'^{\mu} = \tilde{x}^{\mu} + i\gamma^{\mu}(\tilde{x})$ to the null-tetrad vector Z_a^{μ}, such that

$$Z'^{\mu}_{\ a}(x') = \frac{\partial x'^{\mu}}{\partial \tilde{x}^{\mu}} Z_a^{\mu}(\tilde{x}) \tag{203}$$

For the Schwarschild metric written with eq. (202), one uses

$$\tilde{x}^{\mu} = x'^{\mu} + iacos\theta(\delta_0^{\mu} - \delta_1^{\mu}) \tag{204}$$

denoting $x'^{\mu} = (u', r, \theta, \phi')$ reusing notation slightly. The metric found from the Schwarzshild metric is

$$g_{\mu\nu} = \begin{pmatrix} 1 - \frac{r_s r}{\Sigma} & 1 & 0 & asin^2\theta\frac{r_s r}{\Sigma} \\ \cdot & 0 & 0 & -asin^2\theta \\ \cdot & \cdot & -\Sigma & 0 \\ \cdot & \cdot & \cdot & -\sin^2\theta(r^2 + a^2 - a^2 sin^2\theta\frac{r_s}{\Sigma}) \end{pmatrix}, \qquad \text{where} \quad \Sigma \equiv r^2 - a^2 cos\theta \tag{205}$$

Dots (.) indicate $g_{\mu\nu} = g_{\nu\mu}$.

The coordinates $\tilde{x}$ are assumed to be real valued, such that the metric (205) has no mention of complex quantities.

5. For the Schwarzschild metric, the ordinary coordinate transformation

$$u = t - \int dr \frac{a}{\Delta}, \qquad \phi' = \phi - \int dr \frac{r^2 + a^2}{\Delta}, \qquad \Delta \equiv r^2 + a^2 - r_s r \tag{206}$$

shows that the metric (205) is, remarkably, Kerr, now transformed to Boyer-Lindquist coordinates (t, r, θ, ϕ). Note that by the integral above, we mean a indefinite integral without integration constant.

For the Reisner Nordstroem metric, a similar coordinate transformation of the form $u = t + F(r)$, $\phi' = \phi + G(r)$ recovers the Kerr-Newman metric.

E Explanation of code

E.1 Calculations with test particle spin

The code `((official) proper math, optimised) Scattering angle proper math.nb` can handle all calculations with spin. These are included as separate appended files.

Setting up the scattering system in the code
The code needs specifying of the scattering situation in the form of a couple parameters. Below is a list hereof, with a detailed description

- `g`: Scattering metric, written in normal coordinates $\{t, \rho, \phi\}$ restricted to the scattering plane. The coordinates should be denoted by these exact symbols for the code to work.
- `simplifications` and `simplifications2`: Simplifications to be used before and after integrating, respectively.
- `orderInS`: The order in test particle spin S at which the scattering angle should be found. The code will expand in parameter S multiple times throughout, ensuring consistent orders are produced in the final scattering angle.
- `scatteringOrder`: PM order in Newtons gravitational constant, at which the scattering angle should be found. The code ill expand in paramter G multiple times throughout, ensuring consistent orders are produced in the final scattering angle.

Some extra parameters `printExtraInformation` and `progressPrinting` control how the ouput is displayed. The Timeout of `Simplify` in Mathematica can also be set at the top of the document.

Lastly, the test particle spin properties are defined by parameters `PT`, `PPHI` and `tm`, which are discussed below.

Implementing the scattering angle formula in code and implementing spin on the probe
We have now established a scattering metric on which the test particle scatters. This includes a normal coordinate system $\{t, \rho, \phi\}$ to which we restrict ourselves furthermore. The general formula for scattering angles with spin is

$$\chi = \int_{r_m}^{\infty} dr \frac{d\phi}{dr} = \int_{r_m}^{\infty} dr \frac{\mathcal{D}[p_r]}{p_\infty} = \sum_{n=0}^{\infty} \int_0^{\infty} du \left(\frac{d}{du^2}\right)^n \mathcal{D}\left[\frac{r^{2n} U^{n+1}(r,b)}{(n+1)! p_\infty^{2(n+1)}}\right], \quad \text{in last equality } r^2 = u^2 + b^2 \tag{207}$$

$$\mathcal{D} \equiv \partial_b + f_S(r)\partial_S = \partial_b + \left(\frac{p_\infty S}{m\kappa} + \frac{p_\infty \left(a^2 r + 2GM\left(\kappa^2 - r^2\right) - \kappa l r + r^3\right) S^2}{m^2 \kappa^2 \left(\gamma r^3 - a\kappa r\right)}\right)\partial_S + \mathcal{O}(S^3) \tag{208}$$

The scattering metric, with asymptotically spherical coordinates $\{t, r, \phi\}$ is denoted `g` in the code.

Finding $U(r,b)$ and $\mathcal{D}$
Both $U(r,b)$ and $\mathcal{D}$ can be constructed from Justin Vines' unpublished notes. These notes specify

canonical momenta $p_\mu = \{p_t, p_\phi, p_r\}$ and $\frac{d\phi}{dr}$ as

$$\tilde{m}^2/m^2 = g^{\mu\nu}\pi_\mu\pi_\nu \tag{209a}$$

$$\pi_t = -\gamma + GM\kappa\sigma u^3 + \mathcal{O}(\sigma^3) \tag{209b}$$

$$\pi_\phi = l - aGM\kappa\sigma u^3 + GM\kappa\sigma^2 u^3 + \mathcal{O}(\sigma^3) \tag{209c}$$

$$\tilde{m}/m = 1 - \frac{GM(u^3 + 3u^5\kappa^2)\sigma^2}{2} + \mathcal{O}(\sigma^3) \tag{209d}$$

$$\dot{x}^\mu = \frac{1}{\tilde{m}} g^{\mu\nu} p_\nu + \mathcal{O}(S^3) \quad \Rightarrow \quad \frac{d\phi}{dr} = \frac{\dot{\phi}}{\dot{r}} = \frac{u^2}{\widehat{\Delta}^2 \pi_r}\left[\pi_\phi - 2GMu(\pi_\phi + a\pi_t)\right] + \mathcal{O}(S^3) \tag{209e}$$

[46] where we have introduced rescaled quantities

$$\pi_\mu = p_\mu/m, \quad \sigma = S/m, \quad \gamma = E/m, \quad l = J/m - \gamma\sigma = (\pi_\phi)_{r\to\infty}, \quad \kappa = l - \gamma a \tag{211a}$$

$$u = 1/r, \quad \widehat{\Delta} = u^2\Delta = 1 + a^2u^2 - 2GMu \tag{211b}$$

The prefactor $f_S(r)$ in $\mathcal{D}$ as given by eq. (207) may be found by matching eq. (207) with (209e). Constructing the operator in this way, is a trivial step, and completely equivalent to the $h(r)$ structure of the derivation given in our article. The code at the moment uses the operator-form, and is optimised for this form. It would be possible to rewrite the code with the $h(r)$ structure, however would require optimising. $\mathcal{D}$ is simply defined at the top of the code, as quantity `op`.

$U(r, b)$ is found by solving the Hamilton-Jacobi equation (209a) for p_r, then letting $p_r^2 = p_\infty^2 - \frac{L^2}{r^2} - U(r, b)$ where L is the orbital angular momentum. $U(r, b)$ is denoted `R` in the code.

Computing the integrand of eq. (207)

We have now computed both $U(r, b)$ and $\mathcal{D}$. Computing the integrand in eq. (207) is therefor trivial. However, we have not yet imposed specific orders in S and G, at which the scattering angle should be computed. Doing so removes may terms and speeds up calculation.

To do this efficiently, we treat every term in the $\sum_{n=0}^{\infty}$ one by one. Since $U(r, b) \propto G$, we can restrict to look at $n \leqslant$ `scatteringOrder`. For each n, do the following

- Compute the term $\frac{r^{2n}U^{n+1}(r,b)}{(n+1)!p_\infty^{2(n+1)}}$ in eq. (207) up to `scatteringOrder` in G and `orderInS` in S. To minimise expressionlength (which greatly improves performance), $U(r, b)^{n+1}$ is expanded separately in S and G.

- Rewrite all γ's and energies e with velocity v. This simplifies the parameterspace with which Mathematica has to work while doing simplifications.

- Simplify the result. This greatly minimises expression lengths and increases performance.

[46] Note we may also expand $\tilde{m}^2$ directly, as did Vines in "AlignedSpins", to obtain

$$\tilde{m}^2/m^2 = 1 - GM(u^3 + 3u^5\kappa^2)\sigma^2 + \mathcal{O}(\sigma^3) \tag{210}$$

- Impose $r^2 = u^2 + b^2$ explicitly.
- Act with the operators $\mathcal{D}$ and $\left(\frac{d}{du^2}\right)^n$ and keep only relevant orders in S
- Simplify the result
- Integrate the resulting integrand of eq. (207)

Imposing assumptions while integrating and simplifying, such as $b > a$, greatly improves performance. The individual integrands are summed for $n \leqslant$ `scatteringOrder`, which sum to produce the scattering angle.

Simplifying the scattering angle

We now have a scattering angle result which is somewhat overcomplicated. The result may be simplified systematically by using `FullSimplify`, setting everything over a common denominator and gathering powers in v. The resulting scattering angle is very concise and properties such as the light bending limit can readily be surmised. Writing everything in terms of single parameter v, opposed to a possible v, γ form, also provides a very easy way of comparing results ot previous calculations.

E.2 Calculations without test particle spin

As mentioned above calculations without spin are best performed with the `Scattering Angle pure v.nb` code. The general strucuture of the code is very similar to that of the spinning test particle. The appropriate scattering angle formula is in this case

$$\chi = \sum_{n=0}^{\infty} \int_0^{\infty} du \frac{\partial}{\partial b} \left(\frac{d}{du^2}\right)^n \frac{r^{2n} U^{n+1}(r,b)}{(n+1)! p_{\infty}^{2(n+1)}}, \quad r^2 = u^2 + b^2 \tag{212}$$

Again, $U(r,b)$ is calculated from solving the Hamilton-Jacobi equation

$$m^2 = g^{\mu\nu} p_\mu p_\nu \tag{213}$$

where $p_\mu = \{e, L, p_r\}$ with e test particle energy and L test particle angular momentum.

The integrand is then computed exactly as before, with a slightly different simplification method to optimise performance. In the sum over n, each term is treated and integrated separately and the results summed to produce the correct scattering angle.

The simplifications of the final angle are identical with those performed before.

E.3 Reference of quantities and notation used in code

Test particle related quantities

- `m`: Test particle mass
- `v`: Test particle asymptotical velocity
- γ: Test particle asymptotical Lorentz contraction factor

- `e`: Test particle energy
- `J`: Test particle angular momentum (total)
- `b`: Test particle impact parameter (measured at asymptotically flat infinity)
- `S`: Test particle spin
- `tm`: Effective mass of a test particle with spin, appearing in the Hamilton-Jacobi equation
- `PT` and `PPHI`: Canonical test particle momenta in t and ϕ directions which are **input by the user**. They are replaced with p_t and p_ϕ later in the code
- p_t, p_r, p_ϕ: test particle canonical momenta as **used in the internals** of the code.
- $p_{\phi dynReplacement}$ and $p_{tdynReplacement}$: Canonical momenta used in the internals of the code which denote the G-dependent parts of canonical momenta `PT` and `PPHI`

Metric and notation

- $\{t, \rho, \phi\}$: normal coordinates in which the metric is written
- `g`: Scattering metric written in normal coordinates $\{t, \rho, \phi\}$
- `G`: Newtons gravitational constant

Input quantities for the computation

- `op`: Name in code for operator $\mathcal{D}$ producing scattering angle with spin. See below.
- `scatteringOrder`: Order in G at which the scattering angle should be determined
- `orderInS`: Order in S at which the scattering angle should be determined

Additional input parameters

- `printExtraInformation`: Toggles whether things like $U(r, b)$ and T should be printed while doing the calculations. Off by default.
- `progressPrinting`: Toggles whether extra information about the integrands should be printed while they are evaluated.

References

[1] N. E. J. Bjerrum-Bohr, A. Cristofoli, and P. H. Damgaard, "Post-minkowskian scattering angle in einstein gravity," *Journal of High Energy Physics*, vol. 2020, no. 8, p. 38, 2020.

[2] P. H. Damgaard, J. Hoogeveen, A. L. Godoy, and J. Vines, "Scattering angles in kerr metrics." in preparation, Aug 2022.

[3] P. Damgaard and P. Vanhove, "Remodeling the effective one-body formalism in post-minkowskian gravity," *Physical Review D*, vol. 104, 11 2021.

[4] ESA, "A history of astronomy part i: Mapping the sky from ancient to premodern times." `https://sci.esa.int/web/gaia/-/53196-the-oldest-sky-maps`, Sep 2019.

[5] B. P. e. a. Abbott, "Observation of gravitational waves from a binary black hole merger," *Phys. Rev. Lett.*, vol. 116, p. 061102, Feb 2016.

[6] A. Einstein, "On the electrodynamics of moving bodies," *Annals of Physics*, 1905.

[7] A. Einstein, "On the relativity principle and the conclusions drawn from it," *Jahrbuch der Radioaktivitat*, vol. 4, pp. 411–462, 1907.

[8] A. Einstein, "The foundation of the general theory of relativity," *Annalen der Physik*, 1916.

[9] A. Einstein, *Foundations of the General Theory of Relativity.* Leipzig: Barth, 1916.

[10] A. Einstein, "Explanation of the Perihelion Motion of Mercury from the General Theory of Relativity," *Sitzungsber. Preuss. Akad. Wiss. Berlin (Math. Phys.)*, vol. 1915, pp. 831–839, 1915.

[11] C. M. Will, "The confrontation between general relativity and experiment," *Living Reviews in Relativity*, vol. 17, jun 2014.

[12] T. Harmark, "General relativity and cosmology." Lecture Notes, Sep 2019.

[13] R. P. Kerr, "Gravitational field of a spinning mass as an example of algebraically special metrics," *Phys. Rev. Lett.*, vol. 11, pp. 237–238, Sep 1963.

[14] N. Arkani-Hamed, Y.-t. Huang, and D. O'Connell, "Kerr black holes as elementary particles," *Journal of High Energy Physics*, vol. 2020, no. 1, p. 46, 2020.

[15] H. Reissner, "Über die Eigengravitation des elektrischen Feldes nach der Einsteinschen Theorie," Jan. 1916.

[16] E. T. Newman, E. Couch, K. Chinnapared, A. Exton, A. Prakash, and R. Torrence, "Metric of a rotating, charged mass," *Journal of Mathematical Physics*, vol. 6, no. 918, 1965.

[17] L. Blanchet, "Post-newtonian theory and the two-body problem," *Mass and Motion in General Relativity*, vol. 162, 07 2009.

[18] C. M. Will, "On the unreasonable effectiveness of the post-newtonian approximation in gravitational physics," *Proceedings of the National Academy of Sciences*, vol. 108, no. 15, pp. 5938–5945, 2011.

[19] T. Damour and N. Deruelle, "General relativistic celestial mechanics of binary systems. I. The post-Newtonian motion.," *Ann. Inst. Henri Poincaré Phys. Théor*, vol. 43, pp. 107–132, Jan. 1985.

[20] J. Blümlein, A. Maier, P. Marquard, and G. Schäfer, "The fifth-order post-newtonian hamiltonian dynamics of two-body systems from an effective field theory approach: Potential contributions," *Nuclear Physics B*, vol. 965, p. 115352, apr 2021.

[21] A. Buonanno and T. Damour, "Effective one-body approach to general relativistic two-body dynamics," *Physical Review D*, vol. 59, mar 1999.

[22] A. Buonanno and T. Damour, "Transition from inspiral to plunge in binary black hole coalescences," *Phys. Rev. D*, vol. 62, p. 064015, 2000.

[23] T. Damour, P. Jaranowski, and G. Schaefer, "On the determination of the last stable orbit for circular general relativistic binaries at the third postNewtonian approximation," *Phys. Rev. D*, vol. 62, p. 084011, 2000.

[24] T. Damour, "Coalescence of two spinning black holes: An effective one-body approach," *Physical Review D*, vol. 64, 04 2001.

[25] F. Pretorius, "Evolution of binary black-hole spacetimes," *Phys. Rev. Lett.*, vol. 95, p. 121101, Sep 2005.

[26] M. Campanelli, C. O. Lousto, P. Marronetti, and Y. Zlochower, "Accurate evolutions of orbiting black-hole binaries without excision," *Phys. Rev. Lett.*, vol. 96, p. 111101, Mar 2006.

[27] M. Campanelli, C. O. Lousto, and Y. Zlochower, "Spinning-black-hole binaries: The orbital hang up," *Phys. Rev. D*, vol. 74, p. 041501, 2006.

[28] J. Baker, J. Centrella, D.-I. Choi, M. Koppitz, and J. Meter, "Binary black hole merger dynamics and waveforms," *Phys. Rev. D*, vol. 73, 05 2006.

[29] J. G. Baker, J. Centrella, D.-I. Choi, M. Koppitz, J. R. van Meter, and M. C. Miller, "Getting a kick out of numerical relativity," *The Astrophysical Journal*, vol. 653, pp. L93–L96, dec 2006.

[30] J. Baker, M. Campanelli, F. Pretorius, and Y. Zlochower, "Comparisons of binary black hole merger waveforms," *Classical and Quantum Gravity*, vol. 24, 02 2007.

[31] J. A. Gonzalez, U. Sperhake, B. Bruegmann, M. Hannam, and S. Husa, "Total recoil: The Maximum kick from nonspinning black-hole binary inspiral," *Phys. Rev. Lett.*, vol. 98, p. 091101, 2007.

[32] S. Husa, J. A. Gonzalez, M. Hannam, B. Bruegmann, and U. Sperhake, "Reducing phase error in long numerical binary black hole evolutions with sixth order finite differencing," *Class. Quant. Grav.*, vol. 25, p. 105006, 2008.

[33] M. Koppitz, D. Pollney, C. Reisswig, L. Rezzolla, J. Thornburg, P. Diener, and E. Schnetter, "Recoil velocities from equal-mass binary-black-hole mergers," *Physical review letters*, vol. 99, p. 041102, 08 2007.

[34] L. Rezzolla, E. N. Dorband, C. Reisswig, P. Diener, D. Pollney, E. Schnetter, and B. Szilágyi, "Spin diagrams for equal-mass black hole binaries with aligned spins," *The Astrophysical Journal*, vol. 679, pp. 1422–1426, jun 2008.

[35] L. Rezzolla, P. Diener, E. Dorband, D. Pollney, C. Reisswig, E. Schnetter, and J. Seiler, "The final spin from the coalescence of aligned-spin black hole binaries," *The Astrophysical Journal Letters*, vol. 674, p. L29, 12 2008.

[36] M. Boyle, D. A. Brown, L. E. Kidder, A. H. Mroué, H. P. Pfeiffer, M. A. Scheel, G. B. Cook, and S. A. Teukolsky, "High-accuracy comparison of numerical relativity simulations with post-newtonian expansions," *Phys. Rev. D*, vol. 76, p. 124038, Dec 2007.

[37] B. A. et. al., "Improved analysis of GW150914 using a fully spin-precessing waveform model," *Physical Review X*, vol. 6, oct 2016.

[38] A. Einstein, "Approximative Integration of the Field Equations of Gravitation," *Sitzungsber. Preuss. Akad. Wiss. Berlin (Math. Phys.)*, vol. 1916, pp. 688–696, 1916.

[39] A. S. Eddington, "The propagation of gravitational waves," *Proc. R. Soc. Lond.*, vol. 102, pp. 268–282, 1922.

[40] H. Bondi, F. A. E. Pirani, and I. Robinson, "Gravitational waves in general relativity iii. exact plane waves," *Proc. R. Soc. Lond.*, vol. 251, pp. 519–533, 1959.

[41] R. A. Hulse and J. H. Taylor, "Discovery of a pulsar in a binary system.," *Astrophysics Journal*, vol. 195, pp. L51–L53, Jan. 1975.

[42] T. Damour, "1974: the discovery of the first binary pulsar," *Classical and Quantum Gravity*, vol. 32, p. 124009, jun 2015.

[43] LIGO, "Ligo's interferometer." `https://www.ligo.caltech.edu/page/ligos-ifo`, Aug 2022.

[44] LIGO, "Ligo factsheet." `https://www.ligo.caltech.edu/page/facts`, Aug 2022.

[45] LIGO, "Ligo images." `https://www.ligo.caltech.edu/images`, Aug 2022.

[46] M. Cattani and J. Bassalo, "Gravitational waves observation: Brief comments," *Revista Brasileira de Ensino de Física*, vol. 38, 01 2016.

[47] A. Saffer, N. Yunes, and K. Yagi, "The gravitational wave stress–energy (pseudo)-tensor in modified gravity," *Classical and Quantum Gravity*, vol. 35, p. 055011, feb 2018.

[48] B. P. e. a. Abbott, "Gw151226: Observation of gravitational waves from a 22-solar-mass binary black hole coalescence," *Phys. Rev. Lett.*, vol. 116, p. 241103, Jun 2016.

[49] B. P. e. a. Abbott, "Gw170104: Observation of a 50-solar-mass binary black hole coalescence at redshift 0.2," *Phys. Rev. Lett.*, vol. 118, p. 221101, Jun 2017.

[50] B. P. A. et. al., "GW170608: Observation of a 19 solar-mass binary black hole coalescence," *The Astrophysical Journal*, vol. 851, p. L35, dec 2017.

[51] B. P. e. a. Abbott, "Gw170814: A three-detector observation of gravitational waves from a binary black hole coalescence," *Phys. Rev. Lett.*, vol. 119, p. 141101, Oct 2017.

[52] B. P. e. a. Abbott, "Gw170817: Observation of gravitational waves from a binary neutron star inspiral," *Phys. Rev. Lett.*, vol. 119, p. 161101, Oct 2017.

[53] B. P. A. et. al., "GW190425: Observation of a compact binary coalescence with total mass ~ 3.4 $m_{\odot}$," *The Astrophysical Journal Letters*, vol. 892, p. L3, mar 2020.

[54] R. e. a. Abbott, "Gw190412: Observation of a binary-black-hole coalescence with asymmetric masses," *Phys. Rev. D*, vol. 102, p. 043015, Aug 2020.

[55] R. A. et. al., "GW190814: Gravitational waves from the coalescence of a 23 solar mass black hole with a 2.6 solar mass compact object," *The Astrophysical Journal Letters*, vol. 896, p. L44, jun 2020.

[56] A. et. al., "Gw190521: A binary black hole merger with a total mass of 150 $M_{\odot}$," *Phys. Rev. Lett.*, vol. 125, p. 101102, Sep 2020.

[57] R. A. et. al., "Observation of gravitational waves from two neutron star–black hole coalescences," *The Astrophysical Journal Letters*, vol. 915, p. L5, jun 2021.

[58] T. Dietrich and T. Hinderer, "Comprehensive comparison of numerical relativity and effective-one-body results to inform improvements in waveform models for binary neutron star systems," *Phys. Rev. D*, vol. 95, p. 124006, Jun 2017.

[59] C. Palenzuela, "Introduction to numerical relativity," *Frontiers in Astronomy and Space Sciences*, vol. 7, 2020.

[60] B. P. e. a. Abbott, "Properties of the binary black hole merger gw150914," *Phys. Rev. Lett.*, vol. 116, p. 241102, Jun 2016.

[61] B. P. e. a. Abbott, "Directly comparing gw150914 with numerical solutions of einstein's equations for binary black hole coalescence," *Phys. Rev. D*, vol. 94, p. 064035, Sep 2016.

[62] E. Berti, V. Cardoso, and A. O. Starinets, "Quasinormal modes of black holes and black branes," *Class. Quant. Grav.*, vol. 26, p. 163001, 2009.

[63] E. Finch and C. J. Moore, "Modeling the ringdown from precessing black hole binaries," *Phys. Rev. D*, vol. 103, p. 084048, Apr 2021.

[64] N. E. J. Bjerrum-Bohr, P. H. Damgaard, L. Plante, and P. Vanhove, "The SAGEX Review on Scattering Amplitudes, Chapter 13: Post-Minkowskian expansion from Scattering Amplitudes," 3 2022.

[65] B. Bertotti, "On gravitational motion," *Il Nuovo Cimento (1955-1965)*, vol. 4, no. 4, pp. 898–906, 1956.

[66] A. Guevara, A. Ochirov, and J. Vines, "Scattering of spinning black holes from exponentiated soft factors," *Journal of High Energy Physics*, vol. 2019, 09 2019.

[67] P. Di Vecchia, C. Heissenberg, R. Russo, and G. Veneziano, "The eikonal approach to gravitational scattering and radiation at $\mathcal{O}(G^3)$," *Journal of High Energy Physics*, vol. 2021, no. 7, p. 169, 2021.

[68] Z. Bern, J. Parra-Martinez, R. Roiban, M. S. Ruf, C.-H. Shen, M. P. Solon, and M. Zeng, "Scattering Amplitudes, the Tail Effect, and Conservative Binary Dynamics at O(G4)," *Phys. Rev. Lett.*, vol. 128, no. 16, p. 161103, 2022.

[69] N. E. J. Bjerrum-Bohr, L. Planté, and P. Vanhove, "Post-minkowskian radial action from soft limits and velocity cuts," *Journal of High Energy Physics*, vol. 2022, no. 3, p. 71, 2022.

[70] G. U. Jakobsen and G. Mogull, "Conservative and radiative dynamics of spinning bodies at third post-Minkowskian order using worldline quantum field theory," 1 2022.

[71] G. Mogull, J. Plefka, and J. Steinhoff, "Classical black hole scattering from a worldline quantum field theory," *Journal of High Energy Physics*, vol. 2021, no. 2, p. 48, 2021.

[72] G. U. Jakobsen, G. Mogull, J. Plefka, and J. Steinhoff, "Classical gravitational bremsstrahlung from a worldline quantum field theory," *Phys. Rev. Lett.*, vol. 126, p. 201103, May 2021.

[73] G. Jakobsen, G. Mogull, J. Plefka, and J. Steinhoff, "Gravitational bremsstrahlung and hidden supersymmetry of spinning bodies," *Physical Review Letters*, vol. 128, 01 2022.

[74] G. U. Jakobsen, G. Mogull, J. Plefka, and J. Steinhoff, "Susy in the sky with gravitons," *Journal of High Energy Physics*, vol. 2022, no. 1, p. 27, 2022.

[75] T. Damour, "Gravitational scattering, post-minkowskian approximation and effective one-body theory," *Physical Review D*, vol. 94, 09 2016.

[76] J. Vines, "Scattering of two spinning black holes in post-minkowskian gravity, to all orders in spin, and effective-one-body mappings," *Classical and Quantum Gravity*, vol. 35, p. 084002, mar 2018.

[77] M. V. S. Saketh and J. Vines, "Scattering of gravitational waves off spinning compact objects with an effective worldline theory," 2022.

[78] S. V. Iyer and E. C. Hansen, "Strong and weak deflection of light in the equatorial plane of a kerr black hole," *arXiv: General Relativity and Quantum Cosmology*, 2009.

[79] J. Hadamard, *Lectures on Cauchy's Problem in Linear Partial Differential Equations*, ch. Introduction to a kind of improper integral, pp. 134–140. Mrs. Hepsa Ely Silliman Memorial Lecutres, New York: Yale University press, first edition ed., 1923.

[80] L. Blanchet and G. Faye, "Hadamard regularisation," *Journal of Mathematical Physics*, vol. 41, no. 7675, 2000.

[81] M. Riesz, "Integrales de riemann-liouville et potentiels," 1988.

[82] T. Damour and G. Schäfer, "Higher-order relativistic periastron advances and binary pulsars," *Il Nuovo Cimento B (1971-1996)*, vol. 101, no. 2, pp. 127–176, 1988.

[83] T. Damour, "Classical and quantum scattering in post-Minkowskian gravity," *Phys. Rev. D*, vol. 102, no. 2, p. 024060, 2020.

[84] D. Bohm, *Quantum Theory*. Dover Publication Co., New York U.S.A., 1989.

[85] C. R. Keeton and A. O. Petters, "Formalism for testing theories of gravity using lensing by compact objects: Static, spherically symmetric case," *Phys. Rev. D*, vol. 72, p. 104006, Nov 2005.

[86] T. Damour, "High-energy gravitational scattering and the general relativistic two-body problem," *Phys. Rev. D*, vol. 97, no. 4, p. 044038, 2018.

[87] Z. Bern, A. Luna, R. Roiban, C.-H. Shen, and M. Zeng, "Spinning black hole binary dynamics, scattering amplitudes, and effective field theory," *Phys. Rev. D*, vol. 104, no. 6, p. 065014, 2021.

[88] P. H. Damgaard, L. Planté, and P. Vanhove, "On an exponential representation of the gravitational s-matrix," *Journal of High Energy Physics*, vol. 2021, no. 11, p. 213, 2021.

[89] E. T. Newman and A. I. Janis, "Note on the Kerr spinning particle metric," *J. Math. Phys.*, vol. 6, pp. 915–917, 1965.

[90] E. J. Flaherty, "Hermitian and kahlerian geometry in relativity," 1975.

[91] S. P. Drake and P. Szekeres, "Uniqueness of the newman–janis algorithm in generating the kerr–newman metric," *General Relativity and Gravitation*, vol. 32, no. 3, pp. 445–457, 2000.